

THE UNIVERSITY OF CALGARY
PARAMETRIC INVESTIGATION OF THE EFFECTS
OF PRESSURE, RELATIVE PERMEABILITY
AND COMPOSITION UPON LINEAR
GAS-LIQUID DISPLACEMENTS

by

WAYNE ROY HOVDESTAD

A THESIS

SUBMITTED TO THE FACULTY OF GRADUATE STUDIES
IN PARTIAL FULFILLMENT OF THE REQUIREMENTS FOR THE
DEGREE OF MASTER OF ENGINEERING

DEPARTMENT OF CHEMICAL AND PETROLEUM ENGINEERING

CALGARY, ALBERTA

SEPTEMBER, 1989

© WAYNE ROY HOVDESTAD 1989



National Library
of Canada

Bibliothèque nationale
du Canada

Canadian Theses Service Service des thèses canadiennes

Ottawa, Canada
K1A 0N4

The author has granted an irrevocable non-exclusive licence allowing the National Library of Canada to reproduce, loan, distribute or sell copies of his/her thesis by any means and in any form or format, making this thesis available to interested persons.

The author retains ownership of the copyright in his/her thesis. Neither the thesis nor substantial extracts from it may be printed or otherwise reproduced without his/her permission.

L'auteur a accordé une licence irrévocable et non exclusive permettant à la Bibliothèque nationale du Canada de reproduire, prêter, distribuer ou vendre des copies de sa thèse de quelque manière et sous quelque forme que ce soit pour mettre des exemplaires de cette thèse à la disposition des personnes intéressées.

L'auteur conserve la propriété du droit d'auteur qui protège sa thèse. Ni la thèse ni des extraits substantiels de celle-ci ne doivent être imprimés ou autrement reproduits sans son autorisation.

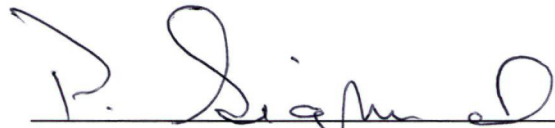
ISBN 0-315-54245-4

THE UNIVERSITY OF CALGARY
FACULTY OF GRADUATE STUDIES

The undersigned certify that they have read, and recommend to the
Faculty of Graduate Studies for acceptance, a thesis entitled,

"PARAMETRIC INVESTIGATION OF THE EFFECTS OF PRESSURE,
RELATIVE PERMEABILITY AND COMPOSITION UPON LINEAR
GAS-LIQUID DISPLACEMENTS"

submitted by Wayne Roy Hovdestad in partial fulfillment of the requirements for
the degree of Master of Engineering.



Dr. P. Sigmund, Chairman
Department of Chemical & Petroleum Engineering



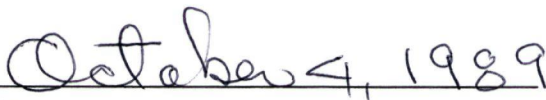
Dr. R.G. Moore,
Department of Chemical & Petroleum Engineering



Dr. A. Badakhshan,
Department of Chemical & Petroleum Engineering



Dr. I. Wierzb,
Department of Mechanical Engineering



Date

ABSTRACT

A parametric investigation of the effects of relative permeability, viscosity ratio and mass transfer upon linear gas-liquid displacements using a numerical model was performed. The objective of this investigation was to quantify the apparent contribution of each process mechanism to the simulated efficiency of a gas-liquid displacement in a permeable, porous medium. The numerical model used in this investigation employed a finite difference formulation of the discretized flow equations with interphase mass transfer calculated by an equation of state. Viscosities were estimated by an empirical correlation.

The computational approach used in this investigation is different than the physical processes it aims to replicate in that process mechanisms active in a given numerical model experiment are programmed into the computer model. While such approaches suffer from uncertainty in physical detail, they do permit a more precise and convenient means of determining the relative contribution of individual process mechanisms to the efficacy of gas-liquid displacements. Numerical parameters used were validated by a sensitivity study of results to the level of discretization and number of grid blocks. The number of grid blocks used was based on converged results as well as

calibration against previously published results.

A total of eighty-five computational flow experiments were performed in this investigation. The results were correlated and, where feasible, compared to both physical and computed results in the open literature.

ACKNOWLEDGMENT

The author wishes to express his gratitude and appreciation to the following people and organizations who have helped to make this work possible:

Dr. P.M. Sigmund, thesis supervisor, who encouraged the author to emphasize scientific fundamentals and to search for a mechanistic explanation of observed results.

The Computer Modelling Group, for permission to use their compositional model in this study.

The Supercomputer Allocation Committee and the Government of Alberta for a grant of time on the Cyber 205 supercomputer at the University of Calgary.

Patricia L. Comer and Kristen Kallstrom at SuperComputing Services, the University of Calgary, for their assistance in using the Cyber 205 supercomputer.

Finally, I would like to thank my beloved wife, Michelle, for her patience and understanding throughout the time required to perform this work.

Table of Contents

| | |
|--|------|
| ABSTRACT | -iii |
| ACKNOWLEDGMENT | -v |
| LIST OF TABLES | -vii |
| LIST OF FIGURES | -ix |
| NOMENCLATURE | -xiv |
| CHAPTER I - INTRODUCTION | -1 |
| CHAPTER II - PHASE BEHAVIOR MODELLING | -6 |
| CHAPTER III - INVESTIGATION OF NUMERICAL GRID REFINEMENT | -14 |
| CHAPTER IV - RELATIVE PERMEABILITY AND VISCOSITY RATIO EFFECTS | -31 |
| Introduction | -31 |
| Relative Permeability Relationships | -37 |
| Fluid Systems | -38 |
| Numerical Model Results | -40 |
| CHAPTER V - INVESTIGATION OF MASS TRANSFER EFFECTS | -48 |
| Introduction | -48 |
| Literature Review | -49 |
| Numerical Model Results | -61 |
| CHAPTER VI - IMPLICATIONS FOR FUTURE RESEARCH | -98 |
| Introduction | -98 |
| Simulation of Laboratory Experiments | -99 |
| Phase Behavior Modelling | -101 |
| Viscous Instabilities | -103 |
| CHAPTER VII - POTENTIAL INDUSTRIAL SIGNIFICANCE | -105 |
| Introduction | -105 |
| Miscible Flood Design and Optimization | -107 |
| Use of Alternative Solvents | -111 |
| Well Models | -113 |
| CHAPTER VIII - SUMMARY OF RESEARCH FINDINGS | -116 |
| CHAPTER IX - REFERENCES | -117 |
| APPENDIX A - DESCRIPTION OF NUMERICAL MODEL | -138 |

LIST OF TABLES

TABLE

- 1 - Composition of Gas-Liquid Systems
- 2 - Physical Properties of Gas-Liquid Systems at 19000 kPa and 71° C
- 3 - Model Parameters
- 4 - Relative Permeability Curves
- 5 - Numerical Model Results, Flash Calculations Suppressed
- 6 - Numerical Model Results, Flash Calculations Active
- 7A - Physical Properties of Gas-Liquid Systems at 14500 kPa and 71° C
- 7B - Physical Properties of Gas-Liquid Systems at 20500 kPa and 71° C
- 8 - Numerical Model Results, Factors Influencing Liquid Recovery
- 9 - Comparison of Numerical Model Results, Effect of Mass Transfer on Pore Volume Liquid Produced
- 10 - Residual Oil Recovery Due to Mass Transfer (at 19000 kPa)

11 - Comparison of Predicted and Actual Liquid Recoveries

LIST OF FIGURES

FIGURE

- 1 - Comparison of the Calculated and Experimental Phase Behavior at 20684 kPa and 71.1°C
- 2 - Comparison of the Calculated Phase Behavior at 71°C for Pressures of 14500, 19000 and 20500 kPa
- 3 - Overall C10 Concentration Profile, Initial Calibration Run - Run 1
- 4 - Overall C10 Concentration Profile, Base Case Run - Run 2
- 5 - Overall C10 Concentration Profile, Fine Grid Sensitivity Run - Run 3
- 6 - Overall C10 Concentration Profile, Coarse Grid Sensitivity Run - Run 4
- 7 - Overall C10 Concentration Profile, Coarse Grid Sensitivity Run - Run 5
- 8 - Dimensionless C10 Concentration Profile, 0.4 PV INJ - RP Original
- 9 - Dimensionless Liquid Saturation, 0.4 PV INJ - RP Original

10 - Dimensionless ClO Concentration Profile, 0.7 PV INJ - RP

Original

11 - Dimensionless Liquid Saturation Profile, 0.7 PV INJ - RP

Original

12 - Original Oil Relative Permeability Curve

13 - Curve I - Concave Oil Relative Permeability Curve

14 - Curve II - Convex Oil Relative Permeability Curve

15 - Curve III - Linear Oil Relative Permeability Curve

16 - Pore Volume Oil Produced Versus Viscosity Ratio At 0.4 PV

Gas Injected

17 - Pore Volume Oil Produced Versus Viscosity Ratio At 0.7 PV

Gas Injected

18 - Total Pore Volume Oil Produced Versus Viscosity Ratio

19 - Total Pore Volume Oil Produced Versus Kinematic Viscosity

Ratio

20 - Comparison of Incremental Oil Recoveries (As A Percentage

of Immiscible Residual Oil Saturation)

(x)

21 - Influence of Pressure On Ultimate Oil Recovery (PVGI=1.2,
Sor=0.3)

22 - Displacement Characteristics For Fluid System D:F at 0.7
PVGI Using Linear Oil Relative Permeability Curve III At 19000
kPa (Run 81)

23 - Displacement Characteristics for Fluid System C:E at 0.7
PVGI Using Linear Oil Relative Permeability Curve III At 19000
kPa (Run 69)

24 - Displacement Characteristics for Fluid System B:M at 0.7
PVGI Using Linear Oil Relative Permeability Curve III At 19000
kPa (Run 57)

25 - Displacement Characteristics for Fluid System A:M at 0.7
PVGI Using Linear Oil Relative Permeability Curve III At 19000
kPa (Run 33)

26 - Displacement Characteristics for Fluid System A:Q at 0.7
PVGI Using Linear Oil Relative Permeability Curve III At 19000
kPa (Run 45)

27 - Methane and n-Decane Concentrations At Grid Block 50 Versus
PVGI Using Linear Oil Relative Permeability Curve III At 19000
kPa for Fluid System D:F (Run 81)

28 - Methane and n-Decane Concentrations At Grid Block 50 Versus
PVGI Using Linear Oil Relative Permeability Curve III At 19000
kPa for Fluid System C:E (Run 69)

29 - Methane and n-Decane Concentrations At Grid Block 50 Versus
PVGI Using Linear Oil Relative Permeability Curve III At 19000
kPa for Fluid System B:M (Run 57)

30 - Methane and n-Decane Concentrations At Grid Block 50 Versus
PVGI Using Linear Oil Relative Permeability Curve III At 19000
kPa for Fluid System A:M (Run 33)

31 - Methane and n-Decane Concentrations At Grid Block 50 Versus
PVGI Using Linear Oil Relative Permeability Curve III At 19000
kPa for Fluid System A:Q (Run 45)

32 - Effect of Pressure on Residual Liquid Saturation for Fluid
System B:M At 0.7 PVGI Using Linear Oil Relative Permeability
Curve III

33 - Effect of Pressure on Residual Liquid Saturation for Fluid
System A:M At 0.7 PVGI Using Linear Oil Relative Permeability
Curve III

34 - Effect of Pressure on Residual Liquid Saturation for Fluid
System A:Q At 0.7 PVGI Using Linear Oil Relative Permeability
Curve III

NOMENCLATURE

| | |
|--------------------|---|
| $^{\circ}\text{C}$ | - degrees Celsius |
| C_{10} | - decane |
| kPa | - pressure in kilopascals |
| k_{rg} | - relative permeability to gas |
| k_{rog} | - relative permeability to oil |
| P_{cog} | - gas-oil capillary pressure |
| PV | - pore volume |
| PVGI | - pore volume gas injected |
| PV INJ | - pore volume injected |
| RLS | - residual liquid saturation |
| RM3/Day | - reservoir volume injected in cubic metres per day |
| ROS | - residual oil saturation |
| RP | - relative permeability |
| S_g | - gas saturation |
| S_o | - oil saturation |
| S_{or} | - residual oil saturation |
| ρ | - density, kg/M^3 |
| μ | - viscosity, centipoise (cp) |
| ν | - kinematic viscosity, centistokes. (cSt) |

CHAPTER I - INTRODUCTION

Gas-liquid displacements are used by the petroleum industry to enhance the recovery of liquid hydrocarbons found in subsurface petroleum reservoirs. Folden [1] reported that the hydrocarbon miscible gas-liquid displacement process had been used, as of 1987, at more than 50 (fifty) locations in the Province of Alberta, with nearly 40 (forty) of these projects using a linear vertical gravity stable gas drive process. Novosad and Costain [2] reported that the actual process mechanisms in some instances were other than those traditionally assumed by the petroleum industry.

The hydrocarbon miscible gas-liquid displacement (hereafter referred to as miscible displacement) process entails using a methane gas sufficiently enriched with hydrocarbons of higher molecular weight such as ethane and propane that it acts as a solvent at the conditions in the subsurface petroleum reservoir. The miscible displacement process achieves a much higher recovery of liquid hydrocarbons than an immiscible gas drive which has no beneficial solvent effect [3]. To date, partially miscible hydrocarbon gas drives intermediate between immiscible and miscible gas drives have not been employed in the Province of Alberta since government regulations generally afford less favorable fiscal treatment given that it is difficult to quantify process performance in those circumstances [4]. An

exception was an experimental immiscible carbon dioxide flooding project [5] which was granted royalty relief since that technology had not been previously used in the Province of Alberta. The same status was also granted to a carbon dioxide miscible flood [6] for the same reason.

The historical development of miscible displacement technology led, in large part, to a premise that high displacement efficiency was achieved for the most part as a result of interfacial tension reduction. The assumed general validity of this premise resulted from an analysis of physical experiments [7] which evaluated the effect of interfacial tension on displacement efficiency in the absence of mass transfer. An indirect consequence was that miscible displacements for multicomponent systems were also assumed to pass through the critical point [8], implying that interfacial tension reduction was the main mechanism to achieve increased oil recoveries.

The historical emphasis on the importance of interfacial tension reduction was further exaggerated by the parallel development of chemical surfactant and polymer technology [9] to enhance oil recovery. Early investigators [10] had used alcohol-water displacement tests to investigate miscible processes, establishing a common fundamental basis for chemical flooding and miscible displacement technologies. The close origins of the two technologies, and the importance of interfacial tension reduction to chemical flooding, further emphasized the perceived

role of interfacial tension reduction in miscible processes. As a practical matter, limitations to experimental procedures and high costs precluded a systematic physical investigation to confirm or disprove this hypothesis. Analytical evaluation was further hampered by the considerable work [11] required to adequately define phase behavior and physical properties in the regions of interest for the miscible displacement process. Other work [12] showed that a kinetic effect existed in miscible displacement respecting the contact time for the solvent to diffuse through rock heterogeneities at the pore throat scale. Significantly, chemical flooding recovered less oil than the solvent in those circumstances, which results were attributed to lower diffusion rates for the chemical agents.

The advent of compositional simulators using an equation of state [13] provided a research tool that could, in principle, be used for a systematic investigation of process mechanisms in miscible displacement. The use of a reservoir simulator to perform numerical model experiments to assess the contribution of the process mechanisms in miscible displacement involved two assumptions; first, that the physics represented by the computational techniques incorporated in the numerical model were adequate to the task, and, second, that the model was used appropriately for the process. These two implicit assumptions were carefully examined and considered in the analysis of results.

A previously described [14] compositional reservoir simulator using the Peng-Robinson equation of state [15] was employed throughout this investigation. The numerical model was calibrated against results reported by Firoozabadi and Aziz [16], who used an earlier version [17] of the compositional reservoir simulator which lacked an adaptive-implicit capability for the mathematical solution of the discretized flow equations. A series of grid refinement experiments were performed to determine the extent of distortion by numerical artifacts. As a result of the grid refinement study, a 100 block model was chosen to be used throughout this investigation. The adequacy of the equation of state to predict phase behavior in the region of interest was also verified in a fashion similar to that reported by Firoozabadi and Aziz [16].

The numerical model experiments performed in this investigation totalled eighty-five (85). Runs 1 to 5 were a series of experiments to assess the effects of grid size upon computed results. Runs 6 to 25 (twenty runs) tested the effects of relative permeability (four curves) and viscosity ratio (five values) upon displacement characteristics. Mass transfer effects were suppressed in Runs 6 to 25 by suspension of equation of state flash calculations. Runs 26 to 85 (sixty runs) tested the effects of relative permeability (four curves), viscosity ratio (five values) and pressure (three values) upon displacement characteristics. These numerical model

experiments, which implicitly assumed an immobile water saturation in a two-phase gas-oil system, are directly applicable to some forty vertical solvent floods in the Province of Alberta. The neglect of capillary forces is warranted since the reservoir rocks are generally carbonates that do not possess a significant water-oil transition zone.

The general approach throughout this investigation was to perform a series of numerical model experiments to permit an assessment of the contribution of each process mechanism to displacement efficiency, as conditions were varied from immiscible to fully miscible. For example, Runs 6 to 25 which were immiscible (flash calculations were suppressed), in addition to defining the relative contribution of viscous forces and phase flow (hereafter referred to as relative permeability, consistent with petroleum industry usage) characteristics on the efficiency of gas-liquid displacements, served as a control population to later numerical model experiments where interphase mass transfer was permitted (flash calculations were active).

CHAPTER II - PHASE BEHAVIOR MODELLING

Phase behavior modelling was performed using a computer program [18] that used the two-parameter Peng-Robinson [15] equation of state, identical to that employed [19] in the compositional reservoir simulator. The phase behavior model applied in this investigation was initially calibrated using a well described [20] ternary system comprised of methane, n-butane, and decane in a fashion similar to that reported by Firoozabadi and Aziz [16]. These three components may also be related to real petroleum reservoir fluids where:

- (1) the methane represents dissolved solution gas;
- (2) the n-butane represents volatile components of intermediate molecular weight; and
- (3) the decane represents the relatively non-volatile heavier ends of higher molecular weight (generally assumed to be hexanes plus).

This choice was based on the fact that a ternary diagram is thermodynamically rigorous for a three-component system. A thermodynamically rigorous approach meant that findings respecting the relationships between phase behavior and displacement characteristics avoided potential complications associated with concerns [21,22] about the validity of pseudocomponent methods (i.e., lumping of several heavier ends

as one component) particularly for the characterization of heavier fractions (e.g., hexanes plus). The calculated and experimental phase envelopes shown in Figure 1 illustrated that an adequate calibration of the phase behavior model used in this investigation was achieved (please observe that the differences between the calculated and the experimental values are exaggerated as a result of the expanded scale). Phase envelopes at the pressures of 14500, 19000 and 20500 kPa specified in the numerical model experiments are shown in Figure 2.

The phase behavior model calibrated in this investigation had some limitations that are intrinsic to all commonly used equations of state similar in concept to that developed by Peng and Robinson [15]. These limitations did not affect the general conclusions of this investigation but do have some bearing in an instance where a precise match of predicted results to a physical experiment was desired. The two-parameter Peng-Robinson equation of state has an attraction parameter and a repulsion parameter that represents the effective molecular volume. However, experience has shown that the repulsion parameter in the Peng-Robinson equation of state does not adequately represent repulsive forces for complex hydrocarbon mixtures. Also, the Peng-Robinson equation of state lacks a means to predict phase viscosities. Wu [23], as well as Jhaveri and Youngren [24], have demonstrated the practical necessity of applying a third parameter to improve liquid density

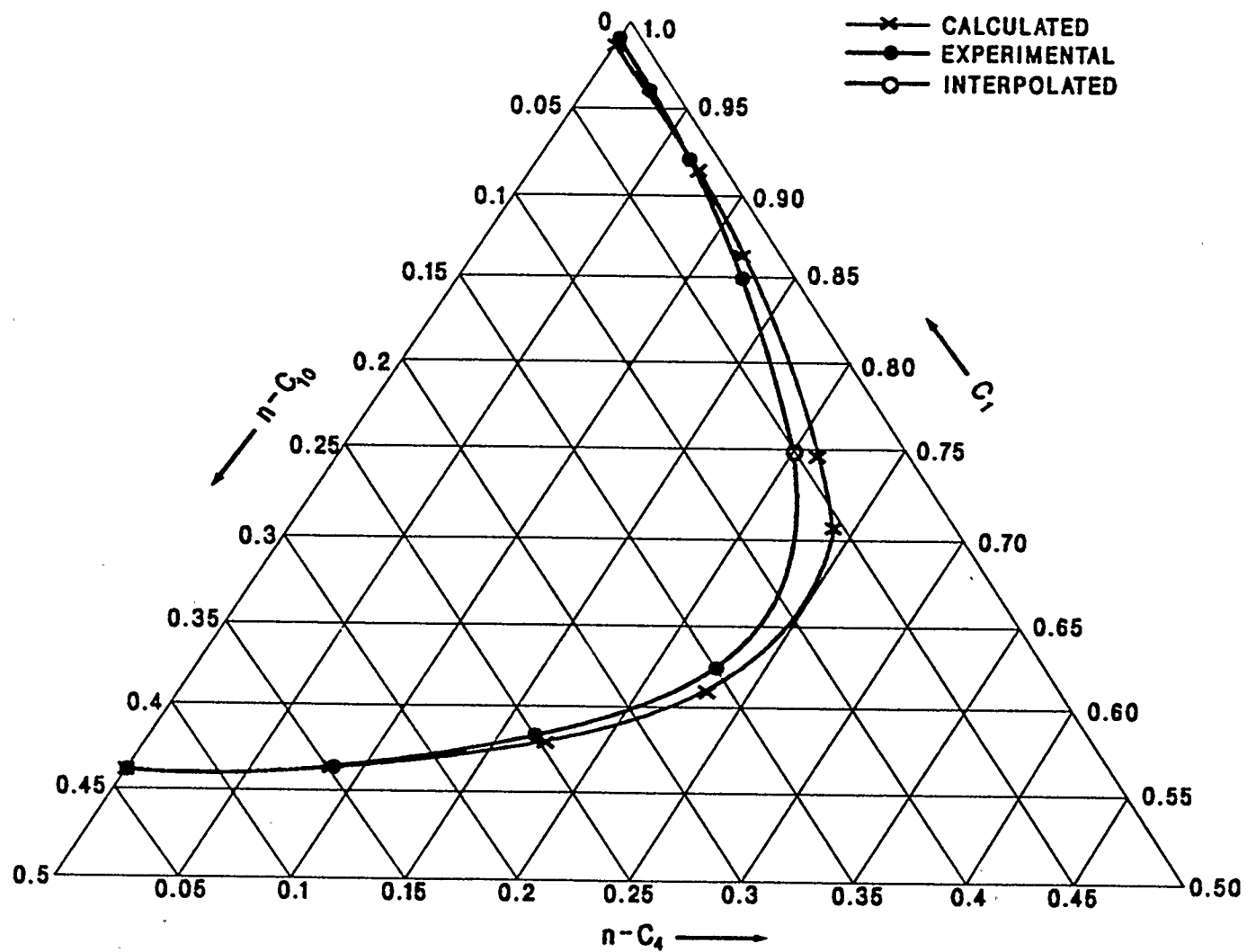


Fig. 1 Comparison of the calculated and experimental phase behavior at 20,684 kPa and 71.1°C

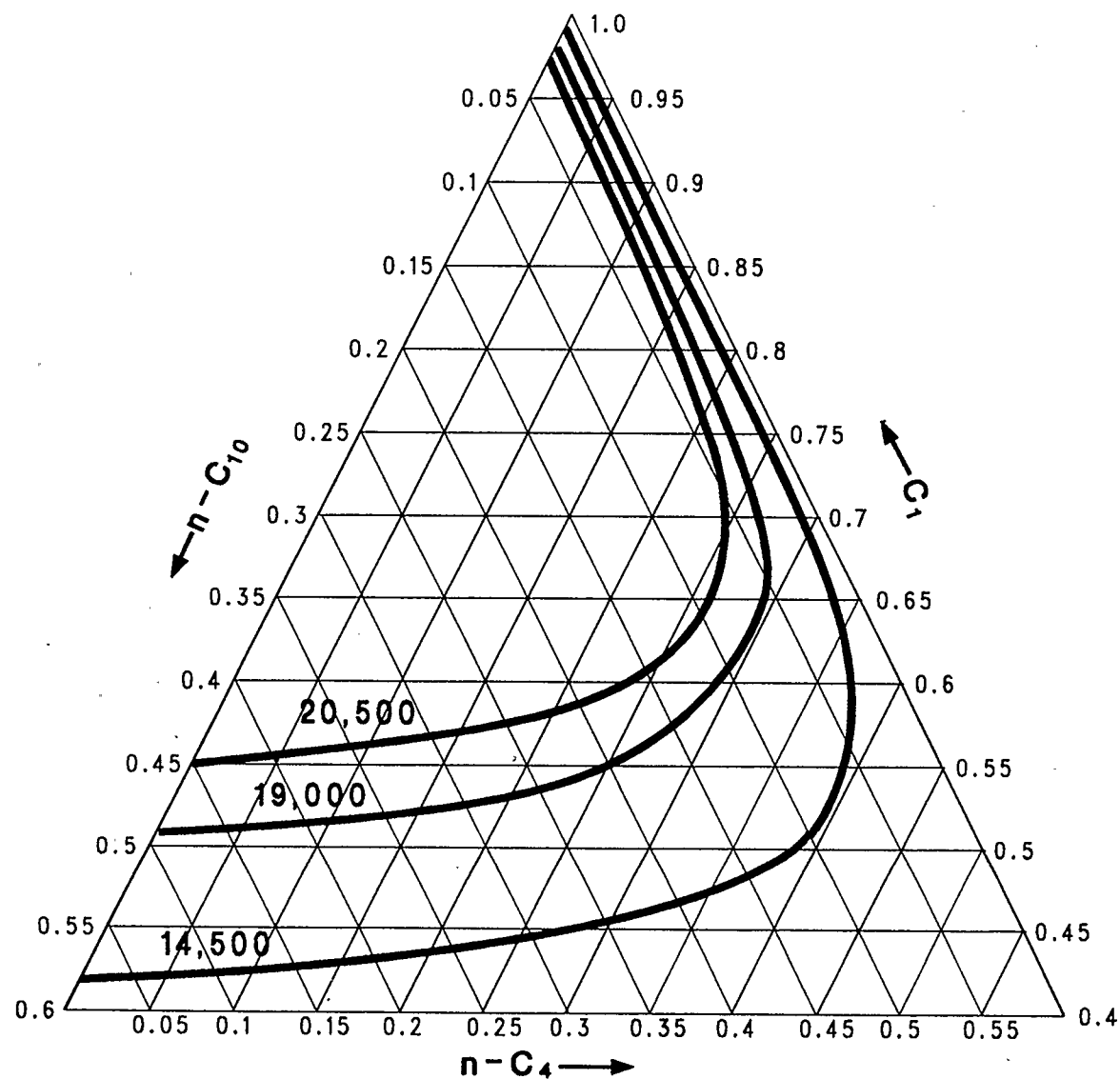


FIG. 2 Comparison of calculated phase behavior at 71.1°C for pressures of 14,500, 19,000 and 20,000 kPa

predictions. Their approach was to use the empirical correction developed by Peneloux et al [25], which does not affect vapor/liquid equilibria calculations made by the unmodified two-parameter equation of state. That correction was not used in this parametric investigation of gas-liquid displacements since the objective was to develop general conclusions regarding the relationship between phase behavior and displacement characteristics. Viscosities were calculated using a correlation [18] reported by Reid, Prausnitz and Sherwood [26] which was assumed to provide satisfactory results. However, some caution was in order when these numerical model experiments were directly compared to physical displacement tests.

Five fluid systems, with the compositions and the (calculated) physical properties shown on Tables 1 and 2, respectively, were selected for use in the numerical model experiments. System A:M was chosen to permit baseline comparisons with the results published by Firoozabadi and Aziz [16]. System B:M was chosen as a control to assist identification of the role of mass transfer in gas-liquid displacements. Systems C:E and D:F, which are equilibrium gas-liquid systems at 19000 kPa, were chosen as controls to assist identification of the role of the relative permeability curve in gas-liquid displacements (and to facilitate correlation with the results of the immiscible Runs 6 to 25 where flash calculations were suppressed). System A:Q, which is a first-contact miscible displacement at 19000 kPa, was

TABLE 1
Composition of Gas-Liquid Systems

| <u>Fluid</u> | <u>Phase</u> | <u>Mole Fraction</u> | | |
|--------------|--------------|----------------------|-----------------|-----------------|
| | | <u>Methane</u> | <u>N-butane</u> | <u>N-Decane</u> |
| A | liquid | 0.00000 | 0.64000 | 0.36000 |
| B | liquid | 0.00000 | 0.00000 | 1.00000 |
| C | liquid | 0.51872 | 0.00000 | 0.48128 |
| D | liquid | 0.60657 | 0.28210 | 0.11133 |
| E | gas | 0.99170 | 0.00000 | 0.00830 |
| F | gas | 0.82136 | 0.16115 | 0.01749 |
| M | gas | 1.00000 | 0.00000 | 0.00000 |
| Q | gas | 0.81350 | 0.18650 | 0.00000 |

Table 2

Physical Properties of Gas-Liquid Systems
At 19000 kPa and 71° C

| Displaced liquid Phase | Displacing gas Phase | μ_L | μ_g | ρ_L | ρ_g | μ_L/μ_g | ν_L x1000 | ν_g x1000 | ν_L/ν_g |
|------------------------------|----------------------------|---------|---------|----------|----------|---------------|------------------|------------------|---------------|
| A | M | .24790 | .01795 | 636.0 | 228.5 | 13.81 | 0.3898 | 0.0786 | 4.96 |
| B | M | .29620 | .01795 | 667.9 | 228.5 | 16.50 | 0.4435 | 0.0786 | 5.64 |
| C | E | .15670 | .01850 | 569.5 | 119.7 | 8.47 | 0.2752 | 0.1546 | 1.78 |
| D | F | .06126 | .02670 | 424.3 | 129.8 | 2.29 | 0.1444 | 0.2057 | 0.702 |
| A | Q | .24790 | .02523 | 636.0 | 214.2 | 9.83 | 0.3898 | 0.1178 | 3.31 |

μ - viscosity, cp

ρ - density, kg/m³

$\nu = \mu/\rho$ - kinematic viscosity, cSt

chosen to complete the range of displacements investigated (from immiscible to fully miscible).

These five systems, as shown in Table 2, also permitted investigation of a wide range of viscosity ratios, including that for kinematic viscosity. Prats [27] observed that "over the years, the use of mobility ratio became so entrenched as being the number that determined the stability of a displacement process" (as indeed it is for processes not characterized by condensation phenomena) "that we lost sight of the fact that it is the value of the pressure gradient ratio that controls the behavior of the displacement front".. Prats then developed an equivalent mobility ratio for steam drives largely based upon the ratio of the kinematic viscosities. An objective of this investigation was to determine if that observation, in principle, also applied to isothermal gas-liquid displacements. That objective was considered appropriate for this investigation since the influence of the ratio of kinematic viscosities on the stability of displacements were easily identified given a horizontal linear one-dimensional system which eliminated potential gravity segregation of the gas and liquid phases.

CHAPTER III - INVESTIGATION OF NUMERICAL GRID REFINEMENT

Numerical grid refinement experiments were performed to assess the effect of grid refinement upon computed results. Aziz and Settari [28] stated "that whenever possible, the necessary grid definition should be determined by a grid sensitivity study. Such a study amounts to performing a series of simulation runs with increasing grid definition until the computed results do not change within the accuracy required." The fundamental reason for the empirical investigation proposed by Aziz and Settari [28] was that the nonlinearities associated with the governing partial differential equations do not provide a mathematical basis to estimate the grid definition required. Technical judgement, similar to the technique of an experimentalist, based on experience, with an understanding of both the physical systems and the formulation method used, is required [29,30]. Details respecting the numerical model used in this investigation are provided in Appendix A.

Past experience published by Firoozabadi and Aziz [16] in which they used 80 grid blocks, was chosen for the initial calibration of the numerical model in Run 1. Emanuel et al [31] in their equilibrium cell model cited 100 to 250 cells as typically being used to simulate a slim tube displacement test; however, they did not provide any assessment of the sensitivity of computed results to the number of equilibrium cells. On that basis, Runs

2 and 3 were performed using 100 and 200 grid blocks, respectively. Additionally, to ensure that "overkill" was avoided, Runs 4 and 5 were performed using 50 and 25 grid blocks, respectively. Model parameters and dimensions used are shown on Table 3.

This investigation of numerical grid refinement yielded unexpected findings, insofar as the results did not converge to a common physical solution. The decane concentration curves for Runs 1 to 5 are presented in Figures 3 to 7. The dimensionless decane concentration and liquid saturation curves, at 0.4 pore volumes gas injection are shown in Figures 8 and 9, and the results at 0.7 pore volumes gas injection are shown in Figures 10 and 11. Interestingly, the lack of convergence to a common physical solution was less marked for the liquid saturation profiles compared to the decane concentration profiles.

The greater, and consistent, disagreement between the concentration profiles, compared with the liquid saturation profiles, suggested that a subtle process was being demonstrated in Runs 1 to 5, versus a purely numerical artifact introduced, for example, by the finite difference technique. It is well known to experimentalists that the solubility of heavier components in a gas may be measured by performing flow experiments [32]. Dry gas is flowed through a packed column containing a heavy residual liquid with the effluent gas chilled to recover evaporated liquids that might not be accurately

Table 3
Model Parameters

| | |
|--|--------------------|
| Grid Blocks: | 100 in x-direction |
| Grid Dimensions | |
| - x-direction: | 0.03 metres |
| - Y & Z: | 0.01 metres |
| Porosity: | 30% |
| Permeability: | 2.5 darcies |
| Injection rate: | |
| - compositional simulator | 0.00009157 RM3/Day |
| Separator Conditions (compositional model) | |
| - 1756, 708, 101.325 kPa | |
| - 32.2, 26.7, 15.0° C | |

Note: Grid dimensions were adjusted appropriately to achieve a total length of 3.0 metres when other than 100 grid blocks were employed.

FIGURE 3

Overall C10 Concentration Profile

INITIAL CALIBRATION RUN - RUN 1

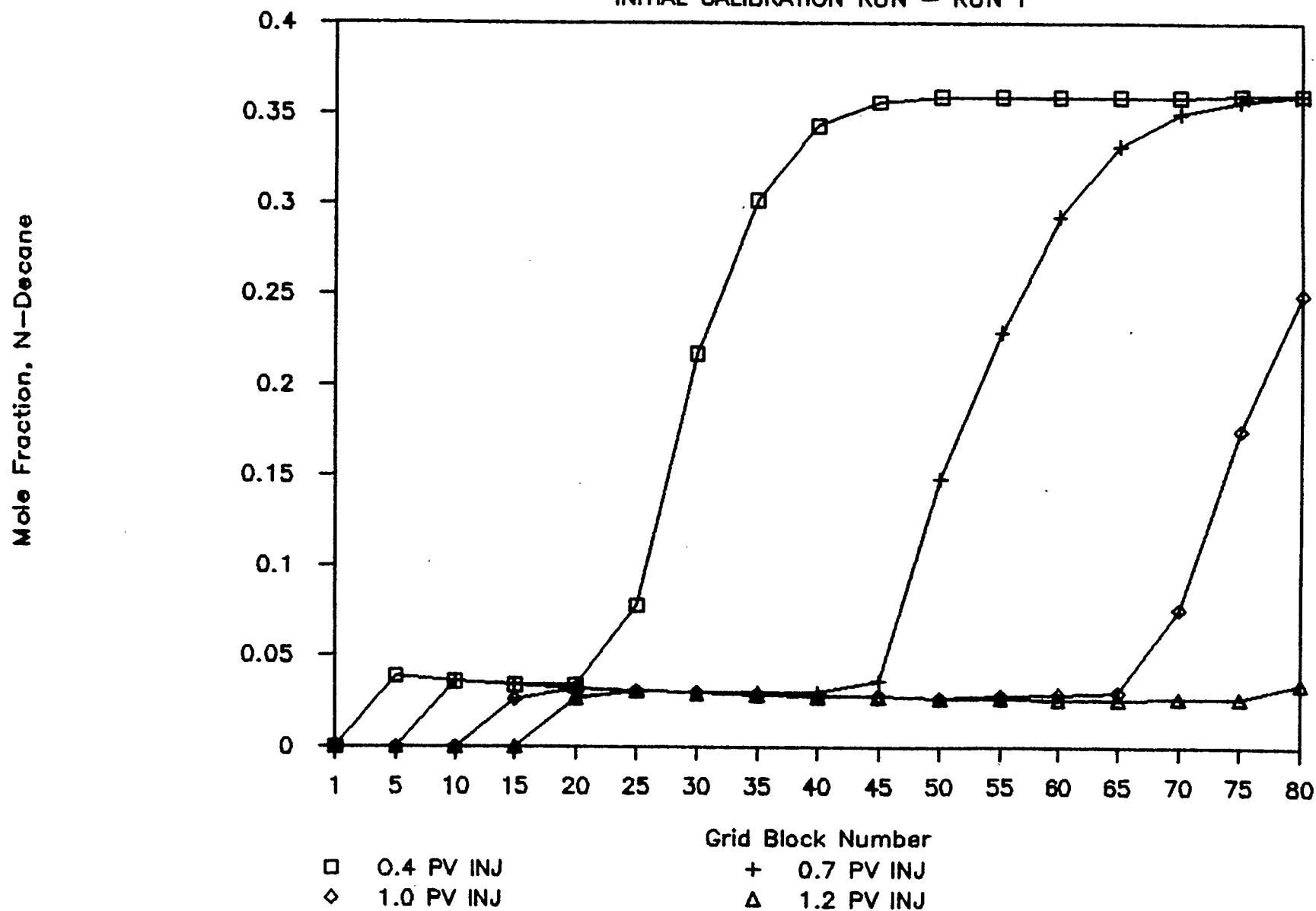


FIGURE 4

Overall C10 Concentration Profile

BASE CASE RUN - RUN 2

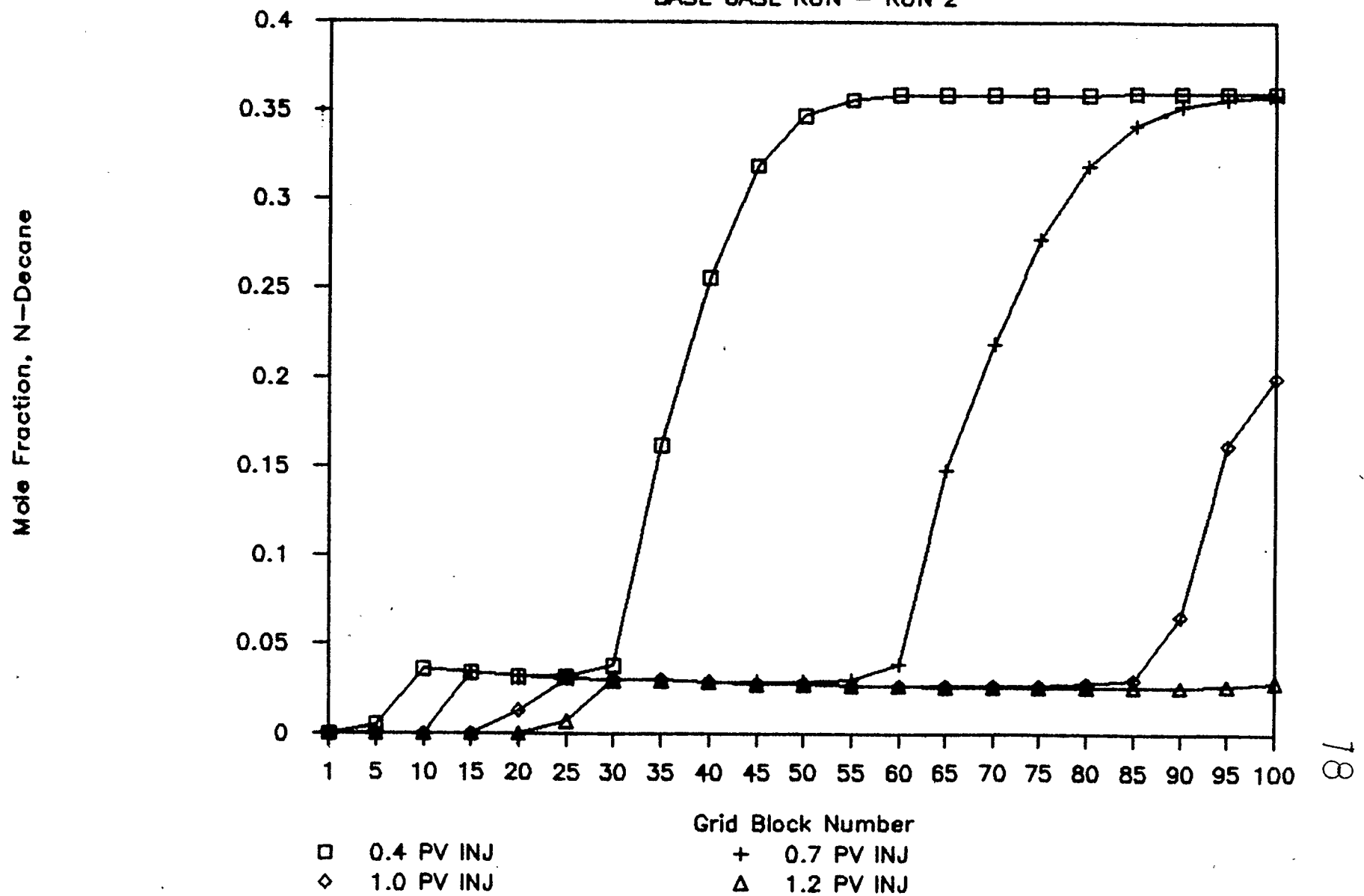


FIGURE 5

Overall C10 Concentration Profile

FINE GRID SENSITIVITY RUN - RUN 3

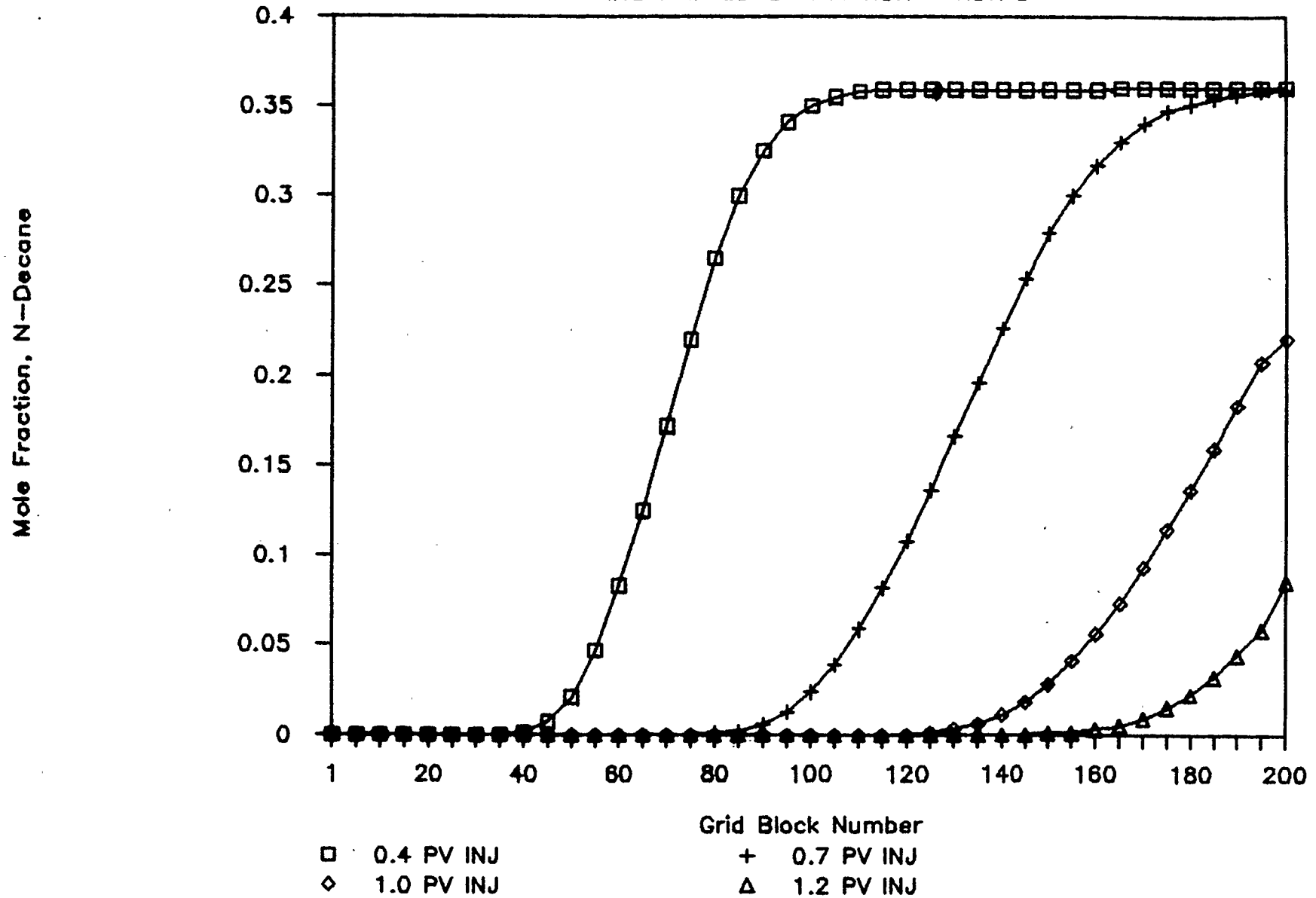


FIGURE 6

Overall C10 Concentration Profile

COARSE GRID SENSITIVITY RUN - RUN 4

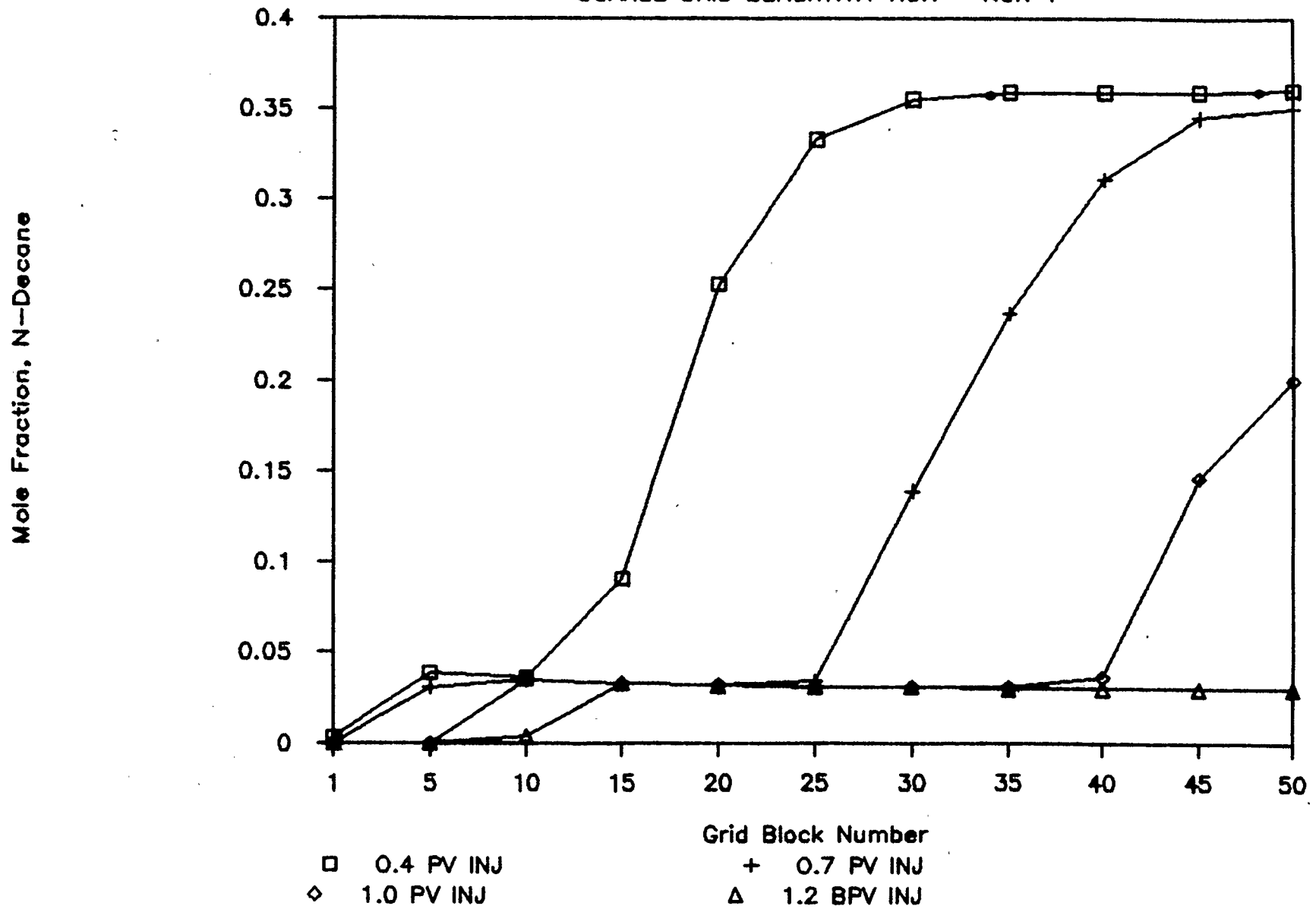


FIGURE 7

Overall C10 Concentration Profile

COARSE GRID SENSITIVITY RUN - RUN 5

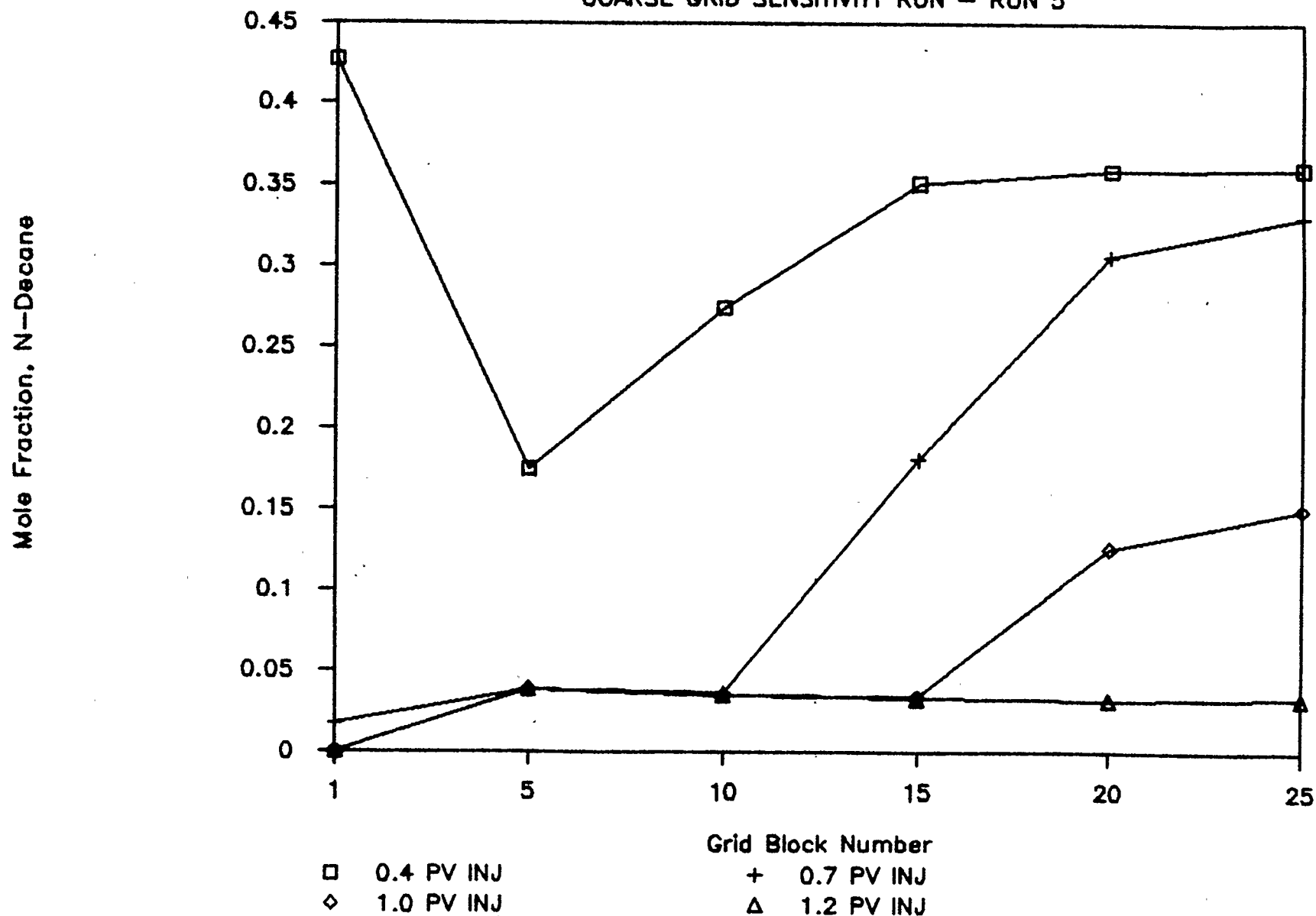


FIGURE 8

Dimensionless C10 Concentration Profile

0.4 PV INJ - RP Original

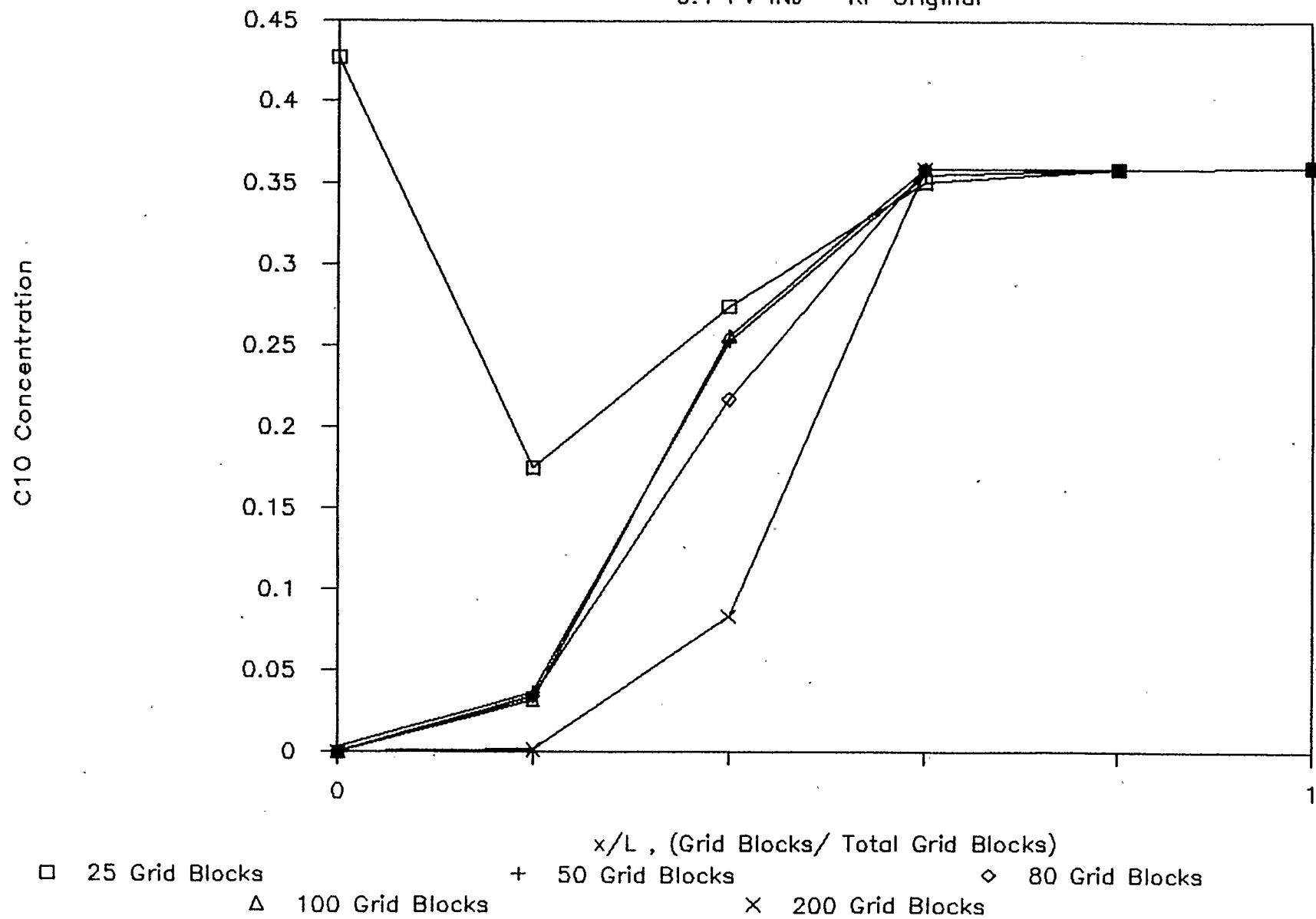


FIGURE 9

Dimensionless Liquid Saturation

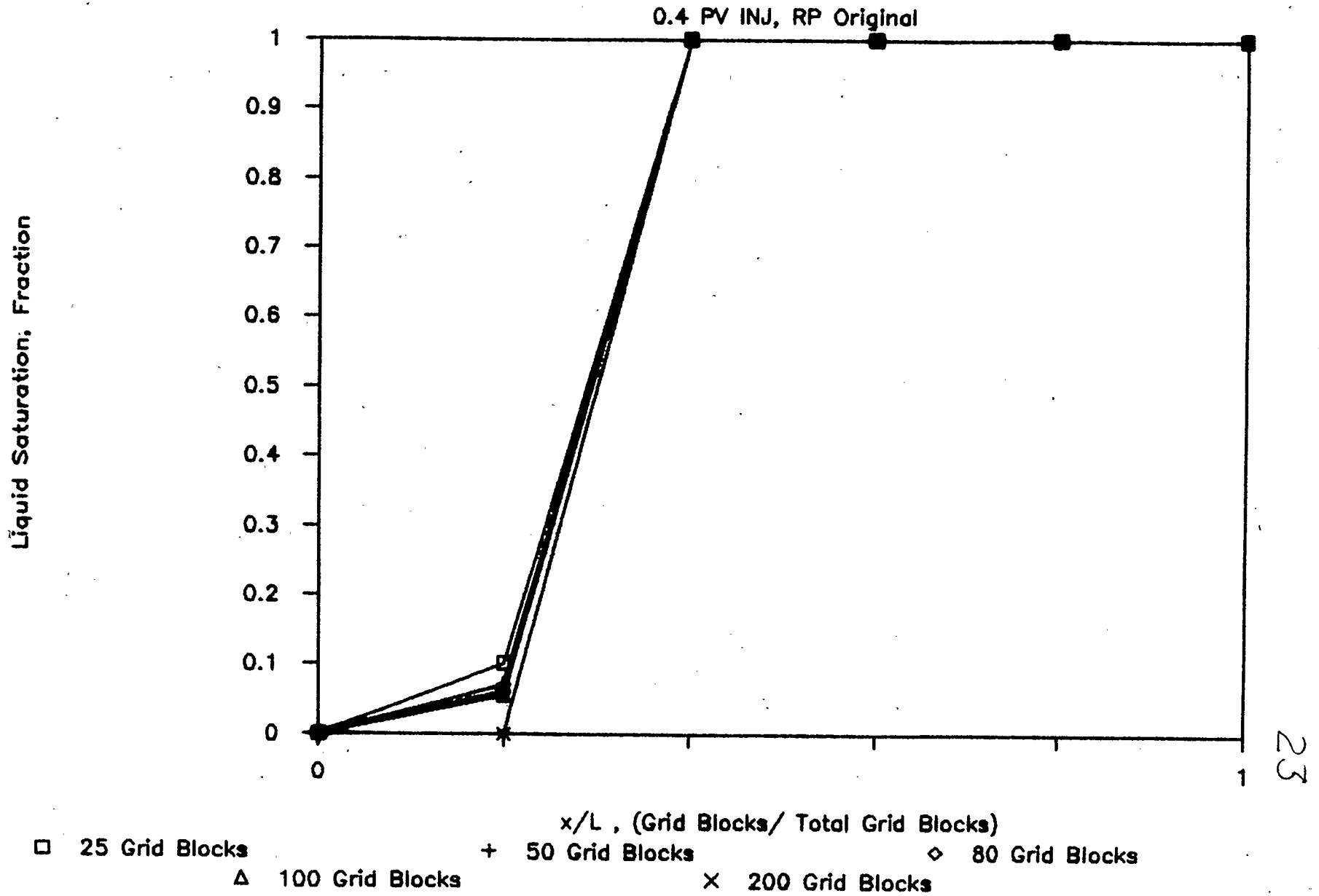


FIGURE 10

Dimensionless C10 Concentration Profile

0.7 PV INJ - RP Original

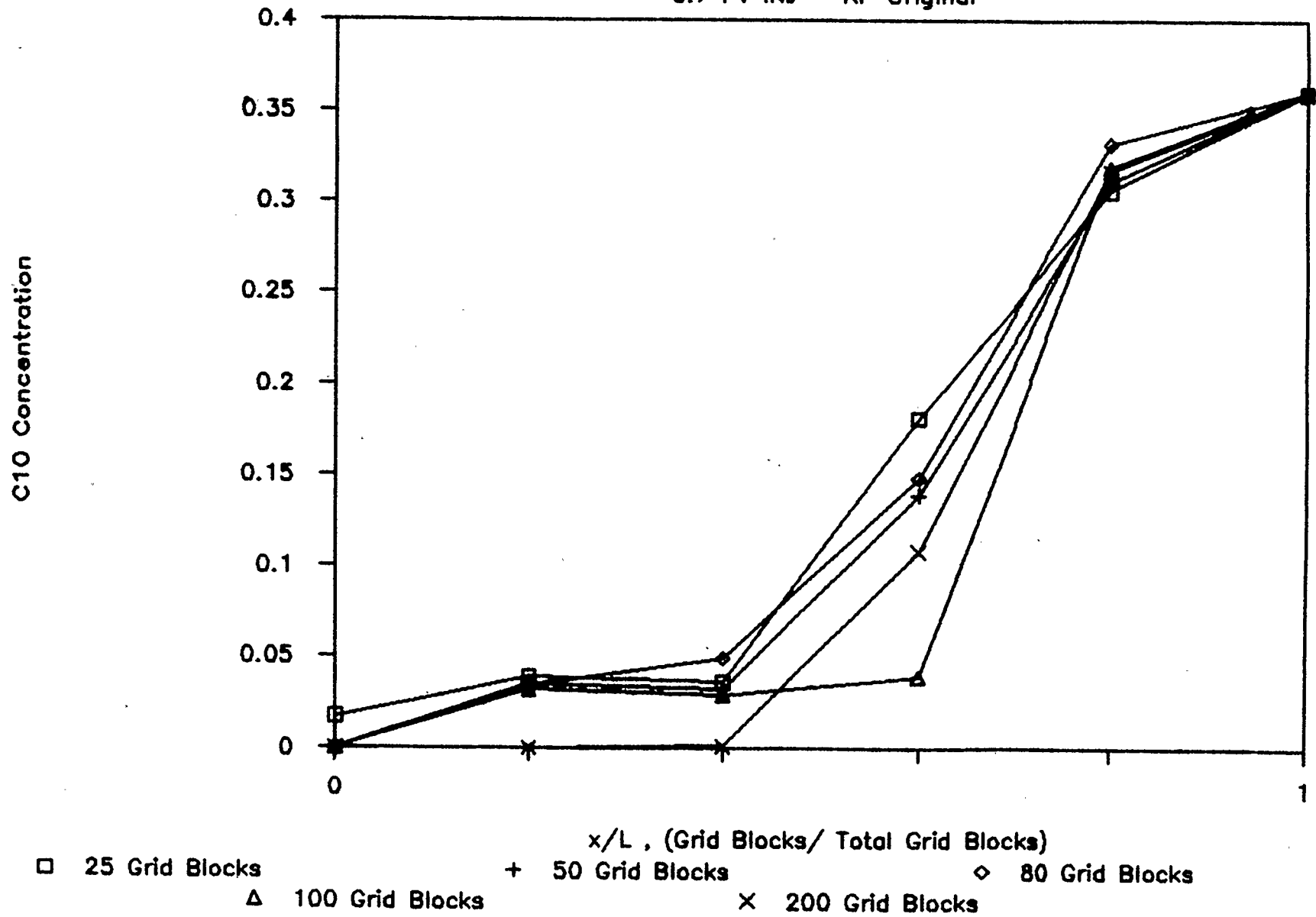
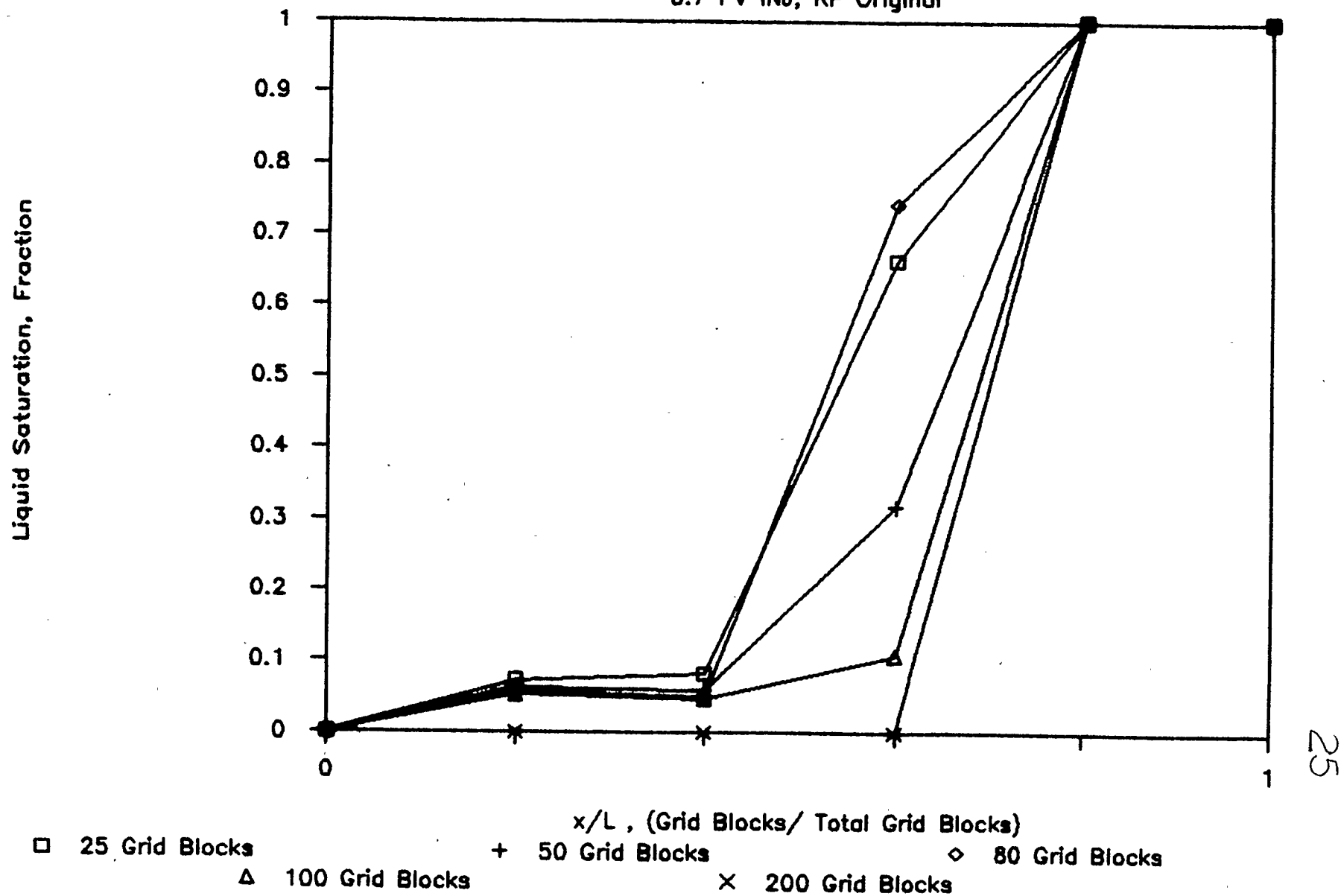


FIGURE 11

Dimensionless Liquid Saturation

0.7 PV INJ, RP Original



measured with a gas chromatograph. Given that there does exist a small pressure gradient across the simulated slim tube, the gas that flows from grid block to grid block will not be in exact equilibrium with the residual liquid. As well, normal oscillations in the mathematical solution of the phase behavior equations may even be sufficient to introduce a non-equilibrium situation for the low liquid solubilities that do exist. The solution to permit effective use of the numerical model was to either adjust the grid block size to limit the influence of this subtle process, which is partially numerical in origin, or to manually override the vapor-liquid equilibria calculations (e.g., calculated K-values). The former solution was used in this work to limit the consequences of small inaccuracies in the phase behavior calculations coupled with the grid block size effect.

Previous researchers did not examine non-equilibrium effects in detail since it is difficult to distinguish between:

- (1) pore scale transport phenomena;
- (2) dispersion caused by one or more of;
 - (i) convective mixing resulting from variations in pore velocities (at one extreme, this may even include viscous fingering or gravity override effects in a "lumped" convective dispersion coefficient);

(ii) molecular diffusion; or

(iii) natural convection (e.g., a natural thermosiphon in the reservoir rock); and

(3) phase behavior effects assuming either;

(i) instantaneous thermodynamic equilibrium; or

(ii) a kinetic effect caused by either by (a) mass transfer rate limitations at an interface, or (b) a contact time effect caused by pore scale transport phenomena;

especially given the complex interaction between each process.

A brief review is required to clarify these points prior to a further evaluation of the numerical model experiments performed to assess the effects of grid size upon computed results.

Pore scale transport phenomena have been extensively investigated [33-36] with recent work [37] examining variations to permeability, interfacial tension and viscosity in the use of the capillary number to correlate the mobilization of residual oil. Mass transfer and diffusion processes have also been investigated using pore scale flow models [38], although more work is required before a direct evaluation of the observed kinetic effect can be obtained from mechanistic first principles. Ypma and Gardner [39] documented this kinetic effect, which they termed residence time, for the residual oil

saturation in linear displacements through reservoir rock samples versus the packed sand used in slim tubes. Coats and Smith [40] developed a differential capacitance model to account for observed experimental results which could not be well matched with a standard diffusion model, postulating a stagnant volume. More recent work [41-43] and the results of a field test [44] which was designed using the Coats-Smith capacitance model have validated this approach. However, the Coats-Smith model assumes that the stagnant reservoir oil in isolated pores contacted by solvent through a diffusion process is miscible upon first contact. Miscible processes that require repeated contacts and mass transfer between the displaced liquid and displacing gas can only be evaluated using the Coats-Smith technique by lumping phase behavior effects and the kinetic or non-equilibrium component of interphase mass transfer into an effective dispersion coefficient which is assumed to remain constant over time. This approach, which would result in a larger solvent volume being required since the dispersion coefficient is higher, has, in fact, been applied in a modified fashion for a large-scale field test [45]. Another pore scale process that may be significant in some instances [46] is the surface film drainage of oil at low saturations at mixed wettability conditions given a favorable ratio of viscous to gravity forces (e.g., low oil viscosities and high vertical relief). In summary, pore scale transport phenomena will not influence grid size selection for the simulation of slim tube

displacement tests since the pore structure of the packed sand and the narrow diameter allow kinetic or residence time effects to be neglected.

Dispersion on the microscopic scale consists primarily of convective mixing and diffusion [47] which can be calculated and used to determine concentration profiles in a permeable, porous medium [48]. Methods have been developed to measure diffusion in a permeable, porous medium [49]. For slim tube displacement tests, it has been reported [50] that contact times for diffusion to occur correspond to flooding rates of approximately 0.6 to 6 metres per hour, which is comparable to actual test rates used in the laboratory. The use of mixing coefficients which included larger scale heterogeneities as well as lumping other effects such as viscous fingering and gravity override, has been applied in a large-scale field test [51]. Natural convection resulting from geothermal gradients (e.g., a thermosiphon effect), especially for fractured formations, has also been reported [52, 53]. In summary, the dispersion that needs to be considered in the simulation of slim tube displacement tests is primarily numerical in origin, which may be evaluated by means of grid refinement experiments.

Phase behavior effects in the simulation of slim tube displacement tests may be assumed to occur instantaneously since the mass transfer rate is not limited by pore structure considerations [39] or a contact time effect [50]. In summary,

it is only necessary to adjust the grid block size to limit the partially numerical artifacts previously discussed respecting evaporation of residual liquid behind the displacement front.

The selection of the optimum number of grid blocks has been narrowed to a range bounded, by the most generous estimate, at somewhere between 50 and 150 grid blocks. The midrange value of 100 grid blocks, which yielded results comparable to the 80 grid blocks used by Firoozabadi and Aziz [16], was chosen for the remainder of this work.

CHAPTER IV - RELATIVE PERMEABILITY AND VISCOSITY RATIO EFFECTS

Introduction

Numerical model experiments were conducted to investigate the effects of relative permeability and viscosity ratio upon linear gas-liquid displacements isolated from the effects of interphase mass transfer. Five fluid systems as shown on Table 2 were used. Numerical model parameters have been summarized on Table 3. Four relative permeability curves as shown on Table 4 and Figures 12 to 15 were used. Flash calculations in the compositional simulator were suppressed to isolate the mass transfer effects. A constant inlet displacement pressure of 19000 kPa was specified in the simulator.

Table 4
Relative Permeability Curves

| | Sg | Krg | Krog |
|--------------------|------|--------|--------|
| ORIGINAL | 0.0 | 0.0 | 1.0 |
| | 0.39 | 0.0310 | 0.37 |
| | 0.5 | 0.0398 | 0.25 |
| | 0.58 | 0.0439 | 0.175 |
| | 0.7 | 0.0500 | 0.082 |
| | 0.75 | 0.0526 | 0.0526 |
| | 0.9 | 0.0658 | 0.0 |
| | 1.0 | 0.1579 | 0.0 |
| CURVE I - CONCAVE | 0.0 | 0.0 | 1.0 |
| | 0.39 | 0.0310 | 0.25 |
| | 0.5 | 0.0398 | 0.12 |
| | 0.58 | 0.0439 | 0.0526 |
| | 0.7 | 0.0500 | 0.0 |
| | 0.75 | 0.0526 | 0.0 |
| | 0.9 | 0.0658 | 0.0 |
| | 1.0 | 0.1579 | 0.0 |
| CURVE II - CONVEX | 0.0 | 0.0 | 0.0 |
| | 0.39 | 0.0310 | 0.57 |
| | 0.5 | 0.0398 | 0.42 |
| | 0.58 | 0.0439 | 0.27 |
| | 0.7 | 0.0500 | 0.0 |
| | 0.75 | 0.0526 | 0.0 |
| | 0.9 | 0.0658 | 0.0 |
| | 1.0 | 0.1579 | 0.0 |
| CURVE III - LINEAR | 0.0 | 0.0 | 1.0 |
| | 0.39 | 0.0310 | 0.44 |
| | 0.5 | 0.0398 | 0.29 |
| | 0.58 | 0.0439 | 0.18 |
| | 0.7 | 0.0500 | 0.0 |
| | 0.75 | 0.0526 | 0.0 |
| | 0.9 | 0.0658 | 0.0 |
| | 1.0 | 0.1579 | 0.0 |

Pcog = 0 for all saturations

Figure 12

ORIGINAL OIL RELATIVE PERMEABILITY CURVE

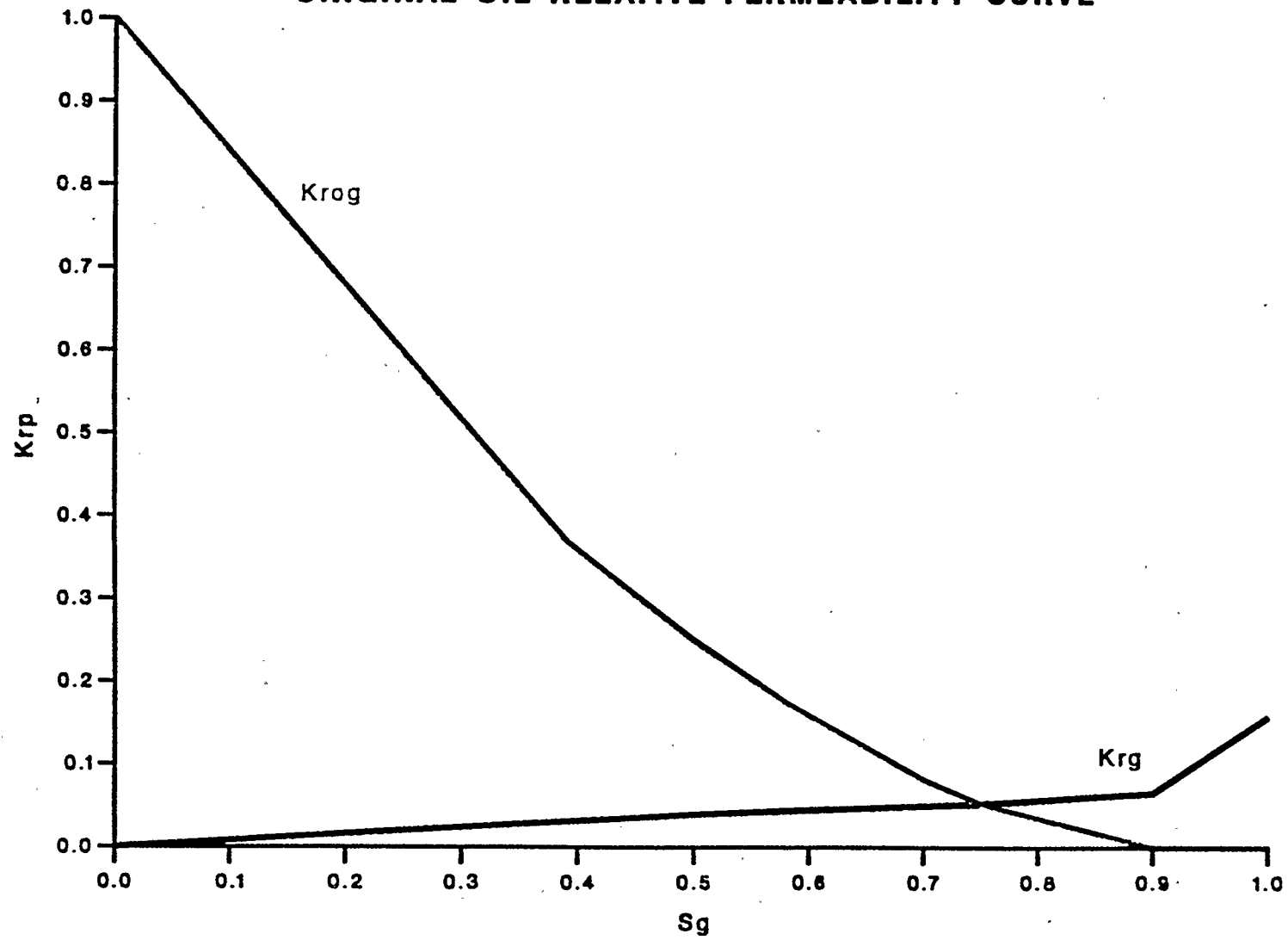


Figure 13

CONCAVE OIL RELATIVE PERMEABILITY CURVE

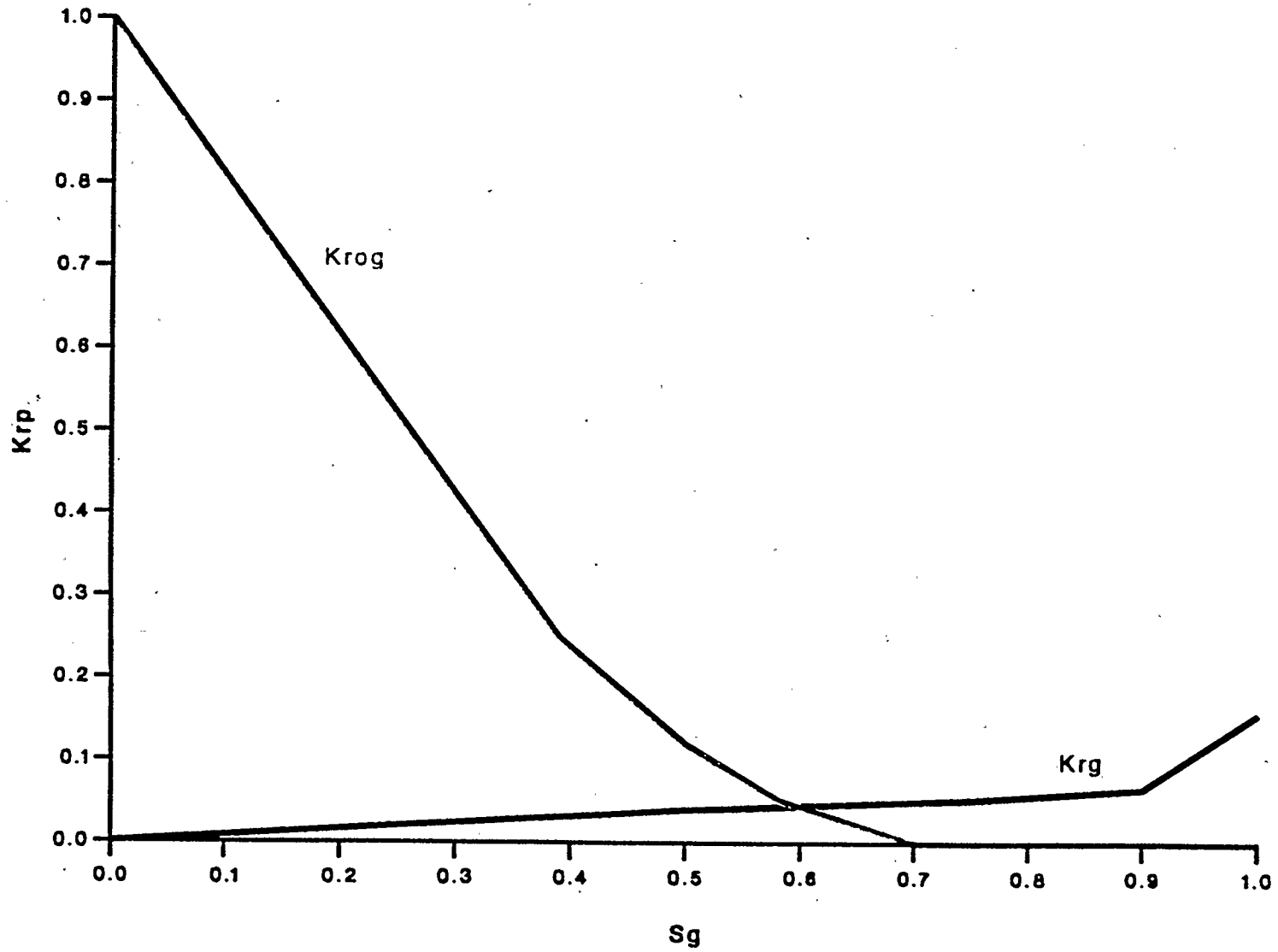


Figure 14

CONVEX OIL RELATIVE PERMEABILITY CURVE

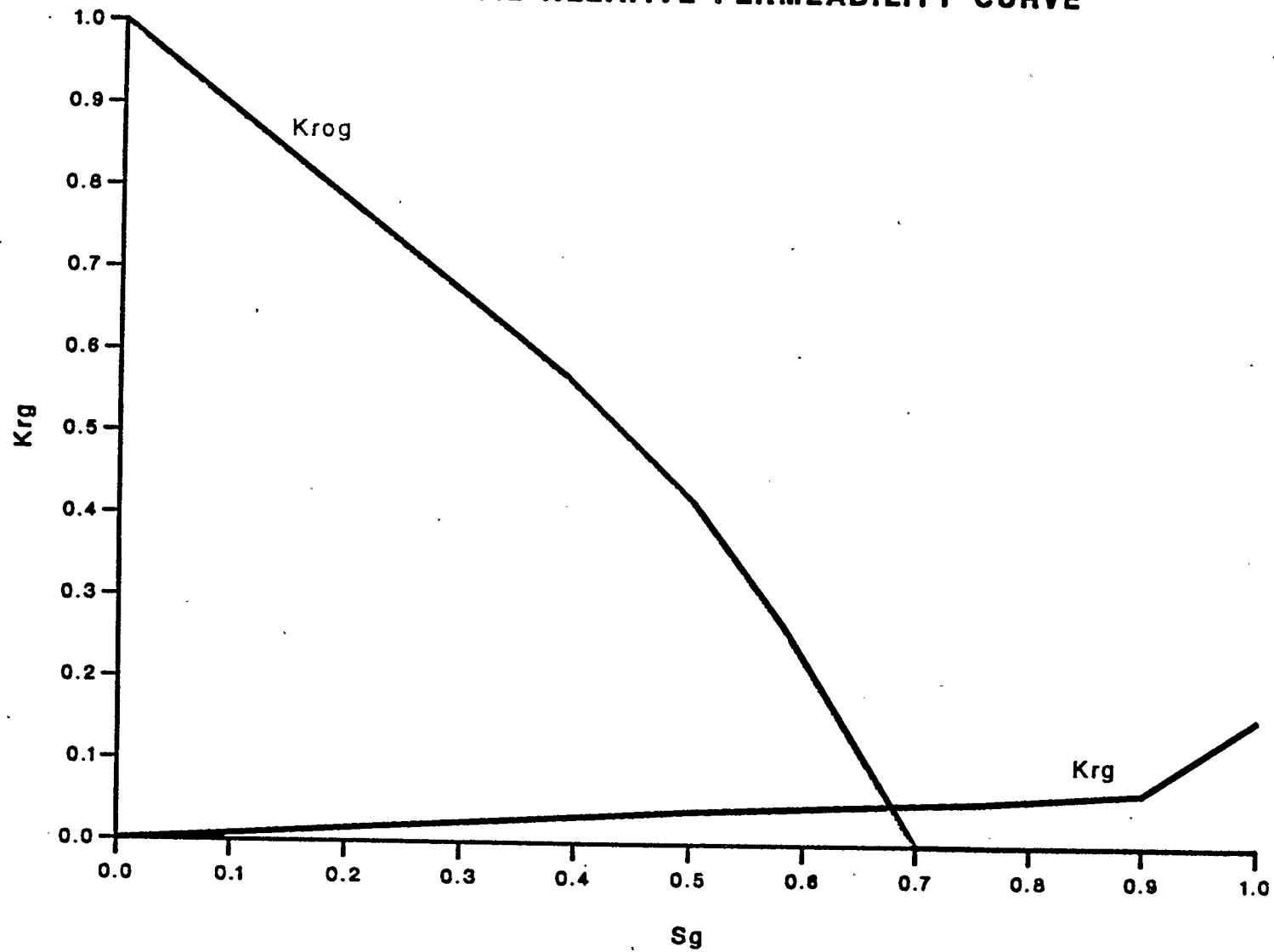
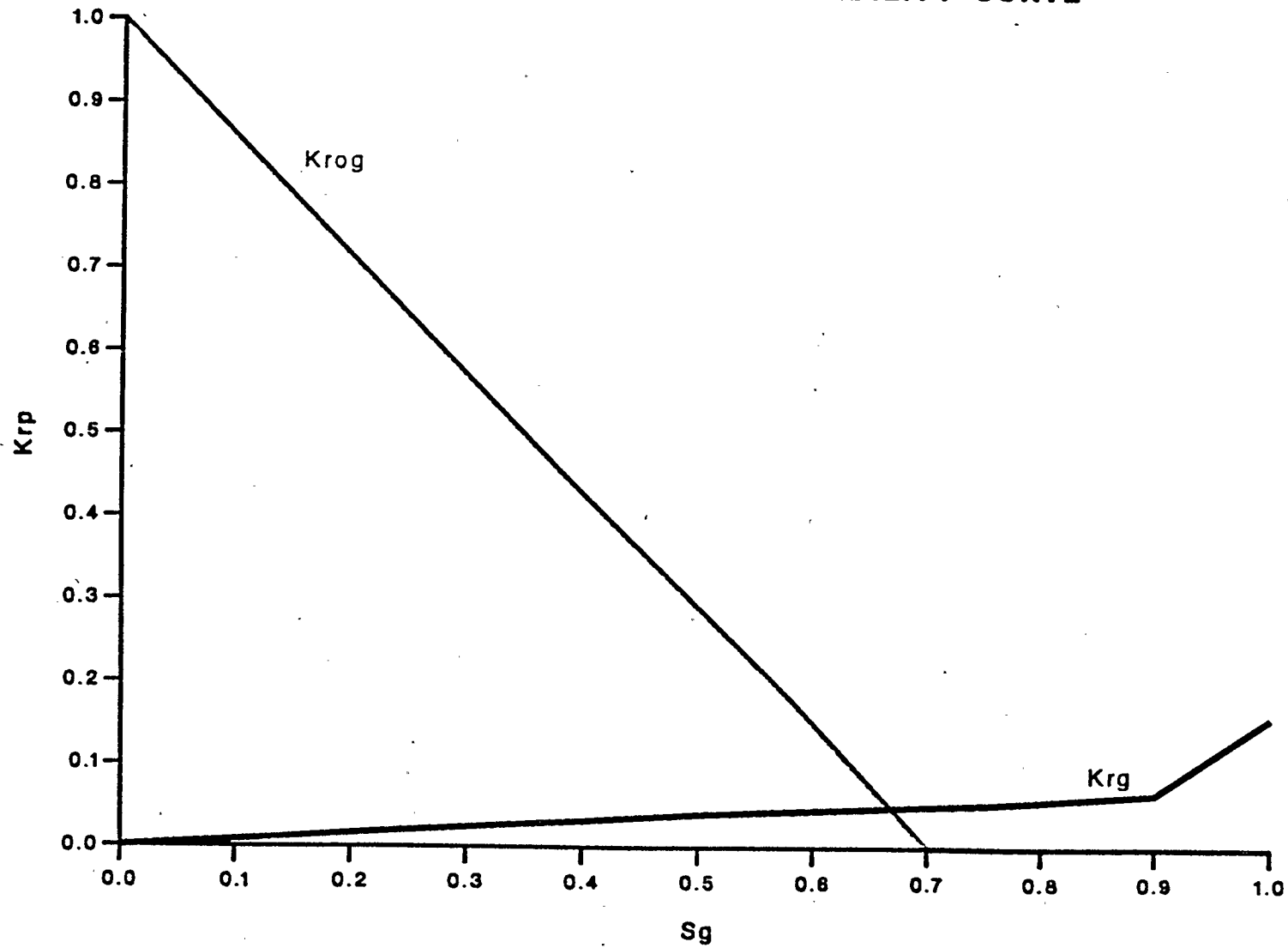


Figure 15

LINEAR OIL RELATIVE PERMEABILITY CURVE



Relative Permeability Relationships

The baseline, or "Original", relative permeability curves, consistent with the results reported by Firoozabadi and Aziz [16], were obtained from Van-Quy et al [54]. The other three sets of relative permeability curves were varied in a systematic fashion by changing the shape of the oil relative permeability curve; as concave Curve I, convex Curve II, and linear Curve III. The critical oil saturation was increased from ten to thirty percent in Curves I, II and III to permit a more convenient comparison to later runs where flash calculations were permitted. The gas relative permeability curve used was the same for each set of oil relative permeability relationships. The water saturation was assumed to be zero for all numerical model experiments.

Fluid Systems

The five fluid systems used in this work were:

(1) System A:M, where liquid A (0.64 n-butane and 0.36 mole fraction n-decane) was displaced by gas M (1.0 mole fraction methane), corresponding to a viscosity ratio of 13.81;

(2) System B:M, where liquid B (1.0 mole fraction n-decane) was displaced by gas M (1.0 mole fraction methane), corresponding to a viscosity ratio of 16.50;

(3) System C:E, an equilibrium gas-liquid system at 19000 kPa, where liquid C (0.51872 methane, and 0.48128 mole fraction n-decane) was displaced by gas E (0.99170 methane and 0.00830 mole fraction n-decane), corresponding to a viscosity ratio of 8.47;

(4) System D:F, an equilibrium gas-liquid system at 19000 kPa, where liquid D (0.60657 methane, 0.28210 n-butane, and 0.11133 mole fraction n-decane) was displaced by gas E (0.82136 methane, 0.16115 n-butane and 0.01749 mole fraction n-decane), corresponding to a viscosity ratio of 2.29; and

(5) System A:Q, a thermodynamic first-contact gas-liquid system at 19000 kPa, where liquid A (0.64 n-butane and 0.36 mole fraction n-decane) was displaced by gas Q (0.8135 methane and 0.1865 mole fraction n-decane), corresponding to a viscosity

ratio of 9.83.

These five fluid systems were selected to cover a wide range, from 2.29 to 16.50, of viscosity ratios (the range for kinematic viscosity ratios was 0.720 to 5.64 as shown on Table 2).

Numerical Model Results

The numerical model results for Runs 6 to 25 have been summarized on Table 5. The results at 0.4 and 0.7 pore volume gas injection shown in Figures 16 and 17, respectively, correlated poorly with the viscosity ratio, which broadly corresponded to the mobility ratio (see Sandrea and Nielsen [55] for a more detailed discussion). These results are consistent with a piston-like displacement process prior to gas breakthrough at the outlet end of the simulated slim tube where the pore volume oil produced is essentially independent of viscosity ratio. These laboratory scale results, however, are contrary to those observed at the field scale for line drive immiscible water-oil displacements [56]. Field scale results have decreased performance efficiencies resulting from a reduced volumetric conformance where the displaced phase is not fully contacted by the displacing phase since gravity segregation often reduces vertical displacement efficiency and viscous instabilities often reduce areal sweep efficiency. The more appropriate comparison is to waterflood (petroleum industry usage for water-oil displacements) displacement tests at the laboratory scale which are less influenced by the factors that reduce volumetric conformance at the field scale [57]. However, waterflood displacement tests are more influenced by viscosity ratio effects since capillary forces are generally stronger than in gas-liquid displacements. Capillary forces in water-oil

Table 5

Numerical Model Results
Flash Calculations Suppressed

| <u>Run No</u> ⁽¹⁾ | <u>Fluid System</u> | <u>Rel. Perm. Curve</u> | <u>PV Oil Produced Vs PV Gas Injected</u> ⁽²⁾ | | | |
|------------------------------|---------------------|-------------------------|--|--------------|--------------|--------------|
| | | | <u>@ 0.4</u> | <u>@ 0.7</u> | <u>@ 1.0</u> | <u>@ 1.2</u> |
| 6 | A:M | OR | 0.341 | 0.610 | 0.885 | 0.890 |
| 7 | A:M | I | 0.347 | 0.617 | 0.678 | 0.678 |
| 8 | A:M | II | 0.347 | 0.617 | 0.678 | 0.678 |
| 9 | A:M | III | 0.347 | 0.619 | 0.678 | 0.678 |
| 10 | A:Q | OR | 0.343 | 0.620 | 0.890 | 0.890 |
| 11 | A:Q | I | 0.359 | 0.637 | 0.722 | 0.722 |
| 12 | A:Q | II | 0.359 | 0.637 | 0.722 | 0.722 |
| 13 | A:Q | III | 0.359 | 0.637 | 0.722 | 0.722 |
| 14 | B:M | OR | 0.293 | 0.534 | 0.788 | 0.890 |
| 15 | B:M | I | 0.289 | 0.534 | 0.699 | 0.699 |
| 16 | B:M | II | 0.289 | 0.534 | 0.699 | 0.699 |
| 17 | B:M | III | 0.289 | 0.534 | 0.699 | 0.699 |
| 18 | C:E | OR | 0.316 | 0.581 | 0.784 | 0.784 |
| 19 | C:E | I | 0.317 | 0.583 | 0.615 | 0.615 |
| 20 | C:E | II | 0.317 | 0.583 | 0.615 | 0.615 |
| 21 | C:E | III | 0.317 | 0.583 | 0.615 | 0.615 |
| 22 | D:F | OR | 0.387 | 0.643 | 0.761 | 0.761 |
| 23 | D:F | I | 0.348 | 0.600 | 0.618 | 0.619 |
| 24 | D:F | II | 0.343 | 0.598 | 0.639 | 0.640 |
| 25 | D:F | III | 0.343 | 0.598 | 0.618 | 0.619 |

(1) Runs 1 to 5 were an investigation of numerical grid refinement.

(2) PV - pore volume (volumes reported are at reservoir conditions).

FIGURE 16

**PORE VOLUME OIL PRODUCED VERSUS
VISCOSITY RATIO AT 0.4 PV GAS INJECTED**

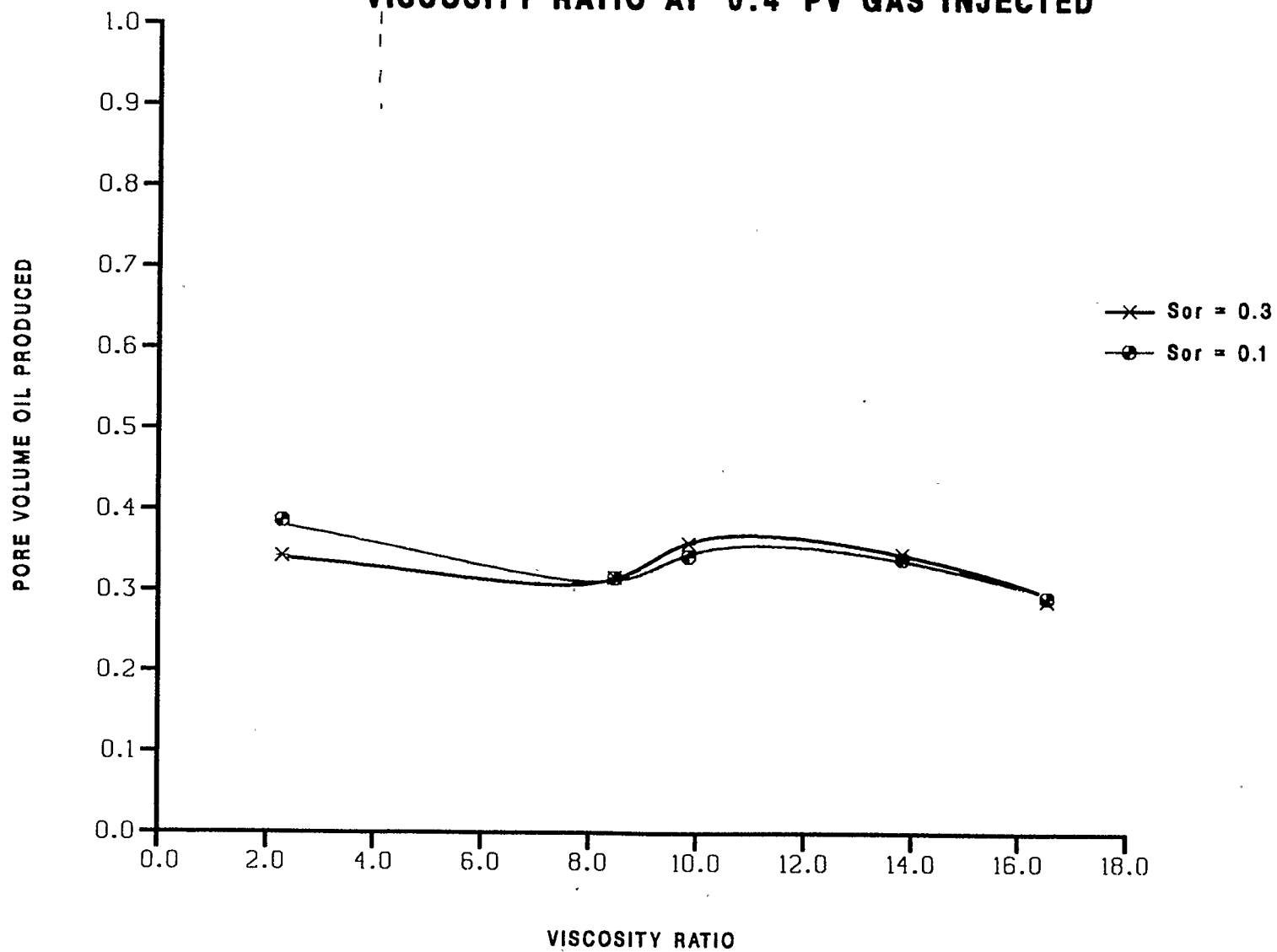
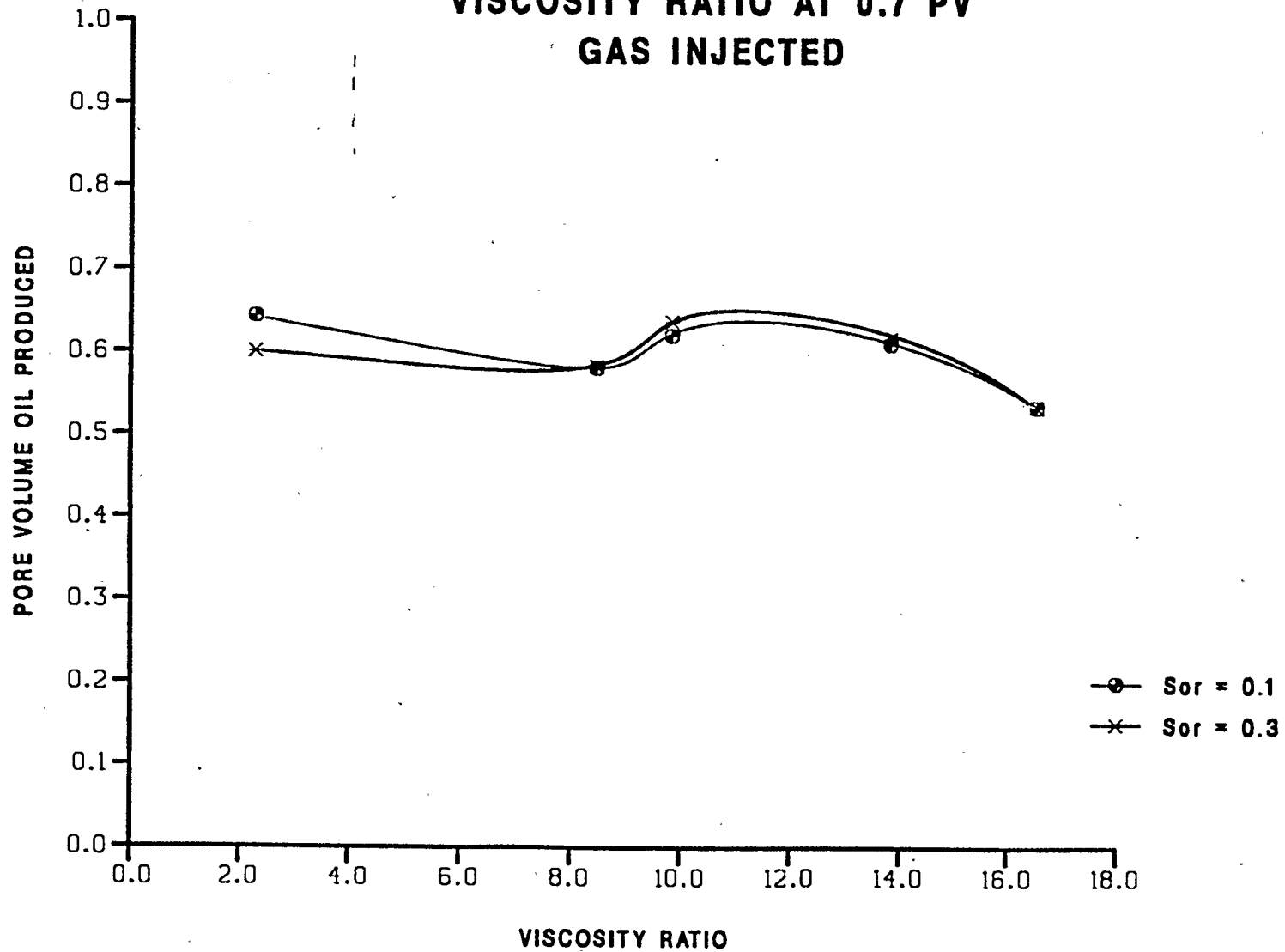


FIGURE 17

**PORE VOLUME OIL PRODUCED VERSUS
VISCOSITY RATIO AT 0.7 PV
GAS INJECTED**



displacements at the laboratory scale strongly affect the influence of viscosity ratio on immiscible displacements [58, 59] and can act to magnify or decrease the sensitivity of results to viscosity ratio depending on wettability [60]. The numerical model experiments performed in this investigation, however, excluded consideration of capillary forces entirely, in order to permit a more convenient comparison of the immiscible and miscible displacements in the numerical model experiments. Examination of the influence of capillary forces and their interaction with other processes was outside the scope of this investigation.

Ultimate recoveries versus both the viscosity ratio and the kinematic viscosity ratio were shown in Figures 18 and 19, respectively. These results were distorted since the simulator found it difficult to distinguish the gas and liquid phases of the equilibrium fluid systems C:E and D:F at the outlet end of the simulated slim tube at high gas-liquid ratios. Consequently, the simulator reported lower ultimate liquid recoveries at the more favorable viscosity ratios of fluid systems C:E and D:F despite the actual reduction of liquid saturations to residual values in the individual grid blocks. The ultimate recoveries were plotted versus kinematic viscosity even though a gravity field was not present in order to verify that anomalous results were not computed by the simulator, which was indeed the case for the non-equilibrium fluid systems. Some

FIGURE 18

TOTAL PORE VOLUME OIL PRODUCED VERSUS VISCOSITY RATIO

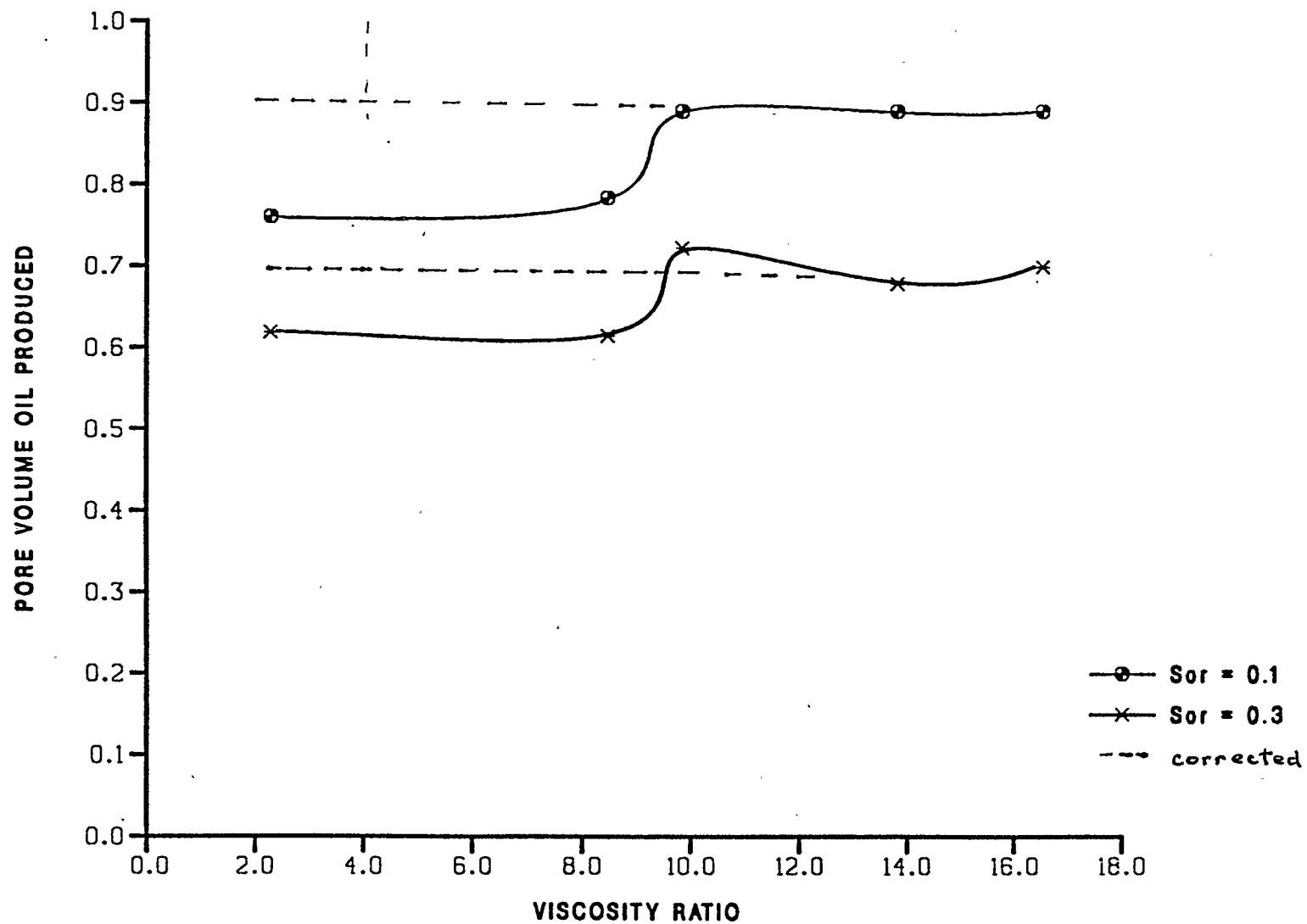
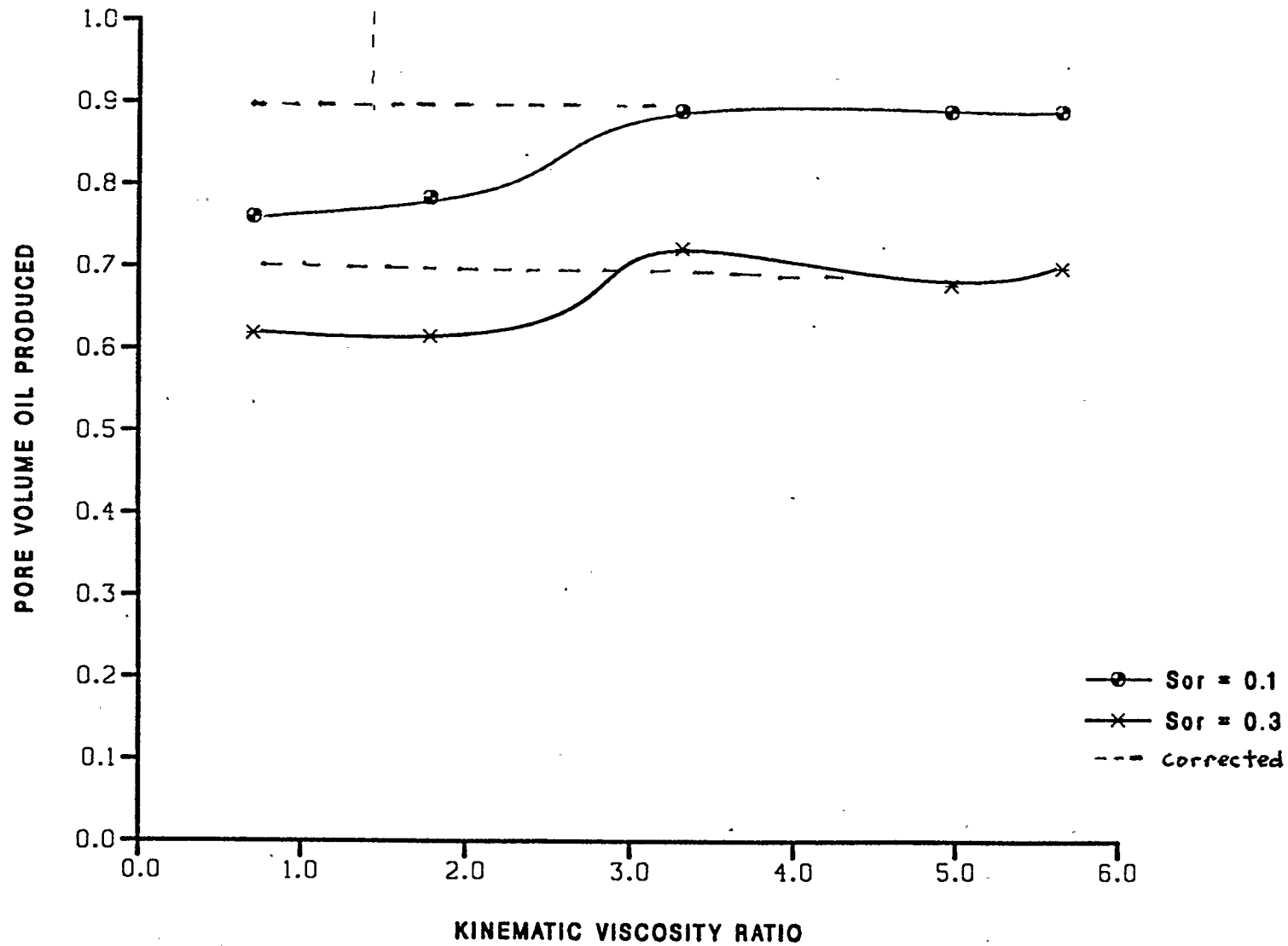


FIGURE 19

**TOTAL PORE VOLUME OIL PRODUCED
VERSUS KINEMATIC VISCOSITY RATIO**



minor discrepancies were also observed for the first-contact miscible fluid system A:Q as shown on Table 5. Liquid recoveries for Runs 11, 12, and 13 slightly exceeded the maximum theoretical value of 70 percent. These results for fluid system A:Q occurred since the simulator did not separate the gas and liquid phases as originally present and permitted solvent condensation into the liquid phase at the outlet end of the simulated slim tube. These observed discrepancies are intrinsic to the use of compositional simulators since, even with flash calculations suppressed, effluent streams can only be distinguished at the outlet by a separator flash calculation. More detailed examination of the influence of viscosity and kinematic viscosity and their interaction with performance characteristics of gas-liquid displacements, as opposed to unit displacement efficiency, was outside the scope of this investigation.

- - - -

CHAPTER V - INVESTIGATION OF MASS TRANSFER EFFECTS

Introduction

Sixty numerical model experiments to investigate the effects of mass transfer upon linear gas-liquid displacement in a permeable, porous medium were performed. Five fluid systems, four relative permeability curves, and three displacement pressures (14500, 19000 and 20500 kPa) were used. This work will directly investigate questions posed by Stalkup [61], in an authoritative monograph on miscible displacement, on the benefits of richer solvents from the fundamental standpoint of phase behavior and miscibility, and the interaction with unit displacement efficiency.

- - - -

Literature Review

Stalkup [62], in a recent work, has examined the influence of dispersion on predicted recovery in simulated slim tube displacement tests. He observed an apparent correlation with the Peclet number ($Pe=Lv/K$, where L =system length, v =interstitial velocity, and K =dispersion coefficient). Stalkup [62] also observed a residual liquid saturation "contrary to traditional concepts about the nature of the miscible displacement process". Later work by Stalkup [63] examined the combined effects of miscible gas enrichment and dispersion upon oil recovery efficiencies predicted by numerical reservoir simulators, arriving at an interpretation that the increase in recovery between dynamic (multicontact) and first-contact (fully-developed) miscibility was both modest and uncertain. This investigation has extended that work to include a systematic examination of mass transfer effects, which allowed a somewhat different interpretation respecting dispersion and mass transfer that was based on a mechanistic hypothesis, where the observed effects may, in large part, be attributed to a number of near-equilibrium contacts between the displacing gas and the displaced liquid causing evaporation of the residual liquid behind the displacement front.

Mansoori and Gupta [64] and Lee et al [65] both performed numerical model compositional simulations of slim tube

displacement tests. Mansoori and Gupta [64] reached the conclusion that solvents required for thermodynamic miscibility could be richer than those required to achieve the high displacement efficiencies encountered in miscible processes. Mansoori and Gupta [64] ascribed observed differences as due to:

- (1) a more complex condensing/vaporizing gas drive process (first simulated by Zick [66]); and
- (2) the influence of dispersion, with the displacement tests and thermodynamic tests providing comparable results at zero dispersion.

Lee et al [65] reached the conclusion that thermodynamic equation of state calculations predicted richer solvents as being required than that observed as necessary in slim tube displacement tests. Lee et al [65] described the displacement process in a linear system as being more complex than previously thought, including up to three mass transfer mechanisms:

- (1) a condensing-gas drive type process at the trailing edge of the displacement;
- (2) a vaporizing-gas drive type process at the leading edge of the displacement; or
- (3) a combined vaporizing/condensing gas drive process that is immiscible, but that attains high displacement efficiencies due to mass transfer effects (consistent with early experimental

work reported by Hall and Geffen [67]).

Lee et al's [65] results did not contradict the agreement between thermodynamic calculations and slim tube tests obtained by Wu et al [68] if it was assumed that only a condensing-gas drive process was being observed. Nonetheless, the lack of a solid theoretical base, including a mechanistic evaluation of the processes contributing to the observed effects of "dispersion" strongly suggested a need for further work in this area. However, it was obvious that researchers have, consistent with this investigation, "dropped" the requirement that the solvent/oil mixture pass through a critical point, which has the implicit assumption that the miscible process is dominated by mass transfer effects versus interfacial tension reduction.

Investigators, as discussed above, have emphasized the critical role of dispersion in promoting the observed disagreements between their thermodynamic calculations and the experimental results of slim tube displacement tests. The mechanisms contributing to dispersion that could be causing the observed "dispersion" include:

- (1) molecular diffusion between the gas and liquid phases;
- (2) convective mixing caused by viscous fingering; and
- (3) interphase mass transfer caused by evaporation of residual liquid behind the displacement front as a result of

non-equilibrium effects.

While a complete examination of dispersion phenomena was beyond the scope of this work, some observations were in order. The influence of longitudinal as compared to transverse [50] molecular diffusion in laboratory-scale processes is small given the high L/D (length/diameter) ratio typical of slim tubes. Convective mixing caused by viscous fingering in a slim tube with a typical diameter of one centimetre should only occur when the displacement rates were high; in short, the effect can be eliminated by appropriate laboratory technique. The remaining, and dominant, physical mechanism was the evaporation of residual liquid behind the displacement front resulting from non-equilibrium effects at least partly numerical in origin. This hypothesis was entirely consistent with the numerical grid refinement experiments in Runs 1 to 5. Those results were caused by mass transfer effects as compared to numerical dispersion caused by discretization of the flow equations. However, for physical systems with dimensions similar to the simulated slim tube, and with extremely adverse viscosity ratios, complete thermodynamic equilibrium between the gas and liquid phase may not be obtained due to the inevitable viscous fingering [69, 70]. In short, the mechanistic bases of the dispersion effects observed by other workers would appear to be primarily interphase mass transfer and viscous fingering (in terms of the viscosity ratio between the displacing gas and the

displaced liquid).

Gardner and Ypma [39] described an experimentally observed residence time (or kinetic) effect in laboratory miscible displacement tests where a minimum "solvent soak" time was required to attain an equilibrium contact between the solvent and the oil. Implications respecting viscosity ratio, optimum laboratory and field displacement rates were not investigated. Gardner and Ypma concluded that a synergistic reaction between phase behavior and viscous fingering reduced oil recovery; analogous to the above hypothesis used herein to explain the "dispersion" effect reported in the open literature.

Stewart and Udell [71] attempted to isolate thermal and hydrodynamic mechanisms for the one-dimensional displacement of residual oil by steam injection. They concluded that "mass-transfer-limited evaporation of the residual oil in the steam zone appears to be the dominant mode of ROS (residual oil saturation) reduction in viscous oil-recovery projects." Stewart and Udell's [71] results were analogous to those reported by Lee et al [65], which distinguished three modes for the dominant process of mass transfer to occur in gas-liquid displacements. The importance of this analogy was that it established a common, if only tentative, physical basis for the various gas injection processes; immiscible or miscible gas injection, steam injection, and air or oxygen injection (for in-situ combustion); which may aid longer term fundamental

research to improve the current understanding of the physical mechanisms governing gas-liquid displacements in a permeable, porous medium.

Sibbald et al [72] and Novosad et al [73], in related papers discussed the numerical simulation of slim tube displacement experiments, and the comparison of slim tube results to those obtained using a rising bubble apparatus (developed by Christiansen and Haines [74]), respectively. Novosad et al [73] obtained a good correlation between the experimental results obtained by the two techniques (i.e., a slim tube and a rising bubble apparatus) and examined methane spikes (where the methane concentration in effluent gas minus the methane concentration in solution gas becomes greater than zero, and then recedes back to zero) observed in some slim tube displacement tests. Novosad et al stated [73] that "gas bubbles or methane spikes are often reported in the effluent of the slim tube tests close to a miscible condition where the two-phase flow (zone) is very short (in length). In miscible condensing gas drives, the gas bubbles correspond to arrival at the outlet of the equilibrium vapour, which forms at the leading, or downstream, edge of the transition zone. On the other hand, the effluent in miscible vapourizing or liquid extraction drives should have neither gas bubbles or methane spikes". Novosad et al [73] came to the observation that a significant methane spike (on the basis of their limited data, a value of 3 mole percent would appear to be

"significant") probably indicates a very efficient immiscible displacement.

Novosad et al [73] also concluded that the rising bubble apparatus test was preferable to the slim tube displacement test as it is faster and less prone to interpretation error respecting whether or not thermodynamic miscibility had indeed occurred. A basic problem in the interpretation of a slim tube displacement test remains the uncertainty as to whether or not the highly efficient displacements observed for immiscible displacements (that benefit from mass transfer) will be achieved in all instances at the field scale due to the need for the oil to be contacted by a high pore volume throughput of drive gas. Thus, prudent operators tend to add a safety factor to solvent designs (by enriching the solvent composition or increasing the operating pressure) based on the results of slim tube displacement tests, which tends to result in thermodynamic miscibility being attained. Operationally, this safety factor also provides flexibility respecting production rates and solvent supplies without fear that regulatory constraints concerning the minimum operating pressure and solvent enrichment might be violated.

Sibbald et al [72] analyzed the fluid systems described by Novosad et al [73] using a compositional simulator and did not find a definitive answer to the question: "how close to miscibility must a solvent/oil system be to allow efficient

displacement in a reservoir?" Sibbald et al [72] also found that "a drastic change in the shapes and endpoints of the (relative permeability) curves from the default case does not significantly affect the recovery level of components predicted by the simulator".

The dominance of mass transfer versus relative permeability has serious consequences respecting the compositional simulation of solvent coning downwards to the producing interval in field scale gravity stable miscible displacements. The high computational cost [75] associated with the combined effects of mass transfer and high pore volume throughputs near the wellbore may necessitate the use of simpler pseudo-miscible models [76] that emulate the actual coning behavior by adjustments to the relative permeability curves in the near wellbore region. Mechanistically, this treatment is equivalent to considering coning as a form of viscous fingering. However, the use of pseudo-miscible models may preclude a match of key parameters such as reservoir pressure [76] since an increasing gas-oil ratio resulting from the production of an oil altered by mixing with the solvent at the solvent-oil interface is not mechanistically simulated. However, recent enhancements to the compositional simulator used in this investigation have made it feasible to perform single well compositional coning studies of gravity stable miscible displacements based on the results of actual test runs [77].

Novosad and Costain [78] have described process mechanisms in miscible displacement as being either:

- (1) liquid extraction by the solvent;
- (2) condensation of the solvent into the oil; or
- (3) a combination of liquid extraction and solvent condensation.

The latter process may result in changes to the composition of the solvent and oil such that the ternary phase envelope does not close. Novosad and Costain [78] showed for mixtures of oil and solvent that "as the solvent concentration in the mixture increases, the saturation pressure, initially a bubblepoint pressure, P_b , becomes a dewpoint and then a bubblepoint again" for pure solvent, and "thus, two critical points have to exist where the bubblepoint and dewpoint lines meet". Consequently, in that instance, the interfacial tension will pass through a minimum where it is a small but finite value since the solvent-oil fluid system does not actually pass through a single-phase critical point. Other workers in laboratory and field studies [79-81] have suggested that displacement efficiencies may be higher at near-miscible or dynamic miscible conditions than for first-contact miscibility as mass transfer acts to stabilize the viscosity ratio, especially where interfacial tension reduction [82] causes relative permeability curves to become linear with a smaller residual liquid saturation. This investigation, which includes a systematic

examination of mass transfer effects, allows a somewhat different interpretation in that what may have occurred was that the combination of liquid extraction and solvent condensation, where the ternary diagram did not close, coupled with interfacial tension reduction in the near critical region, acted to stabilize viscous fingering by comparison to a first-contact miscible process with an adverse viscosity ratio. Further discussion and examination of the influence of interfacial tension reduction effects and their interaction with other processes was outside the scope of this investigation.

Sibbald et al [72] concluded that static, or thermodynamic, miscibility tests may yield more conservative results than a slim tube displacement test for what Lee et al [65] termed a vaporizing-gas drive process at the leading edge of the displacement. In summary, investigators have found that mass transfer has a marked impact on the results of slim tube displacement tests. However, the difficulties in the interpretation of experimental results as well as the most appropriate technique for performing slim tube displacement tests and the resultant implications respecting numerical model results have not been fully discussed elsewhere and were reviewed in the following section.

Experimentalists generally emphasize repeatability as an important indication of the precision of their work; that issue was not at question here, the real issue was how much detail can

be recorded with existing instrumentation at reasonable expense. Randall and Bennion [83] provided a review of recent developments in experimental procedures and a discussion of laboratory factors influencing results [84] for slim tube displacement tests. Randall and Bennion emphasized the need to consider all aspects of observed performance in the interpretation of laboratory measurements, especially subtle aspects of fluid phase behavior such as oil swelling resulting in the mixing of oil and solvent in intimate contact. Earlier work by Yellig and Metcalfe [85] did not address this problem, instead emphasizing that results were reproducible. Also, the slim tube displacement test procedure is not designed to provide a sensitive measure of the chromatographic velocity differences of the individual components [47, 48]. The basic challenge facing the experimentalist was defined, for the purposes of this work, as an inherent limitation on the ability to fully measure fluid compositions and properties throughout the apparatus as the slim tube displacement test proceeds. This inherent limitation also affected the analysis of results using numerical models since it was more difficult to account for phenomena such as oil swelling, the mode of mass transfer and the adequacy of existing well models for flow regimes at the laboratory scale.

Christman and Gorell [86] found that the differences between laboratory and field scale carbon dioxide injectivity were reconciled by the use of the appropriate geometry at the

boundary conditions assumed by the well model. Laboratory simulations required the use of linear formulation while field simulations required the use of a radial formulation. Ong and Butler [87] found that a separate treatment was required for the appropriate scaling of wells when performing scaled physical experiments of the steam-assisted gravity drainage process. Fassihi [88] found that numerical simulations of heavy oil relative permeability tests required consideration of end effects (including some changes to the experimental apparatus) and provision for potentially significant gravity segregation and capillary pressure effects.

Differences in the results of slim tube displacement tests may also be observed due to fluid compressibility depending on whether or not an initial pressure gradient exists across the apparatus from the inlet to the outlet end. A more general problem in numerical reservoir simulation is that few publications ([89], see p. 321) exist respecting the simulation of laboratory models, or the use of numerical models to interpret laboratory experiments. More fundamental work in this area is required to expedite future research beyond the parametric study performed in this investigation.

Numerical Model Results

The numerical model results for Runs 26 to 85 have been summarized on Table 6. Consistent with the results of Runs 6 to 25, and the work of Sibbald et al [72], the shape of the relative permeability curve and endpoint critical saturation only slightly influenced the ultimate oil recovery of two-phase miscible gas-liquid displacements in a linear system. Sigmund et al [90], however, did report that computed recoveries in a miscible carbon dioxide-oil displacement were sensitive to the relative permeability relationships used. These differing results were easily reconciled if it is recalled that multiple liquid phases are more often present in carbon dioxide miscible displacements; therefore, the appropriate comparison is a water alternating hydrocarbon gas miscible displacement, where two liquid phases, oil and water are present, and where hysteresis effects are well-recognized. Further examination of this issue, for which more research work is required, was outside the scope of this investigation.

_ _ _ _

The results for Runs 38 to 49, summarized on Table 6, for fluid system A:Q showed ever increasing oil recovery with increasing solvent injection, even with volumes quoted at reservoir conditions. This anomalous result was observed since some of the solvent continued to condense into the liquid phase after 100 percent recovery of the n-decane originally in place. For a

Table 6

Numerical Model Results
Flash Calculations Active

| Run No. | Fluid System | Rel. Perm. Curve | Pressure kPa | PV Oil Produced Vs. PV Gas Injected | | | |
|---------|--------------|------------------|--------------|-------------------------------------|-------|-------|-------|
| | | | | @ 0.4 | @ 0.7 | @ 1.0 | @ 1.2 |
| 26 | A:M | OR | 14500 | .344 | .616 | .892 | .969 |
| 27 | A:M | I | 14500 | .328 | .588 | .823 | .845 |
| 28 | A:M | II | 14500 | .334 | .594 | .827 | .844 |
| 29 | A:M | III | 14500 | .334 | .592 | .826 | .844 |
| 30 | A:M | OR | 19000 | .349 | .626 | .903 | .984 |
| 31 | A:M | I | 19000 | .339 | .611 | .884 | .907 |
| 32 | A:M | II | 19000 | .344 | .621 | .889 | .911 |
| 33 | A:M | III | 19000 | .344 | .614 | .887 | .911 |
| 34 | A:M | OR | 20500 | .351 | .629 | .904 | .980 |
| 35 | A:M | I | 20500 | .343 | .615 | .889 | .921 |
| 36 | A:M | II | 20500 | .344 | .615 | .889 | .975 |
| 37 | A:M | III | 20500 | .346 | .618 | .893 | .938 |
| 38 | A:Q | OR | 14500 | .351 | .629 | .909 | 1.02 |
| 39 | A:Q | I | 14500 | .338 | .603 | .869 | .929 |
| 40 | A:Q | II | 14500 | .344 | .615 | .886 | .936 |
| 41 | A:Q | III | 14500 | .343 | .612 | .883 | .938 |
| 42 | A:Q | OR | 19000 | .342 | .623 | .909 | 1.04 |
| 43 | A:Q | I | 19000 | .345 | .629 | .916 | 1.05 |
| 44 | A:Q | II | 19000 | .345 | .631 | .919 | 1.04 |
| 45 | A:Q | III | 19000 | .346 | .631 | .919 | 1.06 |
| 46 | A:Q | OR | 20500 | .360 | .641 | .922 | 1.03 |
| 47 | A:Q | I | 20500 | .360 | .640 | .922 | 1.03 |
| 48 | A:Q | II | 20500 | .360 | .641 | .922 | 1.03 |
| 49 | A:Q | III | 20500 | .360 | .641 | .922 | 1.03 |
| 50 | B:M | OR | 14500 | .342 | .611 | .852 | .891 |
| 51 | B:M | I | 14500 | .327 | .584 | .741 | .756 |
| 52 | B:M | II | 14500 | .337 | .600 | .763 | .763 |
| 53 | B:M | III | 14500 | .336 | .597 | .765 | .766 |
| 54 | B:M | OR | 19000 | .352 | .627 | .888 | .930 |
| 55 | B:M | I | 19000 | .339 | .601 | .779 | .789 |
| 56 | B:M | II | 19000 | .345 | .615 | .785 | .785 |
| 57 | B:M | III | 19000 | .343 | .609 | .784 | .786 |
| 58 | B:M | OR | 20500 | .355 | .631 | .897 | .943 |
| 59 | B:M | I | 20500 | .342 | .606 | .787 | .798 |
| 60 | B:M | II | 20500 | .347 | .614 | .793 | .793 |

Table 6 (Continued)

| Run No. | Fluid System | Rel. Perm. Curve | Pressure kPa | PV Oil Produced Vs. PV Gas Injected | | | |
|---------|--------------|------------------|--------------|-------------------------------------|-------|-------|-------|
| | | | | @ 0.4 | @ 0.7 | @ 1.0 | @ 1.2 |
| 61 | B:M | III | 20500 | .346 | .612 | .794 | .794 |
| 62 | C:E | OR | 14500 | .344 | .530 | .630 | .666 |
| 63 | C:E | I | 14500 | .380 | .456 | .502 | .520 |
| 64 | C:E | II | 14500 | .350 | .545 | .549 | .549 |
| 65 | C:E | III | 14500 | .362 | .531 | .547 | .547 |
| 66 | C:E | OR | 19000 | .398 | .691 | .829 | .860 |
| 67 | C:E | I | 19000 | .397 | .634 | .690 | .702 |
| 68 | C:E | II | 19000 | .399 | .694 | .705 | .705 |
| 69 | C:E | III | 19000 | .398 | .689 | .706 | .706 |
| 70 | C:E | OR | 20500 | .391 | .685 | .854 | .883 |
| 71 | C:E | I | 20500 | .389 | .661 | .711 | .719 |
| 72 | C:E | II | 20500 | .392 | .687 | .721 | .721 |
| 73 | C:E | III | 20500 | .391 | .684 | .717 | .717 |
| 74 | D:F | OR | 14500 | .462 | .657 | .719 | .734 |
| 75 | D:F | I | 14500 | .346 | .428 | .451 | .457 |
| 76 | D:F | II | 14500 | .477 | .484 | .490 | .492 |
| 77 | D:F | III | 14500 | .459 | .479 | .485 | .488 |
| 78 | D:F | OR | 19000 | .344 | .599 | .779 | .781 |
| 79 | D:F | I | 19000 | .347 | .599 | .617 | .619 |
| 80 | D:F | II | 19000 | .339 | .595 | .618 | .619 |
| 81 | D:F | III | 19000 | .340 | .596 | .618 | .619 |
| 82 | D:F | OR | 20500 | .299 | .553 | .772 | .805 |
| 83 | D:F | I | 20500 | .294 | .582 | .691 | .701 |
| 84 | D:F | II | 20500 | .334 | .582 | .686 | .701 |
| 85 | D:F | III | 20500 | .334 | .582 | .689 | .703 |

real reservoir fluid system, such artificially high liquid recoveries would not be as large or as easily recognized. These results strongly suggested that post solvent breakthrough recoveries should be carefully examined as to their validity. Indeed, Cardenas et al [91] in the laboratory design of a carbon dioxide miscible flood used a slim tube displacement test criterion of 90 percent oil recovery at carbon dioxide breakthrough (which, based on this work would occur at about 1.0 pore volume gas injection). The experimental results reported by other workers [92] would also support this interpretation. This observation suggests that the common practice of quoting oil recoveries after solvent breakthrough in the absence of an interface may explain some interpretations that slim tube displacement tests predict leaner solvent requirements for a high recovery than static (i.e., thermodynamic) mixing cell tests.

Viscosity ratio and kinematic viscosity ratio data for the displacements at 14500 and 20500 kPa have been shown on Table 7A and 7B, respectively. Close examination of that data indicated some small superficial discrepancies, compared with the data shown on Table 2, as a result of mass transfer caused by thermodynamic considerations. These data and liquid recovery efficiencies have been summarized on Table 8 to illustrate that a straightforward correlation of unit displacement efficiency with viscous forces in a linear system was lost once a

TABLE 7A

Physical Properties of Gas-Liquid Systems
At 14500 kPa and 71° C

| Displaced liquid Phase | Displacing gas Phase | μ_L | μ_g | ρ_L | ρ_g | μ_L/μ_g | $\frac{\nu_L}{\times 1000}$ | $\frac{\nu_g}{\times 1000}$ | $\frac{\nu_L}{\nu_g}$ |
|------------------------------|----------------------------|---------|---------|----------|----------|---------------|-----------------------------|-----------------------------|-----------------------|
| A | M | 0.2294 | .01611 | 628.9 | 96.10 | 14.05 | 0.3648 | 0.1676 | 2.18 |
| B | M | 0.2829 | .01611 | 664.0 | 96.10 | 17.56 | 0.4261 | 0.1676 | 2.54 |
| *C | E | 0.1786 | .01611 | 590.4 | 96.10 | 11.09 | 0.3025 | 0.1676 | 1.80 |
| *D | F | 0.08377 | .01936 | 485.1 | 155.0 | 4.33 | 0.1727 | 0.1249 | 1.38 |
| A | Q | 0.2294 | .02022 | 628.9 | 167.0 | 10.33 | 0.3648 | 0.1211 | 3.01 |

μ - viscosity, cp

ρ - density, kg/m³

$\nu = \mu/\rho$ - kinematic viscosity, cSt

* Oils C & D form a secondary gas saturation at 14500 kPa.

TABLE 7B

**Physical Properties of Gas-Liquid Systems
At 20500 kPa and 71° C**

| Displaced liquid Phase | Displacing gas Phase | μ_L | μ_g | ρ_L | ρ_g | μ_L/μ_g | ν_L x1000 | ν_g x1000 | ν_L/ν_g |
|------------------------------|----------------------------|---------|---------|----------|----------|---------------|------------------|------------------|---------------|
| A | M | 0.2515 | .01868 | 637.3 | 128.6 | 13.46 | 0.3946 | 0.1453 | 2.72 |
| B | M | 0.2987 | .01868 | 668.6 | 128.6 | 15.99 | 0.4468 | 0.1453 | 3.08 |
| C | E | 0.1648 | .01939 | 575.6 | 139.5 | 8.50 | 0.2863 | 0.1390 | 2.06 |
| D | F | 0.05402 | .02834 | 396.8 | 240.5 | 1.91 | 0.1361 | 0.1178 | 1.16 |
| A | Q | 0.2515 | .02682 | 637.3 | 227.6 | 9.38 | 0.3946 | 0.1178 | 3.35 |

μ - viscosity, cp

ρ - density, kg/m³

$\nu = \mu/\rho$ - kinematic viscosity, cSt

Table 8

67

**Numerical Model Results
Factors Influencing Liquid Recovery**

| Fluid System | Pressure kPa | Sor (PV) | ML/Mg | VL/Vg | PV Oil Produced* | |
|--------------|-----------------|-------------|-------|-------|------------------|------------|
| | | | | | @ 1.0 PVGI | @ 1.2 PVGI |
| A:M | 14500 | 0.1 | 14.05 | 2.18 | 0.892 | 0.969 |
| | 14500 | 0.3 | 14.05 | 2.18 | 0.825 | 0.844 |
| | 19000 | 0.1 | 13.81 | 4.96 | 0.903 | 0.984 |
| | 19000 | 0.3 | 13.81 | 4.96 | 0.887 | 0.910 |
| | 20500 | 0.1 | 13.46 | 2.72 | 0.904 | 0.980 |
| | 20500 | 0.3 | 13.46 | 2.72 | 0.890 | 0.945 |
| A:Q | 14500 | 0.1 | 10.33 | 3.01 | 0.909 | 1.02 |
| | 14500 | 0.3 | 10.33 | 3.01 | 0.879 | 0.934 |
| | 19000 | 0.1 | 9.83 | 3.31 | 0.909 | 1.04 |
| | 19000 | 0.3 | 9.83 | 3.31 | 0.918 | 1.05 |
| | 20500 | 0.1 | 9.38 | 3.35 | 0.922 | 1.03 |
| | 20500 | 0.3 | 9.38 | 3.35 | 0.922 | 1.03 |
| B:M | 14500 | 0.1 | 17.56 | 2.54 | 0.852 | 0.891 |
| | 14500 | 0.3 | 17.56 | 2.54 | 0.757 | 0.762 |
| | 19000 | 0.1 | 16.50 | 5.64 | 0.888 | 0.930 |
| | 19000 | 0.3 | 16.50 | 5.64 | 0.783 | 0.787 |
| | 20500 | 0.1 | 15.99 | 3.08 | 0.897 | 0.943 |
| | 20500 | 0.3 | 15.99 | 3.08 | 0.791 | 0.795 |
| C:E | 14500 | 0.1 | 11.09 | 1.80 | 0.630 | 0.666 |
| | 14500 | 0.3 | 11.09 | 1.80 | 0.533 | 0.539 |
| | 19000 | 0.1 | 8.47 | 1.78 | 0.829 | 0.860 |
| | 19000 | 0.3 | 8.47 | 1.78 | 0.700 | 0.704 |
| | 20500 | 0.1 | 8.50 | 2.06 | 0.854 | 0.883 |
| | 20500 | 0.3 | 8.50 | 2.06 | 0.716 | 0.719 |
| D:F | 14500 | 0.1 | 4.33 | 1.38 | 0.719 | 0.734 |
| | 14500 | 0.3 | 4.33 | 1.38 | 0.475 | 0.479 |
| | 19000 | 0.1 | 2.29 | 0.702 | 0.771 | 0.781 |
| | 19000 | 0.3 | 2.29 | 0.702 | 0.618 | 0.619 |
| | 20500 | 0.1 | 1.91 | 1.16 | 0.772 | 0.805 |
| | 20500 | 0.3 | 1.91 | 1.16 | 0.689 | 0.702 |

* versus PVGI (pore volume gas injected)

Note:

1. Irregularities in the kinematic viscosity ratio were caused by quoting values at 19000 kPa from Runs 6 - 25, where flash calculations were suppressed. When the flash calculations are active, mass transfer acts to reduce the density difference between the displacing gas and displaced oil.

significant degree of interphase mass transfer between the displacing gas and the displaced liquid occurred. This observation was more clearly shown on Table 9 where the immiscible (mass transfer suppressed) and miscible (mass transfer active, i.e., thermodynamic equilibrium, or flash, calculations performed) displacement recovery efficiencies were compared.

Fluid systems C:E and D:F were designed to be an equilibrium gas-liquid system at a pressure of 19000 kPa. The immiscible recovery efficiencies for these systems shown on Table 9 tended to be slightly lower than those for the equilibrium gas drive (even after correction for the discrepancies caused by the separator flash calculations for the immiscible runs). However, were the immiscible cases (mass transfer suppressed) to have a more favourable viscosity ratio, a more piston-like displacement essentially identical to that observed for the equilibrium gas drive would occur.

Fluid_system A:Q was designed to be a thermodynamic first-contact miscible gas-liquid system at 19000 kPa. The miscible recoveries at 1.0 pore volume gas injection for immiscible residual oil saturations of both 10 and 30 percent were each about 90 percent as shown on Table 9. The recoveries at 1.2 pore volume gas injection cannot be directly compared since some solvent was condensing into the liquid phase at reservoir conditions. However, an examination of the

Table 9

69

**Comparison of Numerical Model Results
Effect of Mass Transfer
on Pore Volume Liquid Produced**

| <u>Fluid System</u> | <u>Sor (PV)</u> | <u>Mass Transfer Suppressed</u> | | <u>Mass Transfer Active</u> | |
|---------------------|-----------------|---------------------------------|-------------------|-----------------------------|-------------------|
| | | <u>@ 1.0 PVGI</u> | <u>@ 1.2 PVGI</u> | <u>@ 1.0 PVGI</u> | <u>@ 1.2 PVGI</u> |
| A:M | 0.1 | 0.885 | 0.890 | 0.903 | 0.984 |
| | 0.3 | 0.678 | 0.678 | 0.887 | 0.910 |
| A:Q | 0.1 | 0.890 | 0.890 | 0.909 | 1.04 |
| | 0.3 | 0.722 | 0.722 | 0.918 | 1.05 |
| B:M | 0.1 | 0.788 | 0.890 | 0.888 | 0.930 |
| | 0.3 | 0.699 | 0.699 | 0.783 | 0.787 |
| C:E | 0.1 | 0.784 | 0.784 | 0.829 | 0.860 |
| | 0.3 | 0.615 | 0.615 | 0.700 | 0.704 |
| D:F | 0.1 | 0.761 | 0.761 | 0.771 | 0.781 |
| | 0.3 | 0.625 | 0.626 | 0.618 | 0.619 |

Notes:

1. All displacements were performed at 19000 kPa.
2. Sor - residual oil saturation to immiscible displacement (mass transfer suppressed).
3. PVGI - pore volume gas injected.

compositions of the in-situ fluids indicated 100 percent recovery of the n-decane for the first-contact miscible case by 1.2 pore volume gas injection, consistent with the criteria of 99 percent oil recovery at 1.2 pore volume gas injection for first-contact miscibility proposed by Wu et al [68] (Wu et al proposed a criteria of 90 percent oil recovery at 1.2 pore volume gas injection for dynamic miscibility). The results discussed for fluid system A:Q showed excellent agreement with published criteria for first-contact miscibility as measured by slim tube displacement tests or determined using thermodynamic considerations.

Fluid systems A:M and B:M showed liquid recovery efficiencies intermediate between an equilibrium gas drive (where mass transfer does not occur) and a first-contact miscible displacement (where mass transfer is confined to a small mixing zone, and the residual liquid saturation is zero). The incremental recoveries of residual liquid for all cases with mass transfer, as compared to the immiscible case (mass transfer suppressed), were shown on Table 10. As discussed, the incremental recoveries for fluid systems C:E and D:F were due to viscous forces and relative permeability effects tending to reduce recovery for the immiscible case. Similarly, the incremental recoveries for system A:Q shown on Table 10 were consistent with a thermodynamic first-contact miscible displacement process once provision was made for solvent

Table 10

**Residual Liquid Recovery
Due to Mass Transfer
(At 19000 kPa)**

| Fluid System | Sor (PV) | Incremental Oil Produced | | Residual Oil Recovery ¹ | | | |
|------------------|----------|--------------------------|---------|------------------------------------|------------|--------------|------------|
| | | | | Using Sor | | Using Actual | |
| | | | | @ 1.0 PVGI | @ 1.2 PVGI | @ 1.0 PVGI | @ 1.2 PVGI |
| A:M | 0.1 | 0.018 | 0.094 | 18.0 | 94.0 | 15.7 | 85.5 |
| | 0.3 | 0.209 | 0.232 | 69.7 | 77.3 | 64.9 | 72.0 |
| A:Q ² | 0.1 | 0.019 | 0.150 | 19.0 | 100.0 | 17.3 | 100.0 |
| | 0.3 | 0.196 | 0.328 | 65.3 | 100.0 | 70.5 | 100.0 |
| B:M | 0.1 | 0.100 | 0.040 | 100.0 | 40.0 | 47.2 | 36.4 |
| | 0.3 | 0.084 | 0.088 | 28.0 | 29.3 | 27.9 | 29.2 |
| C:E | 0.1 | 0.045 | 0.076 | 45.0 | 76.0 | 20.8 | 35.2 |
| | 0.3 | 0.085 | 0.089 | 28.3 | 29.7 | 22.1 | 23.1 |
| D:F | 0.1 | 0.010 | 0.020 | 10.0 | 20.0 | 4.2 | 8.4 |
| | 0.3 | (0.007) | (0.007) | (2.3) | (2.3) | (1.9) | (1.9) |

Notes:

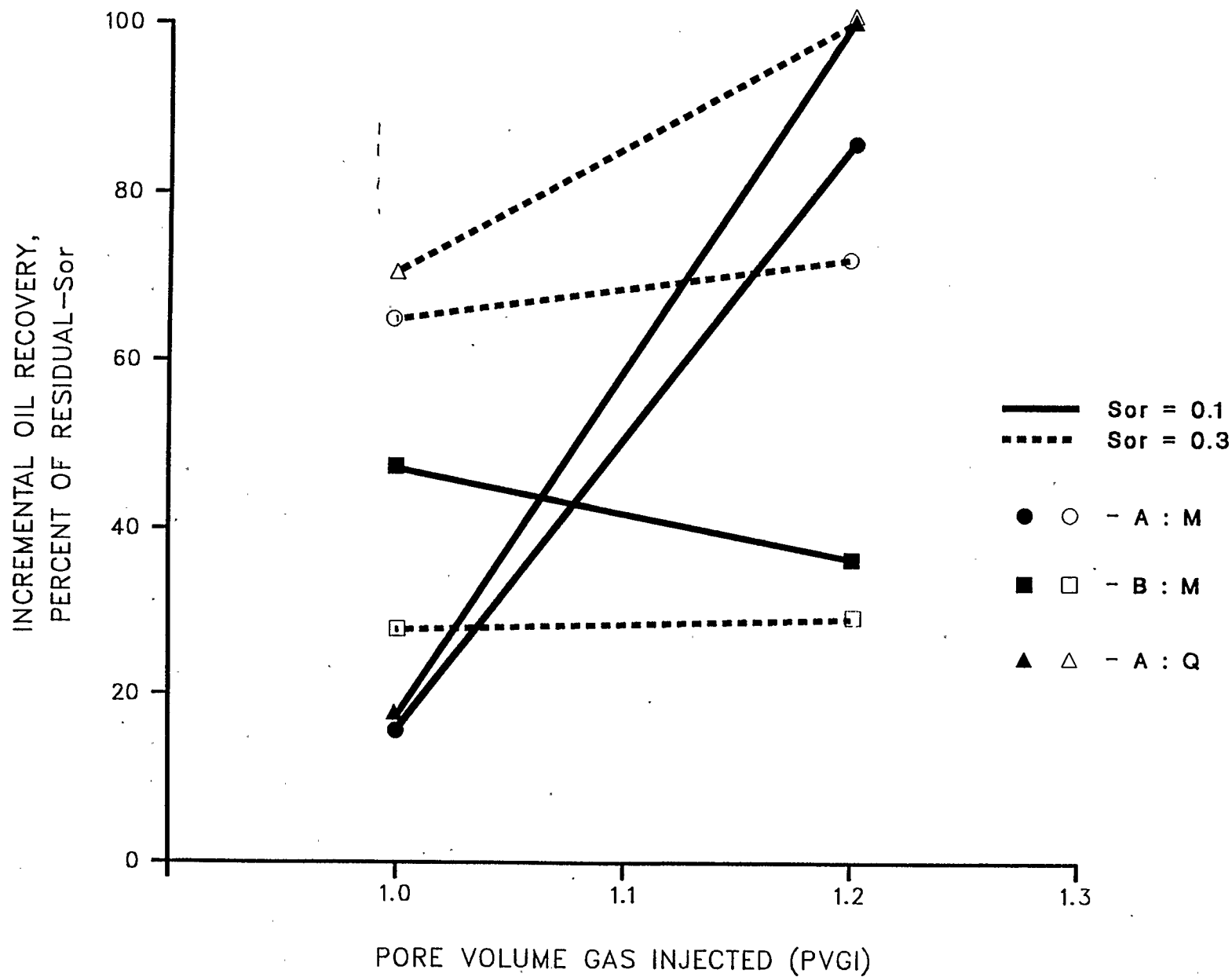
1. The values quoted using the Sor are based on the theoretical residual oil saturations of either 0.1 or 0.3 while the other values quoted are based on the actual oil remaining in the simulated slim tube at the end of the numerical model experiment.
2. Values for residual oil recovery at 1.2 pore volume gas injected (PVGI) were manually adjusted to a maximum 100 percent to account for solvent condensation.

condensation. The results for fluid system A:M and B:M, however, showed some striking differences as shown in Figure 20. The incremental recovery versus pore volume gas injected for fluid system A:M shown in Figure 20 were very similar to those for the fluid system A:Q (a thermodynamic first-contact miscible gas-liquid system). These results strongly suggested that the gas-liquid displacement for fluid system A:M is miscible, with the slightly lower ultimate recoveries indicating conditional (dynamic or multicontact) miscibility. By comparison, the results for fluid system B:M shown in Figure 20 were quite different, having an essentially flat (as opposed to inclined upwards) slope with an ultimate incremental recovery approximately one-half of that observed for the other two systems. Consistent with the work of Lee et al [65] and Sibbald et al [72], the gas-liquid displacement for fluid system B:M would appear to be a highly-efficient, immiscible gas drive.

These results, with the application of baseline immiscible displacements in Runs 6 to 25 (where interphase mass transfer was suppressed) have quantitatively confirmed recent theories in the technical literature respecting the nature of the gas-liquid displacement process, including a highly-efficient, immiscible gas drive. The good agreement between the immiscible gas drive and the equilibrium gas drive results further illustrated the influence of relative permeability when mass transfer was not significant. Taken together, these results clearly demonstrated

FIGURE 20

COMPARISON OF INCREMENTAL OIL RECOVERIES (AS A PERCENTAGE OF IMMISCIBLE RESIDUAL OIL SATURATION)



73

that the gas-liquid displacement process exists as a gradation of design alternatives, with the highly efficient, immiscible gas drive process examined in this work attaining about one-half the incremental oil recovery achieved by employing a miscible as opposed to a purely immiscible displacement process. Equilibrium gas drives were observed to be little better than purely immiscible gas drives since recovery gains caused by interphase mass transfer did not occur. From the standpoint of unit displacement efficiency, many other interrelated factors must also be examined in the design and implementation of field scale tests. In field terms, the baseline equilibrium gas drive corresponds to pressure maintenance by reinjection of produced solution gas. The highly efficient immiscible gas drive corresponds to pressure maintenance by reinjection of stripped solution gas (i.e., intermediate and heavier components removed by surface gas processing facilities) which evaporates residual oil behind the displacement front (analogous to revaporization of retrograde condensed liquids by dry gas). The miscible gas drives involve reinjection of solution gas sufficiently enriched with ethane or propane such that miscibility is achieved. As a practical matter, make-up gas may also be required if a constant reservoir pressure is desired since reinjection of produced solution gas will not completely replace voidage.

Ultimate liquid recoveries versus pressure at 1.2 pore volume gas injected and 0.3 residual liquid saturation were shown in

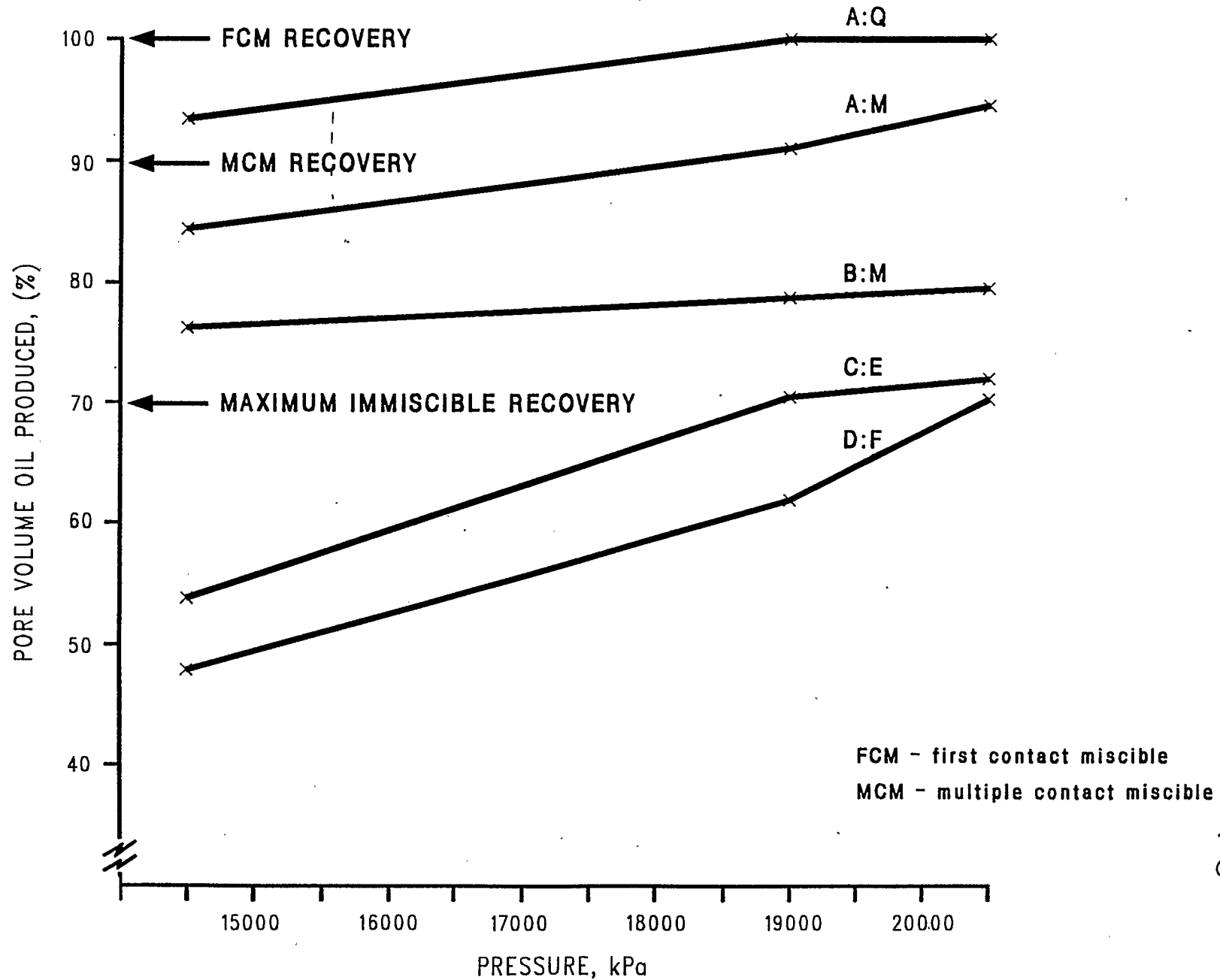
Figure 21. The results showed that the complete gradation from immiscible to fully miscible displacement was investigated in this parametric study. The recoveries for fluid systems C:E and D:F at 14500 kPa were much lower since the original fluids, which were single phase at 19000 kPa, separated into two phases at the lower pressure. At pressures above 19000 kPa, for fluid systems C:E and D:F, liquid recoveries increased due to mass transfer. Numerical model results for fluid system D:F were difficult to interpret as the original liquid was at a near critical state that made it difficult for the simulator to clearly distinguish the gas and liquid phases, necessitating the use of the net recovery of n-decane to estimate equivalent pore volume liquid produced (spot-checks showed that this was a reasonable assumption). These results strongly suggested that there is a need for improvement in the present compositional model for the treatment for critical and near-critical fluids.

Fluid system A:Q displayed dynamic (or multicontact) miscible behavior in terms of displacement efficiency at 14500 kPa and was a thermodynamic first-contact miscible displacement at 19000 kPa and at 20500 kPa. Fluid system A:M displayed near-miscible displacement behavior at 14500 kPa, dynamic miscibility at 19000 kPa, and was about halfway to thermodynamic first-contact miscibility at 20500 kPa. The results for fluid systems A:M and A:Q shown in Figure 21 demonstrated that there were some modest incremental gains in unit displacement efficiency by going from

FIGURE 21

INFLUENCE OF PRESSURE ON ULTIMATE RECOVERY

(PVGI = 1.2, $S_{or}=0.3$)



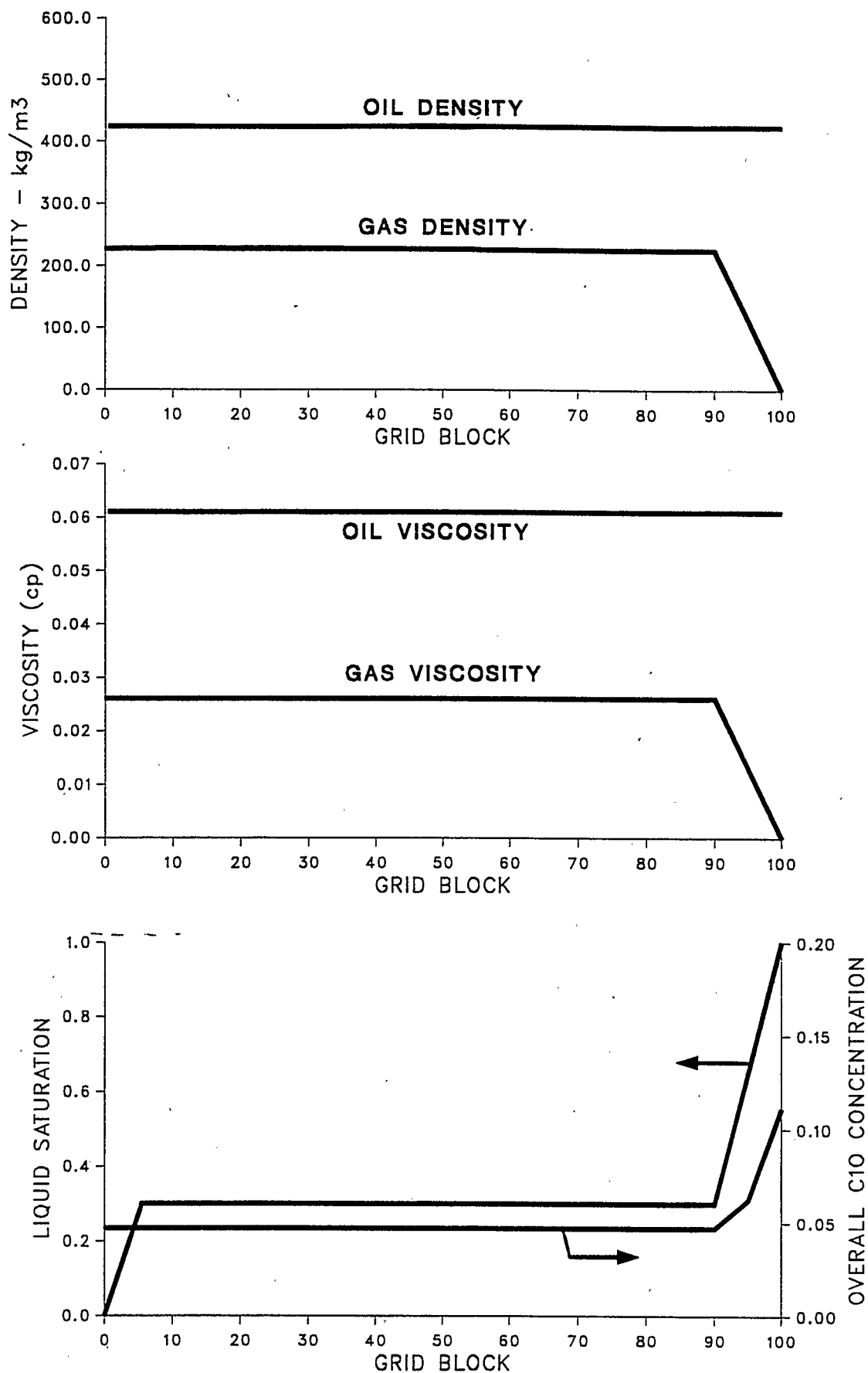
a dynamic to a first-contact miscible gas-drive process in the one-dimensional linear case without gravity or capillary forces.

Fluid system B:M behaved as a highly-efficient, immiscible gas drive that showed a steady increase in recovery as the pressure increased. Stripping (of light ends from the oil) and condensation (of solvent heavy ends) effects, which had complicated the analyses for the other fluid systems, were minimized for fluid system B:M by defining it as pure methane displacing pure n-decane. The importance of stripping and condensation effects was clearly shown by the fact that fluid system B:M had the smallest slope (and increase) in Figure 21 of oil recovery with pressure of any of the fluid systems studied in this investigation. These results suggested that one way to improve solvent design for field scale projects may be to deliberately include oil stripping and solvent condensation effects, as is sometimes done for steamfloods (see Volek and Pryor [93], and Konopnicki et al [94]).

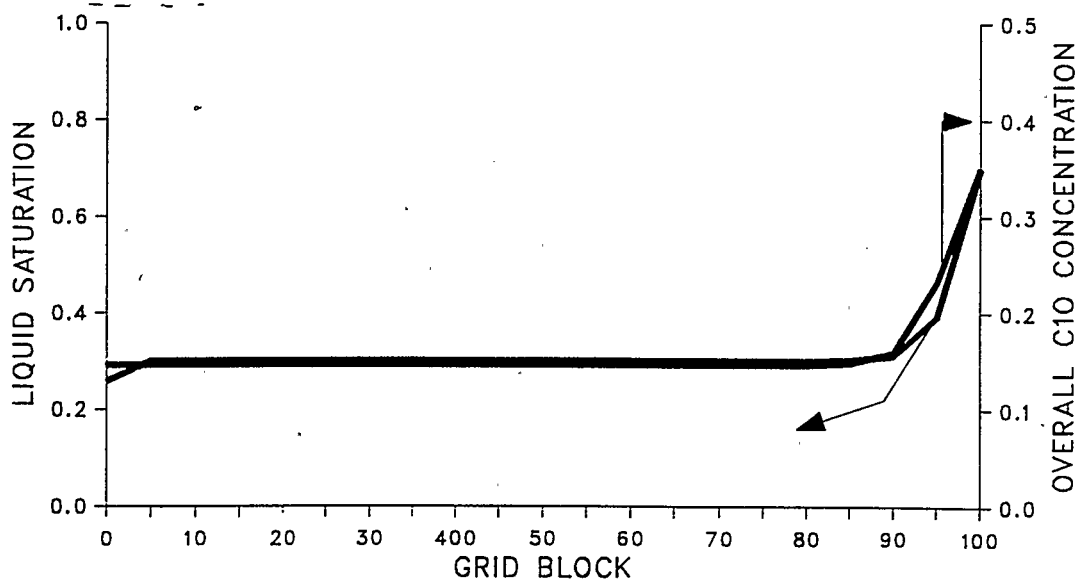
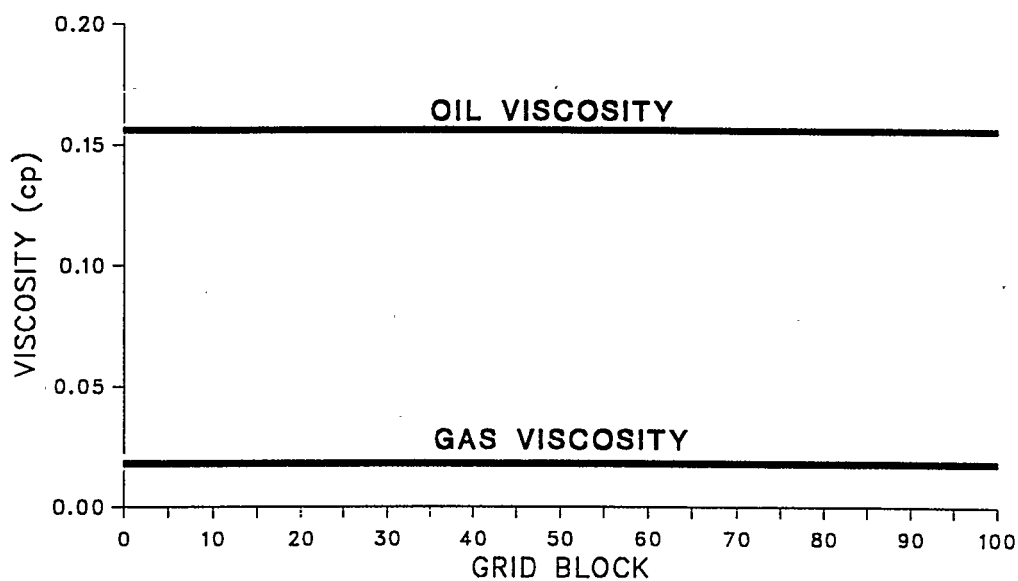
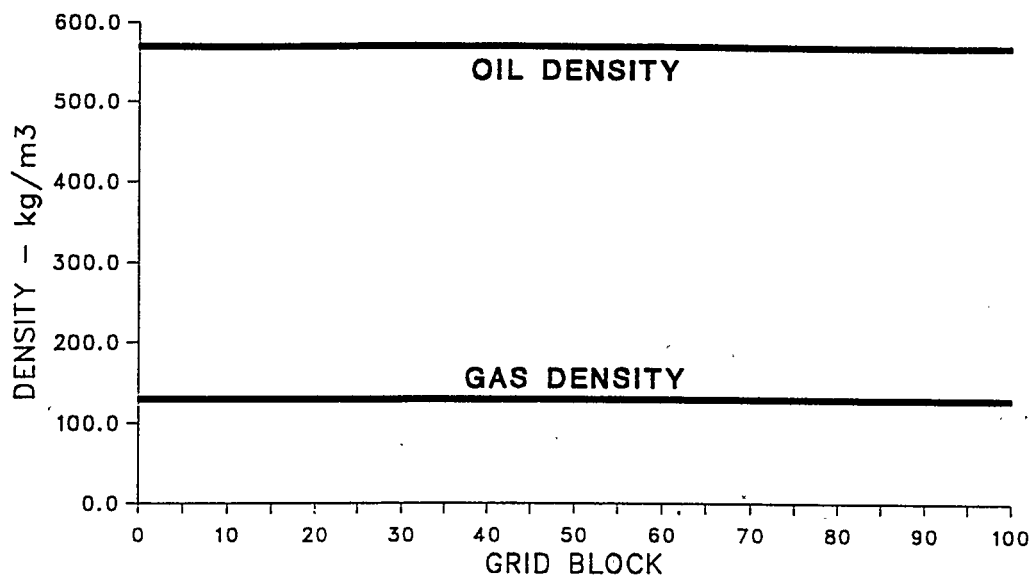
The displacement characteristics for each fluid system were shown in Figures 22 to 26, inclusive, at conditions of 0.7 pore volume gas injection, linear oil relative permeability Curve III, and at 19000 kPa. These conditions were selected since the gas-liquid displacement was well-developed at 0.7 pore volume gas injection, to minimize further unnecessary review of relative permeability effects, and to facilitate comparison to baseline immiscible displacements. Figures 22 to 24 show

FIGURE 22

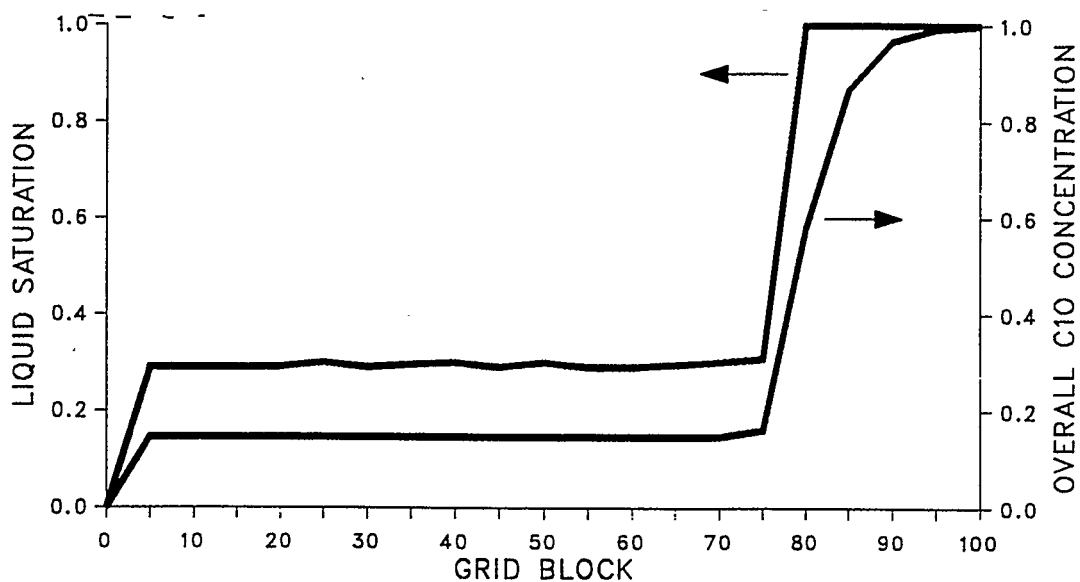
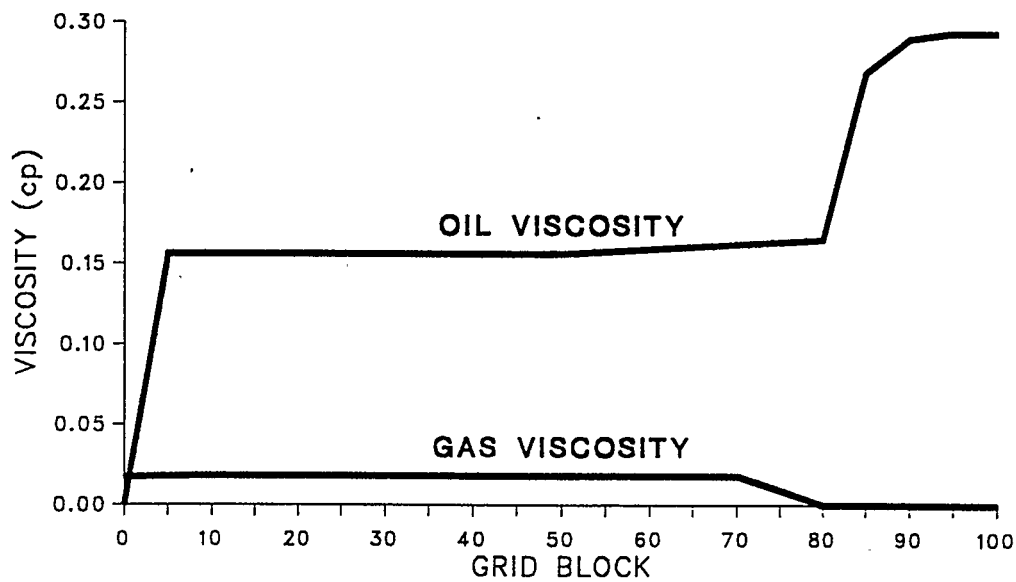
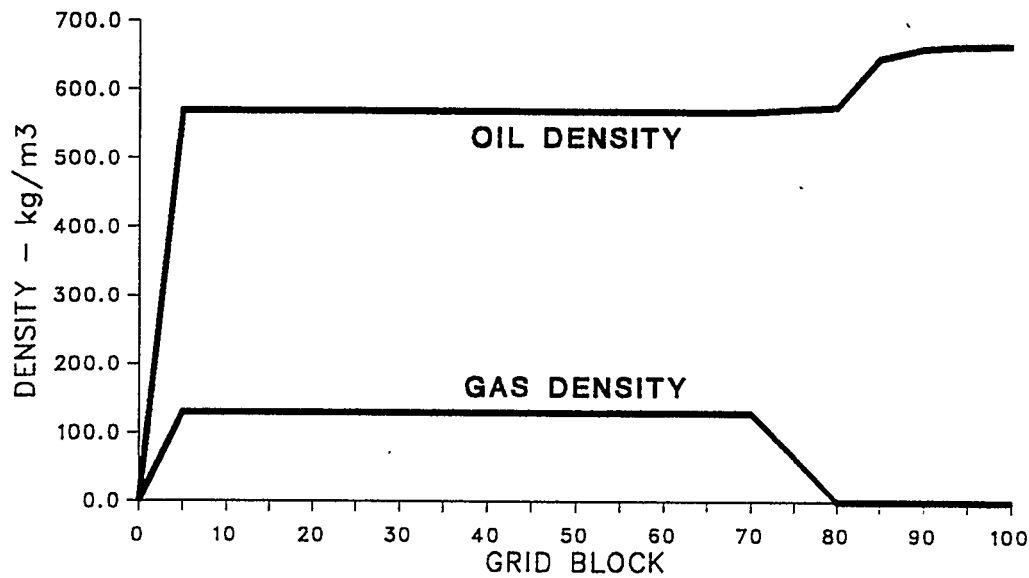
**DISPLACEMENT CHARACTERISTICS FOR FLUID SYSTEM D:F AT
0.7 PVGI USING LINEAR RELATIVE PERMEABILITY CURVE III
AT 19000 kPa (RUN 81)**



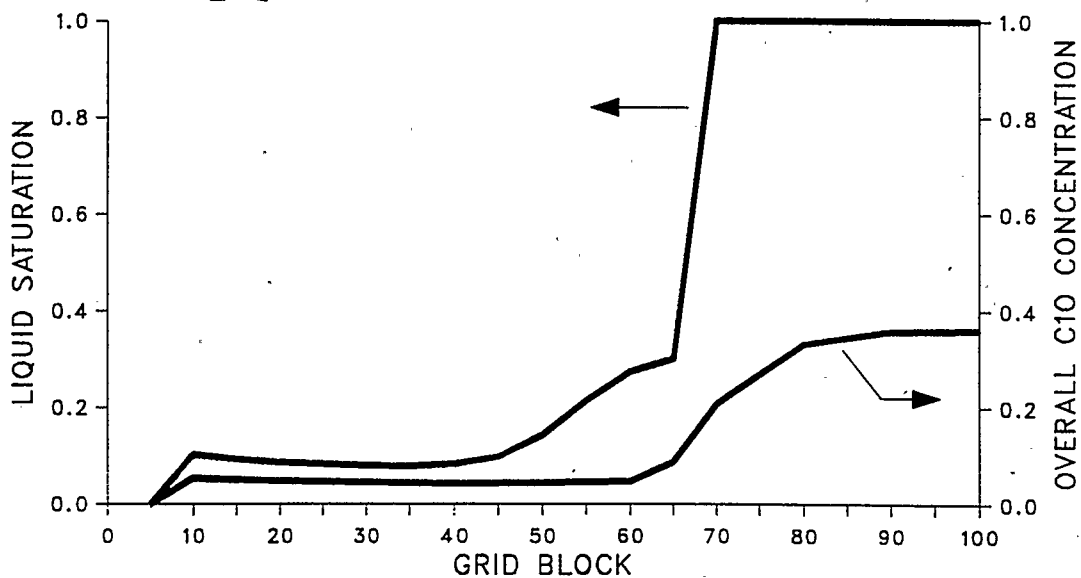
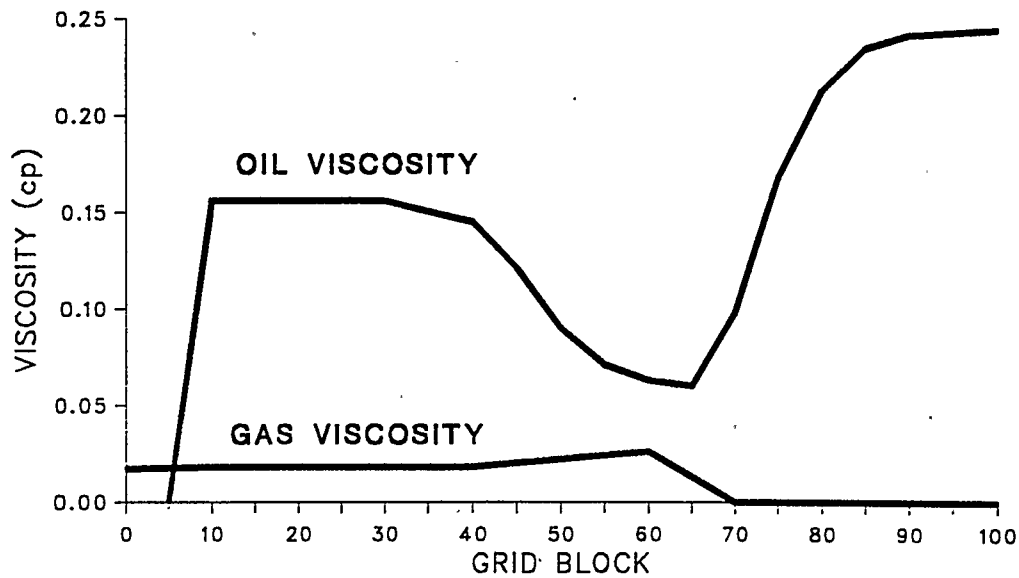
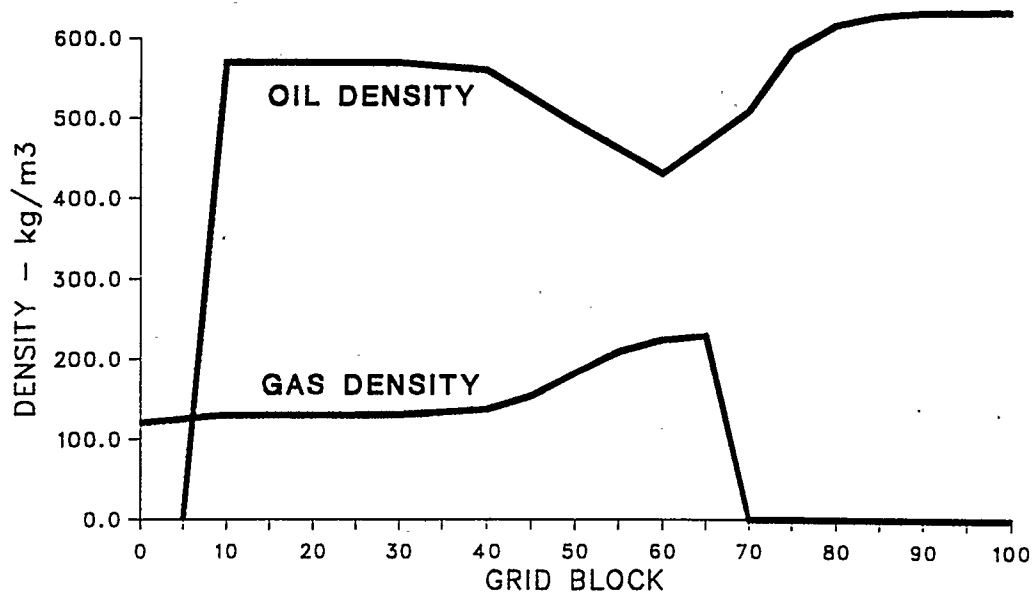
**DISPLACEMENT CHARACTERISTICS FOR FLUID SYSTEM C:E AT
0.7 PVGI USING LINEAR RELATIVE PERMEABILITY CURVE III
AT 19000 kPa (RUN 69)**



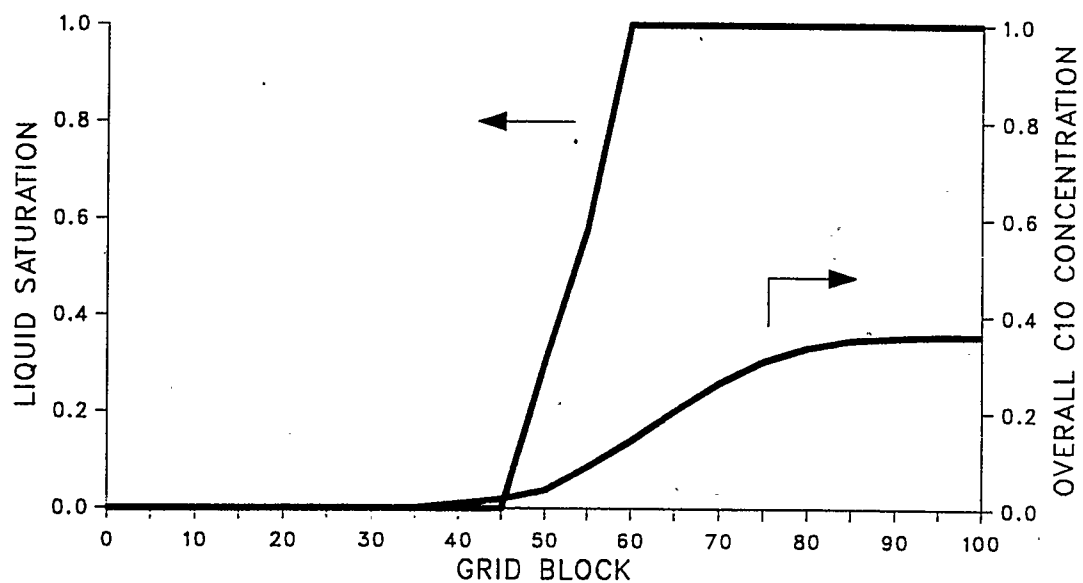
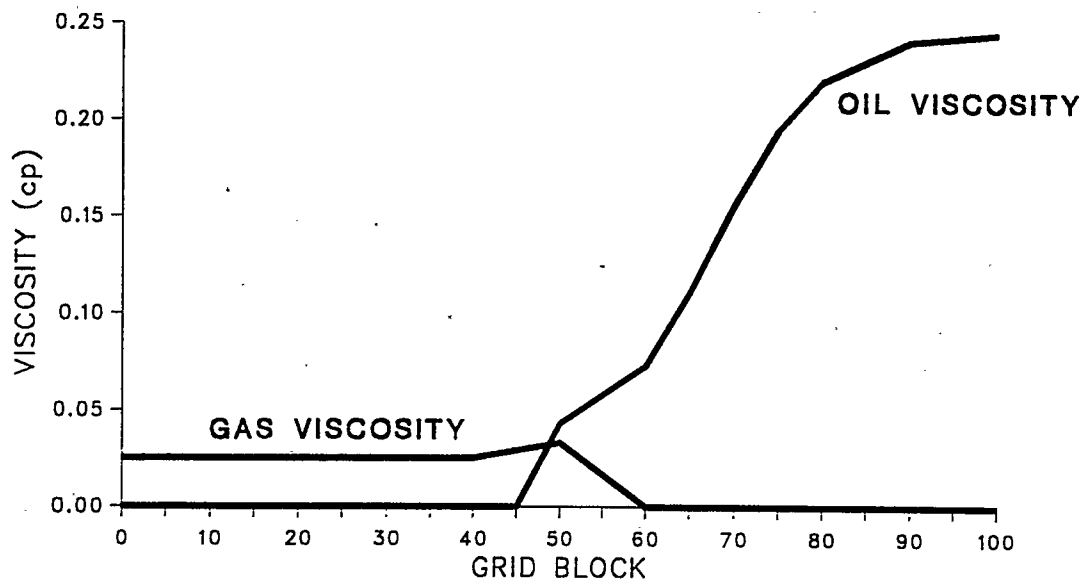
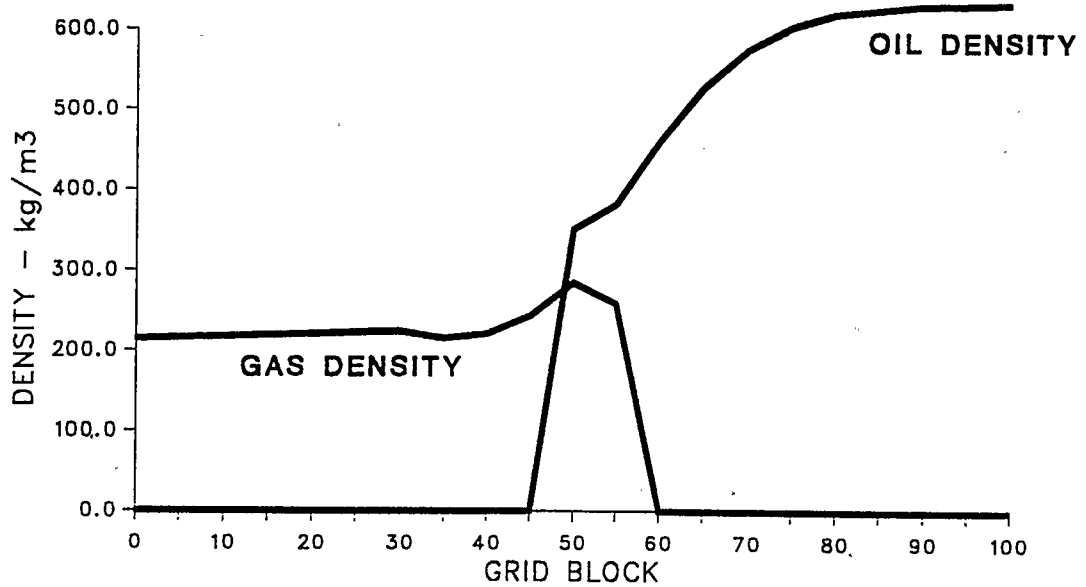
**DISPLACEMENT CHARACTERISTICS FOR FLUID SYSTEM B:M AT
0.7 PVGI USING LINEAR OIL RELATIVE PERMEABILITY CURVE III
AT 19000 kPa (RUN 57)**



**DISPLACEMENT CHARACTERISTICS FOR FLUID SYSTEM A:M AT
0.7 PVGI USING LINEAR OIL RELATIVE PERMEABILITY CURVE III
AT 19000 kPa (RUN 33)**

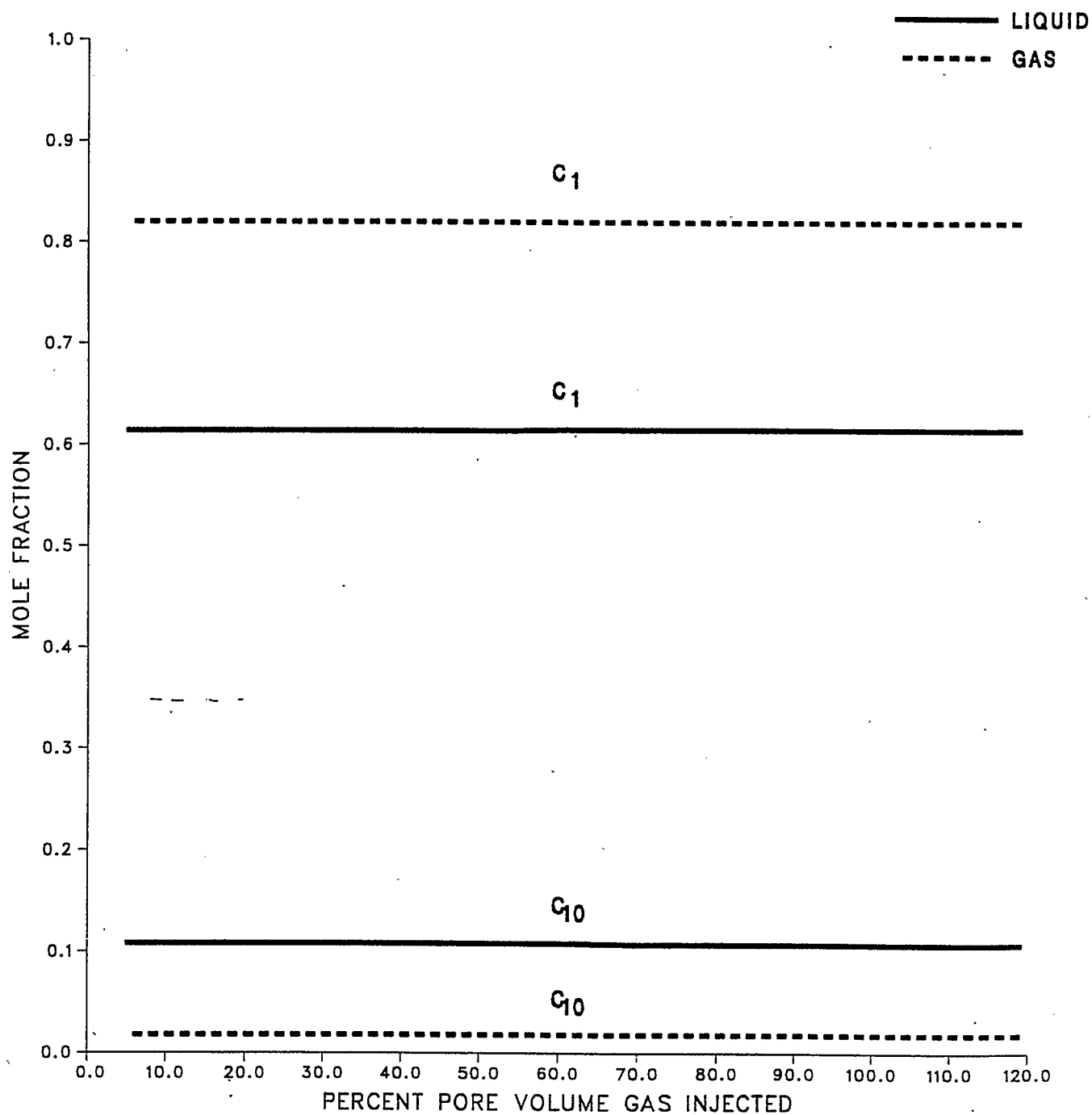


**DISPLACEMENT CHARACTERISTICS FOR FLUID SYSTEM A:Q AT
0.7 PVGI USING LINEAR OIL RELATIVE PERMEABILITY CURVE III
AT 19000 kPa (RUN 45)**

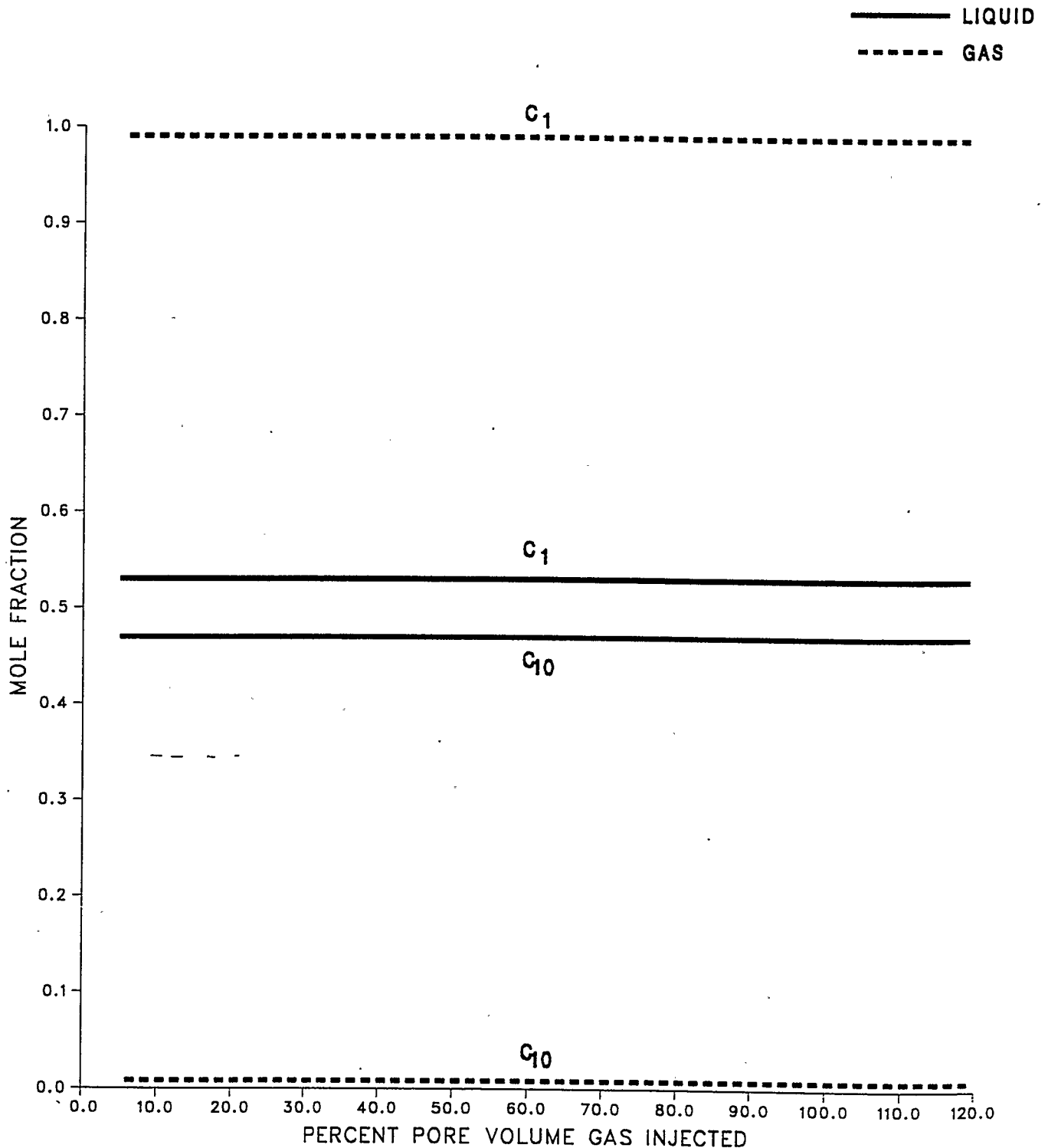


immiscible displacement characteristics for fluid systems D:F, C:E and B:M, with the latter suggesting a modest degree of mass transfer. Figure 25 shows generated or multicontact miscibility for fluid system A:M as the physical properties of the gas and liquid phases become similar at the displacement front. Figure 26 shows a first-contact miscible displacement for fluid system A:Q where the physical properties of the gas and liquid phases become virtually indistinguishable at the displacement front. These results were consistent with the displacement mechanisms considered dominant for each system as previously discussed. However, the "snapshot" portrayal of the displacement process provided limited information on the changes that occurred as the gas-liquid displacement front advanced. To better illustrate these changes, methane and decane concentrations at grid block 50, in the middle of the simulated slim tube, versus pore volume gas injected for each fluid system were shown in Figures 27 to 31, inclusive, using linear oil relative permeability Curve III and at 19000 kPa. These conditions were selected to facilitate comparison with the "snapshot" results shown in Figures 22 to 26, inclusive. The results shown in Figures 29 to 31 clearly illustrate the passing of a displacement front, with an obvious mixing zone where thermodynamic equilibrium was attained between the displaced liquid and displacing gas. Figures 27 and 28 illustrated an equilibrium gas drive for fluid systems D:F and C:E, with constant compositions throughout the displacement. Figure 29 shows a limited degree of mass transfer for fluid

**METHANE AND N-DECANE CONCENTRATIONS AT GRID BLOCK 50
VERSUS PVGI USING LINEAR OIL RELATIVE PERMEABILITY CURVE III
AT 19000 kPa FOR FLUID SYSTEM D:F (RUN 81)**



**METHANE AND N-DECANE CONCENTRATIONS AT GRID BLOCK 50
VERSUS PVGI USING LINEAR OIL RELATIVE PERMEABILITY CURVE III
AT 19000 kPa FOR FLUID SYSTEM C:E (RUN 69)**



**METHANE AND N-DECANE CONCENTRATIONS AT GRID BLOCK 50
VERSUS PVGI USING LINEAR OIL RELATIVE PERMEABILITY CURVE III
AT 19000 kPa FOR FLUID SYSTEM B:M (RUN 57)**

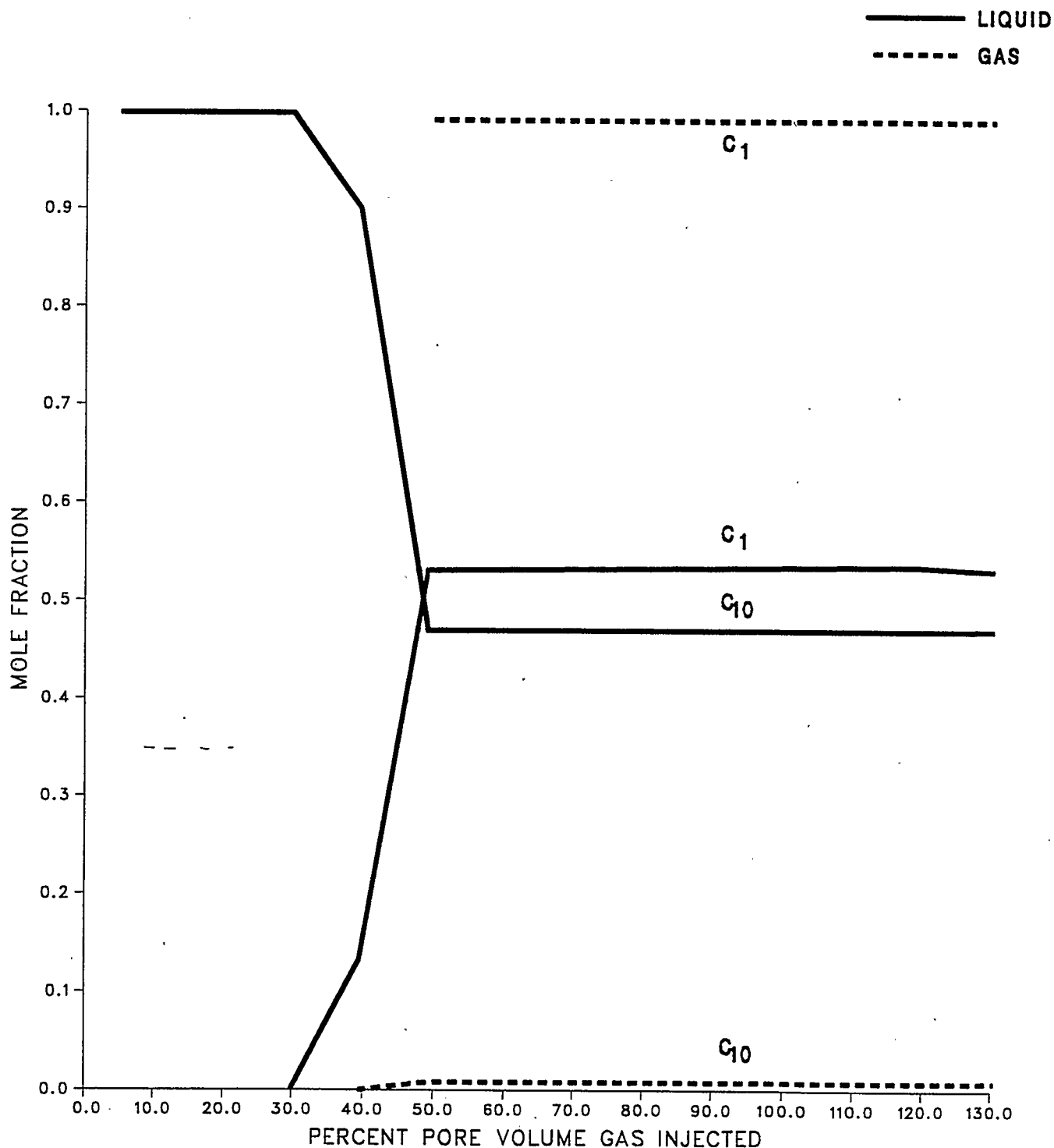


FIGURE 30

**METHANE AND N-DECANE CONCENTRATIONS AT GRID BLOCK 50
VERSUS PVGI USING LINEAR OIL RELATIVE PERMEABILITY CURVE III
AT 19000 kPa FOR FLUID SYSTEM A:M (RUN 33)**

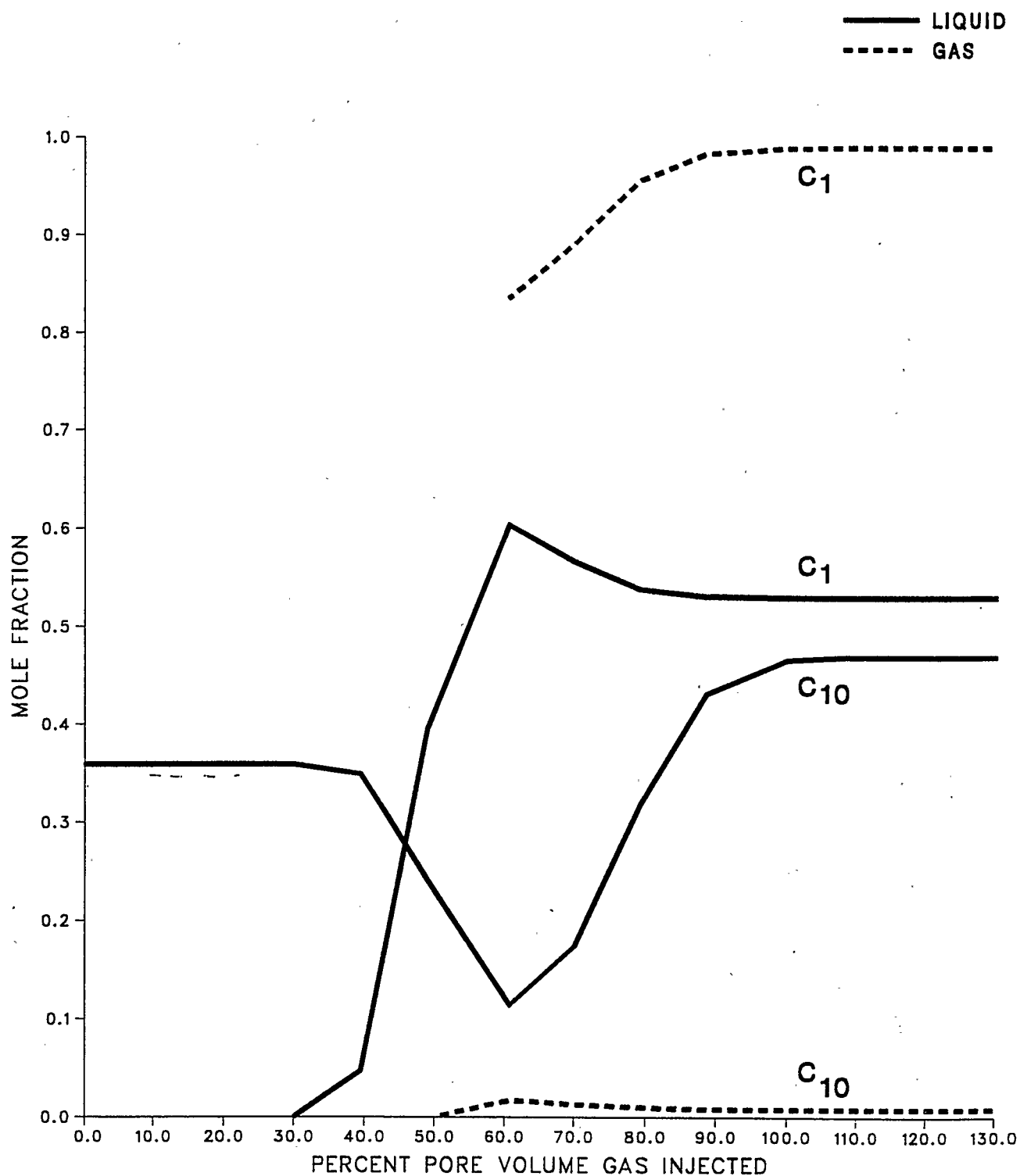
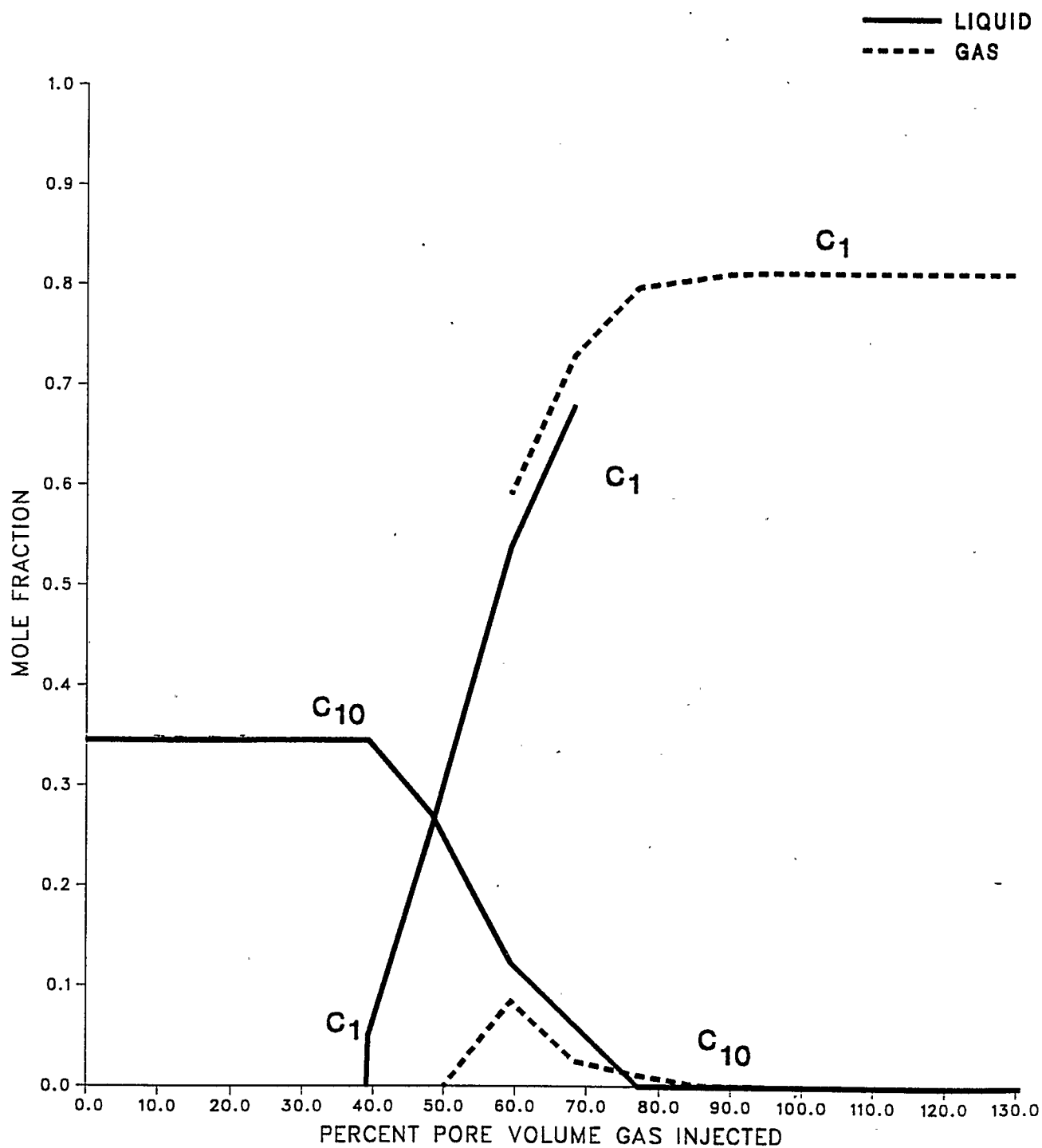


FIGURE 31

**METHANE AND N-DECANE CONCENTRATIONS AT GRID BLOCK 50
VERSUS PVGI USING LINEAR OIL RELATIVE PERMEABILITY CURVE III
AT 19000 kPa FOR FLUID SYSTEM A:Q (RUN 45)**



system B:M until equilibrium compositions similar to fluid system C:E were reached. Figure 30 shows a dynamic miscible displacement for fluid system A:M, with final equilibrium compositions similar to fluid system C:E. These results clearly demonstrate that the mass transfer process acts to recover the intermediate and lighter components of the liquid. Figure 31 shows a first-contact miscible displacement for fluid system A:Q with an obvious transition zone that followed the complete displacement and recovery of the liquid phase. The critical issue, namely the relative efficiency of each displacement, was not immediately obvious from these results.

The effect of pressure and mass transfer on the residual liquid saturations for systems B:M, A:M and A:Q are shown in Figures 32, 33, 34, respectively. Figure 32 showed only a slight change in residual liquid saturation for fluid system B:M as the pressure increased, essentially limited to a modest level of oil vaporization behind the displacement front near the inlet end of the simulated slim tube. Figure 33 shows a transition from an immiscible displacement at 14500 kPa to a miscible displacement at 19000 kPa for fluid system A:M, with a slightly more efficient miscible displacement at 20500 kPa. A zero liquid saturation just behind the displacement front at 20500 kPa occurred when the simulator was unable to distinguish the gas and liquid phases in the critical region. Figure 34 shows a first-contact miscible displacement for fluid system A:Q at

FIGURE 32

**EFFECT OF PRESSURE ON RESIDUAL LIQUID SATURATION
FOR FLUID SYSTEM B:M AT 0.7 PVGI USING
LINEAR OIL RELATIVE PERMEABILITY CURVE III**

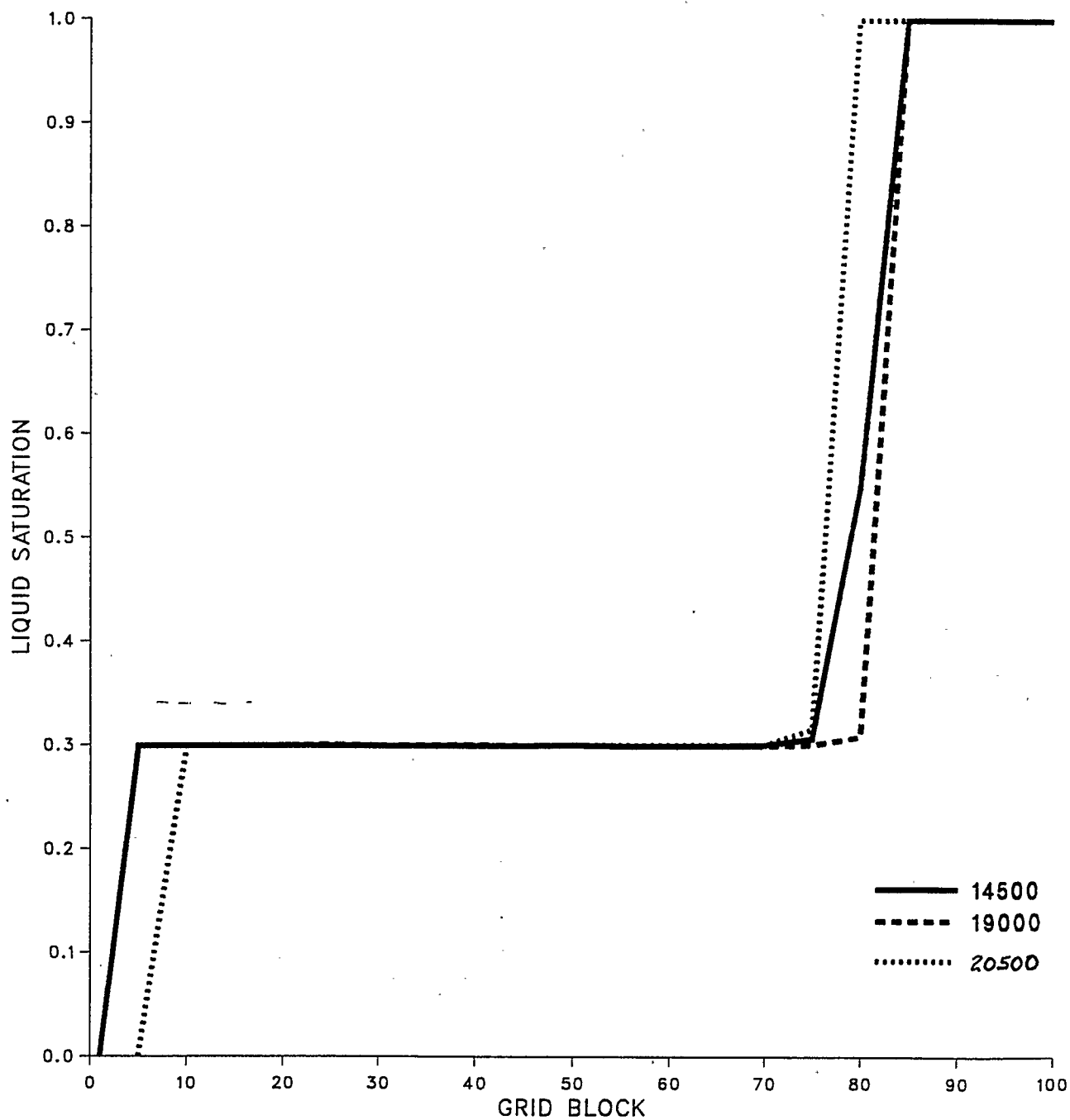


FIGURE 33

**EFFECT OF PRESSURE ON RESIDUAL LIQUID SATURATION
FOR FLUID SYSTEM A:M AT 0.7 PVGI USING
LINEAR OIL RELATIVE PERMEABILITY CURVE III**

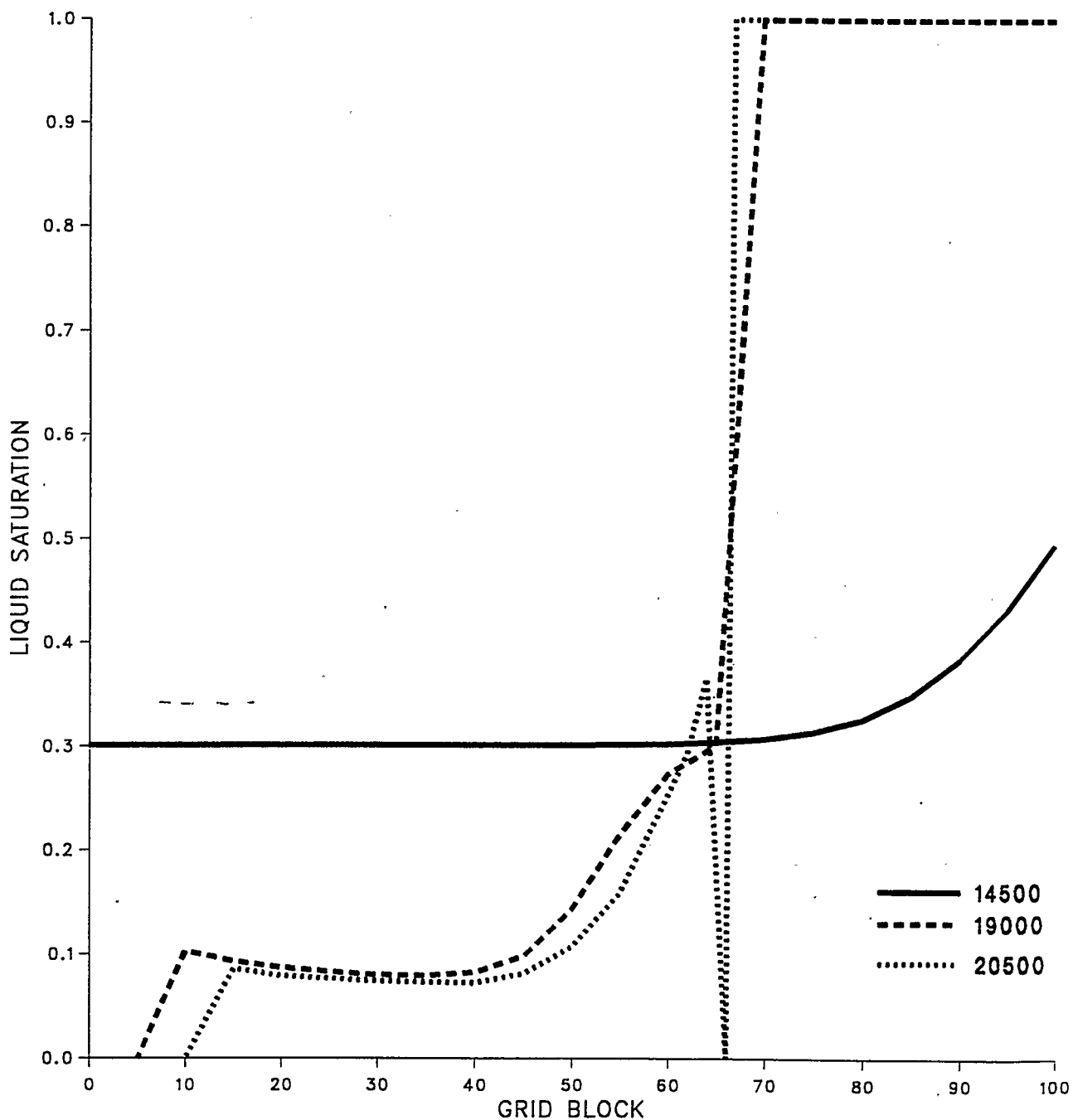
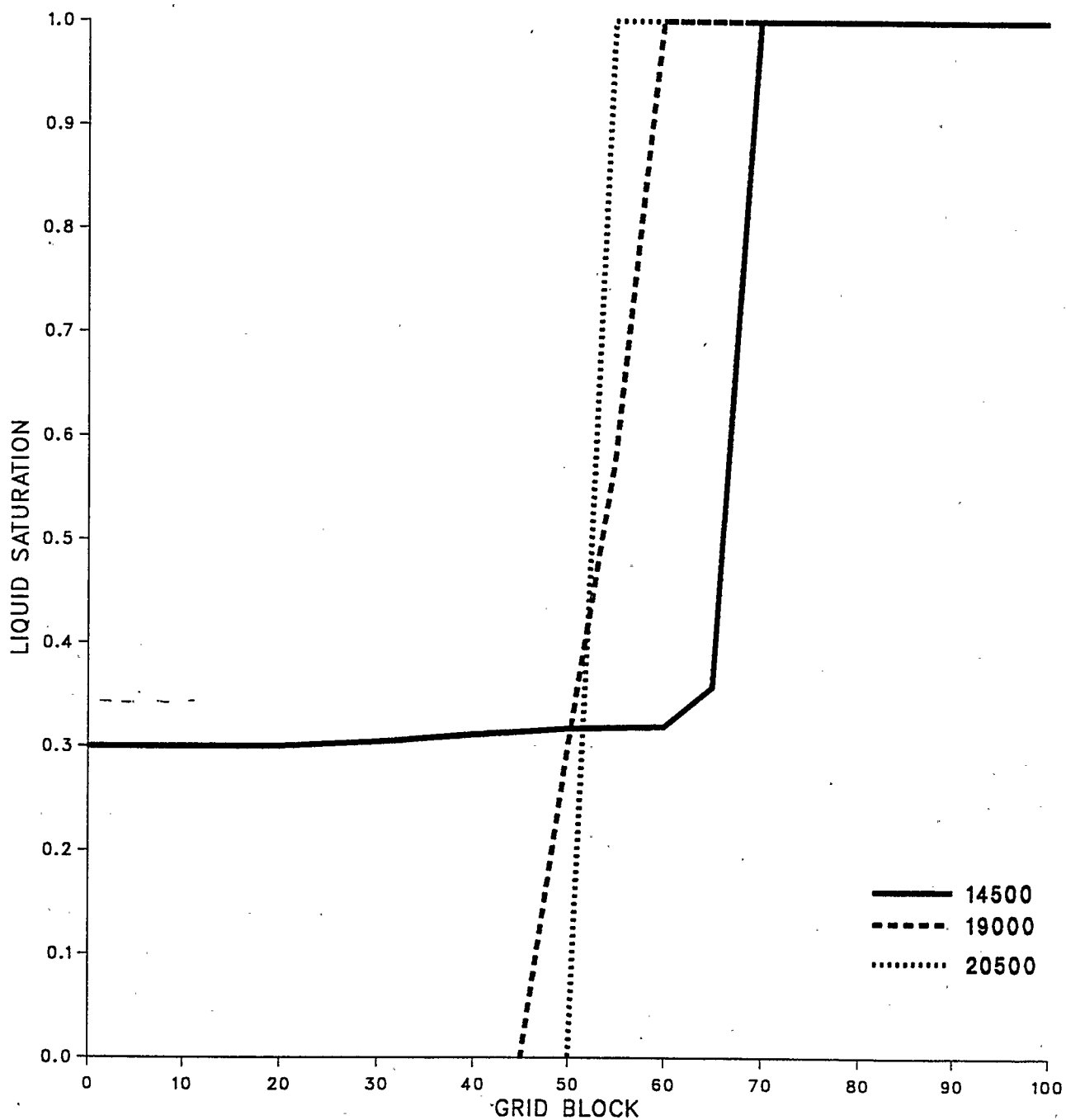


FIGURE 34

**EFFECT OF PRESSURE ON RESIDUAL LIQUID SATURATION
FOR FLUID SYSTEM A:Q AT 0.7 PVGI USING
LINEAR OIL RELATIVE PERMEABILITY CURVE III**



19000 and 20500 kPa. The immiscible displacement characteristics observed at 14500 kPa are misleading in that the active mass transfer between the gas and liquid phases is not apparent, nor is the increased recovery of hydrocarbons observed in the simulation results. With reference to the numerical model results shown on Table 8 for an immiscible residual liquid saturation of 30 percent, this work supports as a criterion for first-contact miscibility the definition used by Cardenas et al [91] who defined miscibility to occur when 90 percent of the liquid was recovered at breakthrough (which, based on this work, would occur at about 1.0 pore volume gas injection). This work is also consistent with Wu et al's [68] criteria of 90 percent oil recovery at 1.2 pore volume gas injection for dynamic miscibility and 99 percent oil recovery at 1.2 pore volume gas injection for first-contact miscibility. It appears that the more straightforward criteria of Cardenas et al [91] result from the fact that only the mixing zone length between the displaced liquid and the displacing gas need be considered in first-contact miscible displacements (limited data [67, 84] suggest that, for well designed slim tube displacement tests, the minimum feasible mixing zone length is about 10 percent of pore volume). By comparison, dynamic miscibility also involves a significant degree of interphase mass transfer, which benefits may not be fully evident at less than 1.2 pore volume gas injection. The results of this work also suggest that quoting liquid recoveries after breakthrough at more than 1.2 pore

volume gas injection may be misleading as solubility (i.e., oil evaporation) effects may so complicate the interpretation of laboratory results as to make their direct application to a field test tenuous and perhaps even unreliable for design calculations. Further research, outside the scope of this investigation, is required to quantify both the magnitude and precise influence of these observed effects upon gas-liquid displacements. The results shown in Figures 32 to 34 clearly demonstrated that the residual liquid saturation decreases as pressure and, hence mass transfer, increased. However, the residual liquid saturation decreased to zero only when thermodynamic first-contact miscibility was achieved. Also, consistent with the published literature, solvent condensation and oil stripping, analogous to the condensing/vaporizing gas drive process, occurred, most noticeably for fluid system A:M. Without more data, a firm conclusion cannot be reached, but it appeared that the occurrence of a vaporizing-gas frontal drive or a condensing-gas drive at the tail end of the process, described by Lee et al [65], was dependent on the characteristics of the particular fluid system as was the highly efficient, immiscible gas drive process. The basic gradation, in terms of linear unit displacement efficiency for two-phase gas-oil systems followed this sequence:

- (1) a purely immiscible lean gas drive with no mass transfer that exhibits a "leaky-piston" displacement behavior since gas

bypasses the liquid as a result of an unfavorable viscosity ratio that yields a low unit displacement efficiency for a given volume of gas injection;

(2) an immiscible gas drive with no mass transfer that as a result of a more favorable viscosity ratio exhibits a more "piston-like" displacement behavior (observed for the equilibrium gas drives studied in this investigation) than the previous case, and yields close to the theoretical maximum unit displacement efficiency for a given volume of gas injection;

(3) a highly efficient, but immiscible gas drive, that significantly benefits from the condensation/vaporization phenomena which improves the effective fractional flow characteristics of the displaced liquid phase;

(4) a dynamic (or multi-contact) miscible displacement process where either the vaporizing or condensing gas-drive process dominates (although both probably occur); and

(5) a thermodynamic first-contact miscible displacement.

The parametric approach used in this investigation was based on limited experimental data and was entirely predictive in nature. The fluid systems in the open literature were not thermodynamically rigorous when presented in a ternary diagram. Public domain data [95] were obtained for twenty slim tube experiments where the liquid was similar to fluid C, and where

four of the tests were performed using a solvent similar to gas E. All twenty slim tube tests were performed at about 14500 kPa and 71°C, comparable to Runs 62 to 65. The results were compared on Table 11 and showed good agreement with those for the longer slim tube. The results from the longer slim tube were reported to provide a better definition of immiscible and miscible displacement, which suggested that the results for the longer slim tube should be used, consistent with findings reported by Flock and Nouar [96].

The other sixteen slim tube experiments used increasingly richer solvents, and while not directly comparable to the results of this numerical model investigation, gave qualitatively similar results. Interestingly, apparent liquid recoveries above 100 percent were observed for the richest solvent, which results were attributed to oil swelling effects. In summary, the numerical model results, while predictive, showed good agreement with actual physical experiments (when such data were obtained).

- - - -

Table 11
Comparison of Predicted and Actual
Liquid Recoveries

| | | <u>PV Oil Produced</u> | |
|------------------|-----------------|------------------------|-----------------|
| | | <u>@ 1.0 PVGI</u> | <u>Ultimate</u> |
| Fluid System C:E | Sor = 0.1 | 0.630 | 0.666 |
| | Sor = 0.3 | 0.533 | 0.539 |
| Forty-Foot Tube | (6 hour test) | 0.481 | 0.500 |
| | (0.5 hour test) | 0.525 | 0.526 |
| Five-Foot Tube | (22 hour test) | 0.716 | 0.732 |
| | (2 hour test) | 0.736 | 0.806 |

Notes:

1. Experimental liquid was 0.413 methane and 0.587 mole fraction n-decane.
2. Experimental gas was 1.000 mole fraction methane.
3. All results based on a slim tube pressure of 14500 kPa and 71° C.

CHAPTER VI - IMPLICATIONS FOR FUTURE RESEARCH

Introduction

The eighty-five numerical model experiments performed in this investigation have been analyzed and evaluated. The results and performance of the numerical model were used to identify areas where future research efforts may be appropriately directed. A separate section on the implications for future research was warranted since the identified areas for potential investigation were more basic and fundamental in nature than expected. Three areas, the simulation of laboratory experiments, phase behavior modelling, and viscous instabilities were examined.

- - - -

Simulation of Laboratory Experiments

Few publications ([89], p. 321) exist respecting the use of numerical models to simulate laboratory experiments. The results of this investigation and the performance of the numerical model has shown that the simulator has a weak or inappropriate treatment of well models for laboratory conditions [86-88]. That limitation fundamentally stems from the assumption that the well inflow and wellbore flow equations at the field scale are also suitable for the different flow regimes and physical geometries existing at the laboratory scale. Consequently, fine details such as the difference in results of slim tube displacement tests that may be observed due to fluid compressibility depending on whether or not an initial pressure gradient exists across the apparatus from the inlet to the outlet end, could not be modelled. The ability to model these fine details is desirable since it would provide the means to resolve uncertainties respecting the significance of what may appear to be minor variations in experimental technique on the reliability of results so obtained. New experimental measurement techniques such as an example application of x-ray computerized tomography reported by Wellington and Vinegar [97] have confirmed the existence of these fine details that are not presently simulated. For example, Wellington and Vinegar described the bypassing of oil in a laboratory coreflood caused by end effects where the flowlines converged to the production

outlet despite adjustments to laboratory equipment to minimize this end effect.

This observed weakness, while not insurmountable, continues to pose a modest logistical barrier to the appropriate use of numerical models to simulate laboratory experiments to either validate the numerical model or to interpret the experimental results. The nature of these identified logistical barriers can also result in a situation where it is almost infeasible to determine precisely what may have caused observed discrepancies between computed and experimental results. In summary, enhancements in the treatment of flow regimes and physical geometries at the laboratory scale are required for numerical models to more accurately simulate these processes.

- - - -

Phase Behavior Modelling

The numerical model experiments performed in this investigation were used as a parametric study of the factors influencing the unit displacement efficiency of gas-liquid displacements in a permeable, porous medium. A precise match of experimental and computed phase behavior was not required in this investigation; even so, some inconvenient, albeit minor, difficulties were encountered. Further research work will likely require a more precise match of computed and experimental phase behavior. Some general improvements that were identified as desirable included:

(1) a need for an improved treatment of critical and near critical fluids in existing two-parameter equations of state (Benmekki and Mansoori [98] reported improved results by using a more appropriate treatment of mixing rules and the unlike three-body attraction);

(2) a need for an improved treatment of the repulsive parameter in two-parameter equations of state to permit a better estimate of liquid densities (Firoozabadi et al [99] reported that better density estimates were obtained with an equation of state that did have a more sophisticated treatment of the repulsive parameter); and

(3) an apparently limited validation of commonly used correlations for estimation of liquid viscosities against

experimental data for fluid systems of interest in petroleum reservoir engineering, particularly for critical and dense gas phase mixtures.

These identified weaknesses fundamentally limit the accuracy of numerical models in regions of the gas-liquid displacement process that are of greatest research and commercial interest. In summary, enhancements in these areas are required for numerical models to more accurately estimate the improvements to unit displacement efficiency for the gradation from a purely immiscible to a thermodynamic first-contact miscible displacement process.

- - -

Viscous Instabilities

The numerical model experiments performed in this investigation also included a grid refinement study that found that the number of grid blocks had to be adjusted to be consistent with the interphase mass transfer between the displaced liquid and the displacing gas behind the displacement front. Numerical model experiments to assess the relationship between the number of grid blocks and viscous forces were not performed. Kremesec and Sebastian [100] found a rough correlation between the number of grid blocks and the gas/liquid viscosity ratio for the displacement of reservoir oils by carbon dioxide in long Berea cores above the minimum miscibility pressure determined from slim tube experiments. However, Kremesec and Sebastian [100] did not perform a rigorous test of the relationship between interphase mass transfer and the number of grid blocks.

These results strongly suggests that there is a relationship between the number of grid blocks, and both viscous forces and mass transfer, in the simulation of gas-liquid displacements in a permeable, porous medium. Some researchers have chosen to characterize the relationship by means of the Peclet number, using an empirically determined "effective mixing coefficient" to describe dispersion (see, for example, Negahban et al [101]) without consideration of the mechanistic basis for the observed results. In summary, further investigation of this topic is

required to fully describe the mechanistic basis for the
observed results.

CHAPTER VII - POTENTIAL INDUSTRIAL SIGNIFICANCE

Introduction

Folden [1] reported that the hydrocarbon miscible gas-liquid displacement process was in use at more than 50 sites within the Province of Alberta in 1987, with nearly 40 of these projects characterized for modelling purposes as a linear vertical gravity-stable process. McCaffery, Sigmund and Wardlaw [102] presented a detailed review and critique of recovery methods in carbonate reservoirs in the Province of Alberta, observing the potential for significant reserves additions by use of miscible gas displacement and other forms of gas-injection operations. Gravity stabilization effects were seen as especially beneficial for vertical displacements. Stelzer [103] demonstrated that models can be reliably used to predict future field performance. The commercial significance of an improved mechanistic understanding of the gas-liquid displacement process that would increase the reliability of numerical models as engineering design tools, with a corresponding reduction of technical risk for the high technology miscible displacement process, is obvious.

A separate section on the potential industrial significance was warranted since the identified areas for potential investigation

were more basic and fundamental in nature than expected. Three areas, miscible flood design and optimization, the use of alternative solvents, and well models were examined.

Miscible Flood Design and Optimization

Industry has been making increasing use of numerical models to design and optimize hydrocarbon recovery projects as shown by published comparative solution projects for commercial reservoir simulators [104-109] and methodologies for engineering control [29-30]. Killough and Kossack [108] presented a comparison of numerical models used to simulate miscible floods, including the numerical model (GEM - General Equation of State Model) used in this investigation, and found reasonable agreement between computed results. However, care had to be taken in the calculation of near well phase mobilities and relative permeabilities when wells were constrained by the flowing bottom hole pressure.

A brief discussion was included herein to clarify the significance of near well and wellbore flow conditions to miscible flood design and optimization when using numerical models. In a field scale project, fluids are produced and injected through a wellbore connecting surface facilities and the subsurface petroleum reservoir. The project operators have, as their only means to influence the performance of the miscible flood, some limited abilities to modify well production performance characteristics by stimulation treatments, the size of the interior tubing, the choice of completion interval (e.g., perforations through the wellbore casing to permit inflow of

fluids from the reservoir) and the use of some form of artificial lift (e.g., pumps) to raise the fluids to the surface. The project operators can more or less control the fluids injected into the petroleum reservoir but cannot directly influence the actual fluid flow in the petroleum reservoir. Therefore, it is crucial that the numerical model adequately represent both the actual physical mechanisms active in the displacement process and the well flow characteristics.

Howes [110] described miscible flood projects in Canada and listed three approaches to increase an inherently low volumetric conformance caused by viscosity ratio and gravity effects:

- (1) gravity stabilization, which is primarily limited to a linear vertical process;
- (2) alternate injection of solvent and water in horizontal miscible floods to limit gravity segregation of the solvent and oil caused by the high density contrast as well as reducing the relative permeability for the flowing gas phase; and
- (3) larger injection volumes of solvent to ensure that more oil is eventually contacted by the solvent.

Tiffin and Kremesec [111] performed a mechanistic evaluation of gravity-assisted miscible flooding and found that it was inherently more efficient than horizontal displacements and that displacement efficiencies increased at lower rates as viscous

fingering decreased. Nutakki [112] examined horizontal miscible displacements in some detail and found that alternate injection of solvent and water may not fully eliminate gravity segregation in the reservoir and that an initial free gas saturation was undesirable since it promoted solvent channeling. Stalkup [61] reported that comparisons of incremental recovery, solvent volume, and solvent richness were "clouded" by the wide variations in reservoir conditions for the various field tests.

However, given the identified limitations of the numerical models used to simulate miscible floods, the results of this investigation do have some bearing on field scale projects:

(1) the highly efficient, immiscible gas-drive process may have some advantages in gravity-stable displacements since there is a higher inherent volumetric conformance and potential benefits from (a) viscous drag effects, (b) vaporization of residual oil behind the displacement front, and (c) gravity drainage of oil at low saturations [46];

(2) the thermodynamic first-contact miscible process may be more desirable in non gravity stable displacements in order to ensure that all oil contacted by the solvent is displaced since viscous fingering [113, 114] acts to decrease volumetric conformance, and, hence, the ultimate oil recovery.

There was an obvious design tradeoff in the above observations. The solvent must, perhaps unconditionally, displace all oil

contacted in a non gravity-stable displacement due to inherent limitations on volumetric conformance. The possible use of less rich solvents for gravity-stable processes recognizes the benefits of gravity drainage and the fact that essentially all oil will be contacted by the solvent due to an inherently high volumetric conformance [110]. However, in non gravity-stable carbon dioxide displacements, the reduced density contrast between the carbon dioxide and the reservoir oil and swelling of the oil by carbon dioxide may reduce somewhat the desirability of employing a first-contact miscible process, since there is some improvement to the effective volumetric conformance as gravity override is reduced. A related, but unresolved, question for gravity stable miscible floods that employ a slug of enriched gas, followed by chase gas, was whether transient gravity segregation of heavier components in the solvent occurred during the life of the project (see Metcalfe et al, [115], and Williams and Dawe, [116]); which would have obvious design implications for the solvent slug process. In summary, fundamental limitations on the reliability of numerical models need to be addressed to reduce the technical risk of the high technology miscible displacement process used widely in the Province of Alberta.

Use of Alternative Solvents

The use of alternative solvents proceeds directly from the previous section where possible advantages of using a highly efficient immiscible gas drive in a gravity-stabilized displacement were discussed. The obvious injection gas was nitrogen, which can be readily extracted from the atmosphere and used at any geographic location. Sayegh et al [117] performed static thermodynamic miscibility experiments, and consistent with Nutakki [112], found that minimum miscibility pressures significantly increased with higher nitrogen content. Sayegh et al [118] also performed slim tube displacement tests using nitrogen and found that although a high oil recovery was observed, miscibility was not achieved at reservoir conditions.

Mechanistic aspects of gravity-stable nitrogen displacements have been investigated by Ypma [119]. Doscher et al [120] found that nitrogen was about as efficient as carbon dioxide in the displacement of crude oil in a gravity stabilized system and stated that it may result from gas drive effects (e.g., viscous drag and relative permeability) being more important than oil swelling and solution effects. Other workers [121-123] have experimentally confirmed that gravity stable immiscible nitrogen displacements can achieve very high displacement efficiencies at certain conditions. These results suggest that conventional slim tube displacement tests may not be the most appropriate

means to evaluate gravity stabilized nitrogen displacements.

Sayegh et al [118] also performed vertical corefloods using a core 28.6 centimetres in length. However, Omole and Osoba [124] reported data for gas-liquid displacements in 50, 150, and 600 centimetre long vertical sandpacks that clearly showed breakthrough recoveries to increase with length, contrary to reported findings for conventional slim tubes [95, 96]. The available data strongly suggest that conventional slim tube tests may underestimate the potential recovery of gravity stabilized nitrogen displacements in field applications. The economics for a highly efficient, immiscible nitrogen gas drive could be enhanced if byproduct oxygen were used in an adjacent fireflood.

In summary, the use of other drive gases such as nitrogen in gravity-stable displacements may warrant more serious consideration and possible field testing once mechanistic and performance uncertainties are resolved.

- - - -

Well Models

Well models used in the simulation of field scale projects are generally assumed to have a radial flow regime while laboratory displacements are assumed to have a linear flow regime [86]. The assumption of a radial flow regime, however, may not be an adequate approximation of the spherical flow regime that does occur in some instances (see Muskat [125]), unless a very refined grid is used. Williamson and Chappelle [126, 127] reviewed the theory and implementation of well models in numerical reservoir simulators and stated, consistent with Killough and Kossack [108], that "some near-well effects may be simulated inadequately", such as the productivity for an injection well, the productivity indices of slanted wells, and backflow. Pedrosa and Aziz [128] described the use of a hybrid grid to improve the treatment of near wellbore flow in field scale simulations. A cylindrical (or elliptical) grid was used for the well blocks with a cartesian grid elsewhere. It was necessary to partially decouple the solution of the flow equations for the well and reservoir regions in order to minimize the imposition of small timestep sizes caused by rapid saturation changes in the vicinity of the wellbore. Pedrosa and Aziz [128] stated that decoupling may not be feasible when a fully implicit treatment is required, which could significantly reduce the savings in computational expense for this approach since small timesteps may be required. Tang and Peaceman [129]

compared analytical and numerical solutions and the effect of boundary conditions on the radial dispersion of solute around an injection well in order to reduce the uncertainties associated with the use of simulators to design enhanced oil recovery projects. Carey and Chow [130] developed a more general treatment of well singularities in reservoir simulation that rigorously verified some existing approaches and allowed for treatment of irregular grids and variable permeability.

The basic engineering problem is that coarse grids are adequate to define reservoir scale flow, while refined grids are necessary to predict solvent breakthrough and coning in miscible processes. In addition, as previously discussed, there are limitations on the adequacy of the theoretical treatment of well boundary conditions in field scale simulation. These concerns are being addressed [131, 132], and may facilitate the direct evaluation of the potential for alternative well configurations such as horizontal wells [133] which are used on an experimental basis [134] at six sites in the Province of Alberta (as of August, 1988). Future enhancements may eliminate the need to treat horizontal wells as a series of point source/sinks in adjacent grid blocks to approximate the actual line source/sink behavior.

In summary, enhancements to field scale reservoir simulation well models are required to facilitate future research and more reliable simulation of design alternatives for field scale

projects.

- - -

CHAPTER VIII - SUMMARY OF RESEARCH FINDINGS

1. Mass transfer between the displaced liquid and displacing gas, when it occurs, dominates the unit displacement efficiencies observed in the numerical model experiments performed in this investigation.

2. There exists a gradation in unit displacement efficiencies between purely immiscible and thermodynamic first-contact miscible displacement, largely caused by mass transfer.

3. Relative permeability and viscosity ratio effects are of secondary importance respecting unit displacement efficiencies by comparison to mass transfer effects caused by variations in the operating pressure or the composition of the displacing drive gas.

4. The highly efficient, immiscible gas drive process, that benefits from mass transfer effects, and the dynamic miscibility process are preferred design alternatives for gravity stabilized gas-liquid displacements.

5. Numerical models can be employed to investigate mechanistic aspects of gas-liquid displacements in a permeable, porous medium.

CHAPTER IX - REFERENCES

- [1] Folden, C.G.: "Enhanced Recovery of light and medium crude oil in Canada", The Journal of Canadian Petroleum Technology (January - February 1987) 37-43.
- [2] Novosad, Zdenka and Costain, Terry: "New interpretation of recovery mechanisms in enriched gas drives", The Journal of Canadian Petroleum Technology (March - April 1988) 54-60.
- [3] Stone, H.L. and Crump, J.S.: "The Effect of Gas Composition Upon Oil Recovery By Gas Drive", Petroleum Trans. AIME, v. 207 (1956) 105-110.
- [4] Kehn, D.M., Pyndus, G.T., and Gaskell, M.H.: "Laboratory Evaluation of Prospective Enriched Gas-Drive Projects", Petroleum Trans. AIME, v. 213 (1958) 382-385.
- [5] Kerr, W.E.: "Retlaw Upper Mannville 'V' Pool unit experimental carbon dioxide flood", The Journal of Canadian Petroleum Technology (January - February 1985) 64-65.
- [6] Ko, S.C.M., Stanton, P.M. and Stephenson, D.J.: "Tertiary recovery potential of CO₂ flooding in Joffre Viking Pool, Alberta", The Journal of Canadian Petroleum Technology (January - February 1985) 36-43.
- [7] Wagner, O.R. and Leach, R.O.: "Effect of Interfacial Tension on Displacement Efficiency", Soc. Pet. Eng. J. (Dec. 1966)

335-344.

[8] Hutchinson Jr., C.A. and Braun, P.H.: "Phase Relations of Miscible Displacement in Oil Recovery", AICHE J. (March 1961) Vol. 7, 64-72.

[9] Society of Petroleum Engineers: "Surfactant/Polymer Chemical Flooding, Vols. I & II", SPE Reprint Series No. 24, 1988.

[10] Society of Petroleum Engineers: "Miscible Processes", SPE Reprint Series No. 8, 1965.

[11] Simon, Ralph, Rosman, A. and Zana, Erdinc: "Phase-Behavior Properties of CO₂ - Reservoir Oil Systems", Soc. Pet. Eng. J. (Feb. 1978) 20-26.

[12] Holm, L.W.: "Status of CO₂ and Hydrocarbon Miscible Oil Recovery Methods", J. Pet. Tech. (Jan. 1976) 76-84.

[13] Coats, K.H.: "An Equation of State Compositional Model", Soc. Pet. Eng. J. (Oct. 1980), see also SPE Reprint Series No. 20, Numerical Simulation II (1986).

[14] Collins, D.A., Nghiem, L.X. and Li, Y.K.: "An Efficient Approach to Adaptive-Implicit Compositional Simulation With an Equation of State", SPE 15133, April 1986.

[15] Peng, D.Y. and Robinson, D.B.: "A New Two-Constant Equation of State", Ind. Eng. Chem. Fund. (1976) Vol. 15,

59-64.

[16] Firoozabadi, Abbas and Aziz, Khalid: "Analysis and Correlation of Nitrogen and Lean-Gas Miscibility Pressure", SPERE (Nov. 1986) 575-582.

[17] Nghiem, L.X., Fong, D.K. and Aziz, K.: "Compositional Modelling With an Equation of State", Soc. Pet. Eng. J. (Dec. 1981) 687-98.

[18] Computer Modelling Group: "CMGPROP Technical Manual, Phase Behavior Package, Version 4.0", March 1988.

[19] Computer Modelling Group: "GEM Program Manual, Equation-of-State Compositional Model, Version 2.3", August 1987.

[20] Reamer, H.H., Fiskin, J.M. and Sage, B.H.: "Phase Equilibria in Hydrocarbon Systems, Phase Behavior in the Methane-n-Butane-Decane System at 160°F", Research on Occurrence and Recovery of Petroleum 1948-1949, The Lord Baltimore Press, Baltimore (1950) 20-24.

[21] Wu, R.S. and Batycky, J.P.: "Pseudocomponent Characterization for Hydrocarbon Miscible Displacement", SPERE (Aug. 1988) 875-883.

[22] Behrens, R.A. and Sandler, S.I.: "The Use of Semicontinuous Description To Model the C7+ Fraction in Equation

of State Calculations", SPERE (Aug. 1988) 1041-1047.

[23] Wu, R.S.: "C7+ Characterization for Fluid Properties Predictions", Petroleum Society of CIM Paper No. 88-39-88, presented at the 39th Annual Technical Meeting of the Petroleum Society of CIM held in Calgary, June 12-16, 1988.

[24] Jhaveri, Bharat S. and Youngren, Gary K.: "Three-Parameter Modification of the Peng-Robinson Equation of State To Improve Volumetric Predictions", SPERE (Aug. 1988) 1033-1040.

[25] Peneloux, A., Rauzy, E. and Freze, R.: "A Consistent Correction for Redlich - Kwong - Soave Volumes", Fluid Phase Equilibria (1982) Vol. 8, 7-23.

[26] Reid, Robert C., Prausnitz, John M. and Sherwood, Thomas K.: The Properties of Gases and Liquids, Third Edition (1977) McGraw-Hill Book Company.

[27] Prats, Michael: Thermal Recovery, SPE Monograph Volume 7 (1982).

[28] Aziz, Khalid and Settari, Antonin: Petroleum Reservoir Simulation, Applied Science Publishers, London and New York (1979).

[29] Saleri, N.G. and Toronyi, R.M.: "Engineering Control in Reservoir Simulation: Part I", SPE 18305 prepared for presentation at the 63rd Annual Technical Conference and

Exhibition of the Society of Petroleum Engineers held in Houston, TX, October 2-5, 1988.

[30] Toronyi, R.M. and Saleri, N.G.: "Engineering Control in Reservoir Simulation: Part II", SPE 17937 prepared for presentation at the SPE Middle East Oil Technical Conference and Exhibition held in Manama, Bahrain, 11-14 March, 1989.

[31] Emanuel, A.S., Behrens, R.A. and McMillen, T.J.: "A Generalized Method for Predicting Gas/Oil Miscibility", SPERE (Sept. 1986) 463-473.

[32] Sigmund, Philip M., and Cameron, Audrey M.: "Recovery of Retrograde Condensed Liquids by Revaporization During Dry Gas Injection", The Journal of Canadian Petroleum Technology (January - March, 1977) 64-76.

[33] Macdonald, I.F. and Dullien, F.A.L.: "Correlating Tertiary Oil Recovery in Water-Wet Systems", J. Pet. Tech. (Feb. 1976) 7-9.

[34] Rošmaň, A. and Simon, R.: "Flow Heterogeneity in Reservoir Rocks", J. Pet. Tech. (Dec. 1976) 1427-1429.

[35] Chatzis, I. and Dullien, F.A.L.: "Modelling Pore Structure by 2-D and 3-D Networks With Application to Sandstones", The Journal of Canadian Petroleum Technology (January - March, 1977) 97-108.

[36] Yadav, G.D., Dullien, F.A.L., Chatzis, I. and Macdonald, F.: "Microscopic Distribution of Wetting and Nonwetting Phases in Sandstones During Immiscible Displacements", SPERE (May 1987) 137-147.

[37] Morrow, N.R., Chatzis, I. and Taber, J.J.: "Entrapment and Mobilization of Residual Oil in Bead Packs", SPERE (Aug. 1988) 927-934.

[38] Mahers, Eric G. and Dawe, Richard A.: "Gravitational Effects During Diffusional Mass Transfer at the Pore Scale", SPEFE (April 1986) 184-192.

[39] Gardner, J.W. and Ypma, J.G.J.: "An Investigation of Phase-Behavior/Macroscopic-Bypassing Interaction in CO₂ Flooding", SPE Reprint Series No. 18, Miscible Processes II, 1985 Edition (see also Soc. Pet. Eng. J., Oct. 1984, 508-20).

[40] Coats, K.H. and Smith, B.D.: "Dead-End Pore Volume and Dispersion in Porous Media", SPE Reprint Series No. 18, Miscible Processes II (1985 Edition) 290-301.

[41] Bretz, Robert E. and Orr Jr., Franklin M.: "Interpretation of Miscible Displacements in Laboratory Cores", SPERE (Nov. 1987) 492-500.

[42] Bretz, R.E., Specter, R.M. and Orr Jr., F.M.: "Effect of Pore Structure on Miscible Displacement in Laboratory Cores", SPERE (Aug. 1988) 857-866.

[43] Jasti, Jay K., Vaidya, Ramimadhav N., and Fogler, H. Scott: "Capacitance Effects in Porous Media", SPERE (Nov. 1988) 1207-1214.

[44] Martin, William Earl and Young, M.N.: "The Wizard Lake D-3A Pool Miscible Flood", SPE Reprint Series No. 18, Miscible Processes II, 1985 Edition.

[45] Chen, S.M., Olynyk, J. and Asgarpour, S.: "Effect of multiple-contact miscibility on solvent slug size determination", The Journal of Canadian Petroleum Technology (May - June, 1986) 29-35.

[46] Salathiel, R.A.: "Oil Recovery by Surface Film Drainage in Mixed-Wettability Rocks", J. Pet. Tech. (Oct. 1973) 1216-1224.

[47] Sigmund, Phillip M.: "Prediction of Molecular Diffusion At Reservoir Conditions. Part I - Measurement and Prediction of Binary Dense Gas Diffusion Coefficients", The Journal of Canadian Petroleum Technology (April - June, 1976) 48-57.

[48] Sigmund, Phillip M.: "Prediction of Molecular Diffusion At Reservoir Conditions. Part II - Estimating the Effects of Molecular Diffusion and Convective Mixing In Multicomponent Systems", The Journal of Canadian Petroleum Technology (July - September, 1976) 53-62.

[49] Renner, T.A.: "Measurement and Correlation of Diffusion Coefficients for CO₂ and Rich-Gas Applications", SPERE (May

1988) 517-523.

[50] Grogan, A.T., Pinczewski, V.W., Ruskauff, Gregory J. and Orr Jr., F.M.: "Diffusion of CO₂ at Reservoir Conditions: Models and Measurement", SPERE (Feb. 1988) 93-102.

[51] Asgarpour, S., Singhal, A.K., Card, C.C., Wong, T.W. and Springer, S.: "Re-Evaluation of Solvent Requirements for a Hydrocarbon Miscible Flood", SPERE (Feb. 1988) 227-234.

[52] Aziz, K., Bories, S.A. and Combarnous, M.A.: "The Influence of Natural Convection in Gas, Oil and Water Reservoirs", The Journal of Canadian Petroleum Technology (April - June, 1973) 41-47.

[53] Reiss, Louis H.: The Reservoir Engineering Aspects of Fractured Formations, Gulf Publishing Company, 1980.

[54] Van-Quy, N., Simandoux, P. and Corteville, J.: "A Numerical Study of Diphasic Multicomponent Flows", Soc. Pet. Eng. J. (April 1972) 171-84.

[55] Sandrea, Rafael, and Nielsen, Ralph F.: Dynamics of Petroleum Reservoirs Under Gas Injection, Gulf Publishing Company (1974).

[56] Craig Jr., F.F.: The Reservoir Engineering Aspects of Waterflooding, SPE Monograph Volume 3 (1971).

[57] Willhite, G. Paul: Waterflooding, SPE Textbook (1986).

[58] Brandner, C.F. and Slotboom, R.A.: "Vertical Immiscible Displacement Experiments in a Non-Homogeneous Flow Cell", Paper No. 374014 presented at the 25th Annual Technical Meeting of the Petroleum Society of CIM in Calgary, May 7-10, 1974.

[59] Lenormand, R.: "Scaling Laws for Immiscible Displacements With Capillary and Viscous Fingering", SPE 15390 prepared for presentation at the 61st Annual Technical Conference and Exhibition of the Society of Petroleum Engineers held in New Orleans, LA, October 5-8, 1986.

[60] Wang, F.H.L.: "Effect of Wettability Alteration on Water/Oil Relative Permeability, Dispersion and Flowable Saturation in Porous Media", SPERE (May 1988) 617-628.

[61] Stalkup Jr., Fred I.: Miscible Displacement, SPE Monograph Volume 8 (1983).

[62] Stalkup Jr., Fred I.: "Displacement Behavior of the Condensing/Vaporizing Gas Drive Process", SPE 16715 prepared for presentation at the 62nd Annual Technical Conference and Exhibition of the Society of Petroleum Engineers held in Dallas, TX September 27-30, 1987.

[63] Stalkup Jr., Fred I.: "Effect of Gas Enrichment and Numerical Dispersion on Compositional Simulator Predictions of Oil Recovery in Reservoir Condensing and Condensing/Vaporizing Gas Drives", SPE 18060 prepared for presentation at the 63rd

Annual Technical Conference and Exhibition of the Society of Petroleum Engineers held in Houston, TX October 2-5, 1988.

[64] Mansoori, J. and Gupta, S.P.: "An Interpretation of the Displacement Behavior of Rich Gas Drives Using An Equation-of-State Compositional Model", SPE 18061 prepared for presentation at the 63rd Annual Technical Conference and Exhibition of the Society of Petroleum Engineers held in Houston, TX October 2-5, 1988.

[65] Lee S-T., Lo, H. and Dharmawardhana, B.T.: "Analysis of Mass Transfer Mechanisms Occurring in Rich Gas Displacement Process", SPE 18062 prepared for presentation at the 63rd Annual Technical Conference and Exhibition of the Society of Petroleum Engineers held in Houston, TX October 2-5, 1988.

[66] Zick, A.A.: "A Combined Condensing/Vaporizing Mechanism in the Displacement of Oil by Enriched Gases", SPE 15493 presented at the 61st Annual Technical Conference and Exhibition of the Society of Petroleum Engineers held in New Orleans, LA Oct. 5-8, 1986. - - - -

[67] Hall, H.N. and Geffen, T.M.: "A Laboratory Study of Solvent Flooding", Petroleum Trans. AIME, v. 210 (1957) 48-57.

[68] Wu, R.S., Batycky, J.P., Harker, B. and Rancier, D.: "Enriched gas displacement: design of solvent compositions", The Journal of Canadian Petroleum Technology (May - June 1986)

55-59.

[69] Sigmund, P., Sharma, H., Sheldon, D. and Aziz, K.: "Rate Dependence of Unstable Waterfloods", SPERE (May 1988) 401-409.

[70] Fayers, F. John and Newley, Trevor M. J.: "Detailed Validation of an Empirical Model for Viscous Fingering With Gravity Effects", SPERE (May 1988) 542-550.

[71] Stewart, L.D. and Udell, K.S.: "Mechanisms of Residual Oil Displacement by Steam Injection", SPERE (No. 1988) 1233-1242.

[72] Sibbald, L.R., Novosad, Z. and Costain, T.G.: "Analysis of One-Dimensional Rich Gas Displacements With An Equation of State Simulator", Petroleum Society of CIM Paper No. 89-40-5, presented at the 40th Annual Technical Meeting of the Petroleum Society of CIM held in Banff, May 28 to 31, 1989.

[73] Novosad, Z., Sibbald, L.R. and Costain, T.G.: "Design of Miscible Solvents For A Rich Gas Drive Comparison of Slim Tube Tests With Rising Bubble Tests", Petroleum Society of CIM Paper No. 89-40-3, presented at the 40th Annual Technical Meeting of the Petroleum Society of CIM held in Banff, May 28 to 31, 1989.

[74] Christiansen, Richard L. and Haines, Hiemi Kim: "Rapid Measurement of Minimum Miscibility Pressure With the Rising-Bubble Apparatus", SPERE (Nov. 1987) 523-527.

[75] Settari, A. and Karcher, B.: "Simulation of enhanced

recovery projects - the problems and the pitfalls of the current solutions", The Journal of Canadian Petroleum Technology (November - December 1985) 22-28.

[76] Bennion, D.W. and Stewart, B.: "Simulation of a directly miscible vertical displacement hydrocarbon solvent flood", The Journal of Canadian Petroleum Technology (January February 1987) 97-103.

[77] Private Meeting With Y.K. Li, Computer Modelling Group, August 23, 1989.

[78] Novosad, Z. and Costain, T.G.: "Mechanisms of Miscibility Development in Hydrocarbon Gasdrives: New Interpretation", SPERE (Aug. 1989) 341-347.

[79] Giraud, A., Thomere, R., Gard, J. and Charles, M.: "A Laboratory Investigation Confirms the Relative Inefficiency of True Miscible Drives, and Outlines New Concepts for Maximizing Oil Recovery by Gas Injection", SPE 3486, presented at the 46th Annual Fall Meeting of the Society of Petroleum Engineers, New Orleans, LA, Oct. 3-6, 1971.

[80] Auxiette, G. and Chaperon, I.: "Injection de Gaz Miscible sur Modeles Lineares, Analyse Compositionnelle et Experimentales", paper presented at the Second European Symposium on Enhanced Oil Recovery of ARTEP, Paris, France, Nov. 8-10, 1982.

[81] Arthur, K.B., Rioche, M.A. and Sakthikumar, Soma: "The Use of a 3-D Compositional Numerical Reservoir Model in the Design of a Miscible Gas Injection Project", SPE 11484 presented at the Middle East Oil Technical Conference of the Society of Petroleum Engineers held in Manama, Bahrain, March 14-17, 1983.

[82] Bardon, C. and Longeron, D.G.: "Influence of Very Low Interfacial Tensions on Relative Permeability", Soc. Pet. Eng. J. (Oct. 1980) 391-401.

[83] Randall, T.E. and Bennion, D.B.: "Recent developments in slim tube testing for hydrocarbon-miscible flood (HCMF) solvent design", The Journal of Canadian Petroleum Technology (November - December 1988) 33-44.

[84] Randall, T.E. and Bennion, D.B.: "Laboratory factors influencing slim tube test results", The Journal of Canadian Petroleum Technology (July - August 1989) 60-70.

[85] Yellig, W.F. and Metcalfe, R.S.: "Determination and Prediction of CO₂ Minimum Miscibility Pressures", J. Pet. Tech. (Jan. 1980) 160-68 (see also SPE Reprint Series No. 18, Miscible Processes II, 1985 Edition).

[86] Christman, P.G. and Gorell, S.B.: "A Comparison of Laboratory and Field-Observed CO₂ Tertiary Injectivity", SPE 17335 prepared for presentation at the SPE/DOE Enhanced Oil Recovery Symposium held in Tulsa, Oklahoma, April 17-20, 1988.

[87] Ong, Tee S. and Butler, Roger M.: "Wellbore Flow Resistance in Steam-Assisted Gravity Drainage", Petroleum Society of CIM Paper No. 89-40-58 presented at the 40th Annual Technical Meeting of the Petroleum Society of CIM held in Banff, May 28 to 31, 1989.

[88] Fassihi, Mohammad R.: "Estimation of relative permeability from low rate, unsteady-state tests - a simulation approach", The Journal of Canadian Petroleum Technology (May-June 1989) 29-38.

[89] Society of Petroleum Engineers: Numerical Simulation II, SPE Reprint Series No. 20, 1986 Edition.

[90] Sigmund, P.M., Aziz, K., Lee, J.I., Nghiem, L.X. and Mehra, R.: "Laboratory CO₂ Floods and Their Computer Simulation", Proc. 10th World Pet. Cong., Bucharest (1979) Vol. 3, 243-50 (see also SPE Reprint Series No. 18, Miscible Processes II, 1985 Edition).

[91] Cardenas, R.L., Alston, R.B., Nute, A.J. and Kokolis, J.P.: "Laboratory Design of a Gravity-Stable, Miscible CO₂ Process", J. Pet. Tech. (Jan. 1984) 111-18 (see also SPE Reprint Series No. 18, Miscible Processes II, 1985 Edition).

[92] Alonso, M. Morineau, Y., Simandoux, P., Bradshaw, A.D., and Bennion, D.W.: "A Laboratory Investigation of the Enriched Gas Displacement Process in Vertical Models", (including Comments by

L.R. Smith and J.L. Shelton, and the Authors' Reply) The Journal of Canadian Petroleum Technology (January - March, 1973) 47-58.

[93] Volek, C.W. and Pryor, J.A.: "Steam Distillation Drive Brea Field, California", J. Pet. Tech. (Aug. 1972) 899-906 (see also SPE Reprint Series No. 7, Thermal Recovery Processes, 1985 Edition).

[94] Konopnicki, D.T., Traverse, E.F., Brown, A. and Deiberg, A.D.: "Design and Evaluation of the Shiells Canyon Field Steam-Distillation Drive Pilot Project", J. Pet. Tech. (May 1979) 546-52 (see also SPE Reprint Series No. 7, Thermal Recovery Processes, 1985 Edition).

[95] Texaco Inc., Research and Technical Department (Burnett, D.B. and Lim, F.H.): "Determination of Solvent Compositions for Miscible Floods", August 1971, ERCB Open Files.

[96] Flock, D.L. and Nouar, Akli: "Parametric analysis on the determination of the minimum miscibility pressure in slim tube displacements", The Journal of Canadian Petroleum Technology (September - October 1984) 80-88.

[97] Wellington, S.L. and Vinegar, HJ.J.: "X-Ray Computerized Tomography", J. Pet. Tech. (Aug. 1987) 885-898.

[98] Benmekki, E.H., and Mansoori, G.A.: "Minimum Miscibility Pressure Prediction With Equations of State", SPERE (May 1988) 559-564.

[99] Firoozabadi, A., Nutakki, R., Wong, T.W. and Aziz, K.: "EOS Predictions of Compressibility and Phase Behavior in Systems Containing Water, Hydrocarbons, and CO₂", SPERE (May 1988) 673-84.

[100] Kremesec Jr., V.J. and Sebastian, H.M.: "CO₂ Displacements of Reservoir Oils From Long Berea Cores: Laboratory and Simulation Results", SPERE (May 1988) 496-504.

[101] Negahban, S., Shiralkar, G.S. and Gupta, S.P.: "Simulation of the Effects of Mixing in Gas Drive Core Tests of Reservoir Fluids", SPE/DOE 17377 prepared for presentation at the SPE/DOE Enhanced Oil Recovery Symposium held in Tulsa, Oklahoma, April 17-20, 1988.

[102] McCaffery, F.G., Sigmund, P.M., and Wardlaw, N.C.: "A Treatise on Hydrocarbon Recovery From Carbonate Reservoirs", Petroleum Recovery Institute, Research Report RR-36, May 1978.

[103] Stelzer, R.B.: "Model Study vs. Field Performance, Cycling the Paluxy Condensate Reservoir", API Drilling and Production Practice (1956) 336-342.

[104] Odeh, A.S.: "Comparison of Solutions to a Three - Dimensional Black Oil Reservoir Simulation Problem", J. Pet. Tech. (Jan. 1981) 13-25.

[105] Weinstein, H.G., Chappellear, J.E., and Nolen, J.S.: "Second Comparative Solution Project: A Three-Phase Coning

Study", J. Pet. Tech. (March 1986) 345-353.

[106] Kenyon, D.E. and Behie, G.A.: "Third SPE Comparative Solution Project: Gas Cycling of Retrograde Condensate Reservoirs", J. Pet. Tech. (Aug. 1987) 981-997.

[107] Aziz, K., Ramesh, A.B. and Woo, P.T.: "Fourth SPE Comparative Solution Project: Comparison of Steam Injection Simulators", J. Pet. Tech. (Dec. 1987) 1576-1584.

[108] Killough, J.E., and Kossack, C.A.: "Fifth Comparative Solution Project: Evaluation of Miscible Flood Simulators", SPE 16000 presented at the Ninth SPE Symposium on Reservoir Simulation held in San Antonio, Texas, February 1-4, 1987.

[109] Firoozabadi, A. and Thomas, L.K.: "Sixth Comparative Solution Project: A Comparison of Dual-Porosity Simulators", SPE 18741 presented at the Tenth SPE Symposium on Reservoir Simulation, February 6-8, 1989, Houston, Texas.

[110] Howes, Barbara J.: "Enhanced oil recovery in Canada: success- in -progress", The Journal of Canadian Petroleum Technology (November - December 1988) 80-88.

[111] Tiffin, D.L. and Kremesec Jr., V.J.: "Mechanistic Study of Gravity-Assisted CO₂ Flooding", SPERE (May 1988) 524-532.

[112] Nutakki, Ramagopal: "The Influence of Phase Behavior and Solvent Channeling on Miscible Gas Flood Performance", MS

Thesis, U. of Calgary, Calgary, Alta. (September 1983).

[113] Sarma, Hemanta Kumar: "An Experimental Study of Instability and Viscous Fingering in Porous Medium ", MS Thesis, U. of Calgary, Alta. (October 1983).

[114] Soucemarianadin, A., Touboul, E., Bourlion, M., Nittmann, J. and Lenormand, R.: "Sweep Efficiency in Multilayered Porous Media: Contrast Between Stable and Unstable Flow", SPE 16955 prepared for presentation at the 62nd Annual Technical Conference and Exhibition of the Society of Petroleum Engineers held in Dallas, TX, September 27-30, 1987.

[115] Metcalfe, R.S., Vogel, J.L. and Morris, R.W.: "Compositional Gradients in the Anschutz Ranch East Field", SPERE (August 1988) 1025-32.

[116] Williams, John K. and Dawe, Richard A.: "Near-Critical Condensate Fluid Behavior in Porous Media - A Modelling Approach", SPERE (May 1989) 221-27.

[117] Sayegh, S.G., Wang, S.T. and Najman, J.: "Multiple contact phase behavior in the displacement of crude oil with nitrogen and enriched nitrogen", The Journal of Canadian Petroleum Technology (November - December 1987) 31-39.

[118] Sayegh, S.G., Wang, S.T. and Fosti, J.E.: "Recovery of crude oil by nitrogen injection laboratory displacement data", The Journal of Canadian Petroleum Technology (November December

1988) 74-79.

[119] Ypma, Jan G.J.: "Compositional Effects in Gravity - Dominated Nitrogen Displacements", SPERE (August 1988) 867-74.

[120] Doscher, T.M., Oyekan, R.O., and El Arabi, M.: "The Displacement of Residual Crude by CO₂ and Nitrogen in Gravity Stabilized Systems", SPE Trans. Vol. 277 (1984) 593-596.

[121] Kantzas, A., Chatzis, I. and Dullien, F.A.L.: "Mechanisms of Capillary Displacement of Residual Oil by Gravity-Assisted Inert Gas Injection", SPE 17506 prepared for presentation at the SPE Rock Mountain Regional Meeting, held in Casper, WY, May 11-13, 1988.

[122] Kantzas, A., Chatzis, I. and Dullien, F.A.L.: "Enhanced Oil Recovery by Inert Gas Injection", SPE/DOE 17379 prepared for presentation at the SPE/DOE Enhanced Oil Recovery Symposium held in Tulsa, Oklahoma, April 17-20, 1988.

[123] Chatzis, I., Kantzas, A. and Dullien, F.A.L.: "On the Investigation of Gravity-Assisted Inert Gas Injection Using Micromodels, Long Berea Sandstone Cores, and Computer-Assisted Tomography", prepared for presentation at the 63rd Annual Technical Conference and Exhibition of the Society of Petroleum Engineers held in Houston, TX, October 2-5, 1988.

[124] Omole, O. and Osoba, J.S.: "Effect of column length on CO₂ - crude oil miscibility pressure", The Journal of Canadian

Petroleum Technology (July - August 1989) 97-102.

[125] Muskat, M.: Physical Principles of Oil Production, (1949) IHRDC.

[126] Williamson, Alexander S. and Chappellear, John E.: "Representing Wells in Numerical Reservoir Simulation: Part 1 - Theory", SPE Trans. Vol. 271 (1981) 323-338.

[127] Chappellear, John E. and Williamson, Alexander S.: "Representing Wells in Numerical Reservoir Simulation: Part 2 - Implementation", SPE Trans. Vol. 271 (1981) 339-344..

[128] Pedrosa Jr., Oswaldo A. and Aziz, Khalid: "Use of a Hybrid Grid in Reservoir Simulation", SPERE (Nov. 1986) 611-621.

[129] Tang, D.H.E. and Peaceman, D.W.: "New Analytical and Numerical Solutions for the Radial Convection-Dispersion Problem", SPERE (Aug. 1987) 343-359.

[130] Carey, G.F. and Chow, S.S.: "Well Singularities in Reservoir Simulation", SPERE (Nov. 1987) 713-719.

[131] Winterfeld, P.H.: "Simulation of Pressure Buildup in a Multiphase Wellbore/Reservoir System", SPEFE (June 1989) 247-252.

[132] Lee, S.H.: "Analysis of Productivity of Inclined Wells and Its Implications for Finite-Difference Reservoir Simulation", SPEFE (May 1989) 173-180.

[133] Butler, Roger M.: "The potential for horizontal wells for petroleum production", The Journal of Canadian Petroleum Technology (May-June 1989) 39-47.

[134] Alberta Oil Sands Technology and Research Authority:
"Alberta Heavy Oil, Oil Sands and Enhanced Recovery,
Experimental Pilot Projects", August 1988.

APPENDIX A

DESCRIPTION OF NUMERICAL MODEL

A phase behaviour package [A-1] and an equation-of-state compositional model [A-2], that were developed by the Computer Modelling Group, were used throughout this investigation. Compositional models such as the General Equation of State Model (GEM) applied in this investigation are widely used [A-3, A-4] to simulate design alternatives and optimization strategies for improved oil recovery processes. The compositional model GEM has also been successfully applied to the simulation of laboratory displacement experiments [A-5] similar in concept to the numerical model experiments performed in this investigation.

The general flow equations have been derived elsewhere [A-6] and are presented in summary form below (symbols are defined in the nomenclature to Appendix A):

$$\psi_P = \nabla T_P (\nabla p - \gamma \nabla z) - \frac{\partial}{\partial t} (\rho \phi S)_P + q_{n_c+1} = 0 \quad (1)$$

where:

$$T_P = \left(\rho \frac{k k_r}{\mu} \right) \quad (2)$$

Equation (1) is the general partial differential equation for the flow of a compressible fluid [A-6] with the phase transmissibility defined by equation (2). The governing discretized flow equations for the compositional simulator GEM have been presented by Collins, Nghiem

and Li [A-7] and are summarized below (symbols are defined in the nomenclature to Appendix A):

$$\begin{aligned}
 \psi_p &= \Delta T_o^m (\Delta p^{n+1} - \gamma_o^m \Delta D) \\
 &+ \Delta T_g^m (\Delta p^{n+1} + \Delta p_{cog}^m - \gamma_g^m \Delta D) \\
 &+ \theta \Delta T_w^m (\Delta p^{n+1} - \Delta p_{cwo}^m - \gamma_w^m \Delta D) + \sum_{i=1}^{n+1} q_i^{n+1} \\
 &+ \theta q_{n_c+1}^{n+1} - \frac{V}{\Delta t} \left[\phi^{n+1} (\rho_o S_o + \rho_g S_g + \theta \rho_w S_w)^{n+1} \right. \\
 &\left. - \phi^n (\rho_o S_o + \rho_g S_g + \theta \rho_w S_w)^n \right] = 0
 \end{aligned} \tag{3}$$

$$g_i = \ln f_{ig} - \ln f_{io} = 0 \quad i=1, \dots, n_c \tag{4}$$

$$S_m = (N_m / \rho_m) / \left[\sum_q (N_q / \rho_q) \right] \quad \begin{matrix} m=o, g, w \\ q=o, g, w \end{matrix} \tag{5}$$

Equation (3) represents the discretized flow equation with thermodynamic equilibrium defined by equation (4) and fluid saturations defined by equation (5). These equations are solved numerically.

NOMENCLATURE

| | |
|------------|--|
| D | - depth |
| f_{im} | - fugacity of Component i in Phase m ($m=0,g$) |
| g | - phase equilibrium equation |
| k | - absolute permeability to flow, μm^2 |
| k_r | - relative permeability |
| N_i | - moles of Component i per unit of pore volume ($i=1,\dots,n_c+1$) |
| N_g | - moles of gas per unit of pore volume |
| N_o | - moles of oil per unit of pore volume |
| N_{im} | - moles of Component i in Phase m ($m=0,g$) per unit of pore volume |
| p | - oil-phase pressure |
| p_{cog} | - gas-oil capillary pressure |
| p_{cwo} | - oil-water capillary pressure |
| q_i | - molar injection/production rate of Component i |
| S_m | - saturation of Phase m ($m=0,g,w$) |
| t | - time |
| T_m | - molar transmissibility of Phase m ($m=0,g,w$) |
| V | - block volume |
| y_{im} | - gradient of Phase m ($m=0,g$) |
| γ_m | - gradient of Phase m ($m=0,g,w$) |
| ∇ | - gradient operator |
| Δ | - difference operator |
| θ | - scaling factor for water equation and variables |
| ρ_m | - molar density of Phase m ($m=0,g,w$) |

ϕ - porosity

ψ - material balance equation

Superscripts

m - old or new time level
n - old time level
n+1 - new time level

Subscripts

i,j,s - subscripts for components
g - gas phase
m,p - subscripts for phases
o - oil phase
w - aqueous phase

REFERENCES

- [A-1] Computer Modelling Group: "CMGPROP Technical Manual, Phase Behaviour Package, Version 4.0", March 1988.
- [A-2] Computer Modelling Group: "GEM Program Manual, Equation-of-State Compositional Model, Version 2.3", August 1987.
- [A-3] Kenyon, D.E. and Behie, G.A.: "Third SPE Comparative Solution Project: Gas Cycling of Retrograde Condensate Reservoirs", J.Pet.Tech. (Aug. 1987), 981-997.
- [A-4] Killough, J.E. and Kossack, C.A.: "Fifth Comparison Solution Project: Evaluation of Miscible Flood Simulators", SPE 16000 presented at the Ninth SPE Symposium on Reservoir Simulation held in San Antonio, Texas, February 1-4, 1987.
- [A-5] Firoozabadi, Abbas and Aziz, Khalid: "Analysis and Correlation of Nitrogen and Lean-Gas Miscibility Pressure", SPERE (Nov.1986) 575-582.
- [A-6] Aziz, Khalid, and Settari, Antonin: Petroleum Reservoir Simulation, Applied Science Publishers, London and New York (1979).
- [A-7] Collins, D.A., Nghiem, L.X. and Li, Y.K.: "An Efficient Approach to Adaptive-Implicit Compositional Simulation With An Equation of State", SPE 15133, April 1986.